STRATHCLYDE INSTITUTE OF PHARMACY & BIOMEDICAL SCIENCES

University of Strathclyde Science

Discovering the biological and clinical implications of modulating glucocorticoid action using metabolomic profiling of human plasma samples

Mohammad A. A. Alwashih

A Thesis Submitted in Fulfillment of the Requirements for the Award of Degree of Doctor of Philosophy in Strathclyde Institute of Pharmacy and Biomedical Sciences at the University of Strathclyde

2016

Declaration

‘I declare that, except where specifically indicated, all the work presented in this report is my own and I am the sole author of all parts.’

Signed: _____

Date: _____

Acknowledgments

I wish to express my sincerest gratitude to Allah for providing me with health, commitment and patience to complete my PhD studies. I am deeply grateful to my principal supervisor, Dr David G Watson, for his immense support, continuous encouragement and motivation throughout my PhD studies. My thanks is also extended to our collaborators Prof Brian R Walker, Prof Ruth Andrew, and Prof Roland Stimson from Edinburgh University, and Prof David MacFarlane from Aberdeen University, for their help in providing samples, advice and valuable insights.

Particular thanks are owed to all my friends and colleagues in SIPBS for their support during my study.

I wish also to offer my sincere gratitude to my parents for their emotional support and prayers, and to my brothers and sisters for their encouragement. I am grateful to my wife and my sons for their patience, support and love. I also wish to thank all my friends, especially Dr. Bandar Alshammary, Dr. Abdulrahman Alharthi, Dr. Abdulaziz Alqadi, Mr. Feras Alshehri, Dr. Adel Alharf, Dr. Khalid Aldajani and Mr. Daifallah Alwadani for their support during my stay in Glasgow.

Finally, I wish to thank the Saudi Ministry of Interior for sponsoring my PhD study.

Table of Contents

Table of Contents

Declaration i

Acknowledgments ii

Table of Contents iii

List of Figures x

List of Tables xiii

List of Abbreviations xv

Terms used interchangeably xviii

Papers published/submitted and posters presented xix

Abstract xx

1 Introduction 2

1.1 General background 2

1.2 Glucocorticoids 4

1.3 Physiological role of GC 7

1.1 Actions of GC in peripheral tissues 10

1.1.1 Muscle 10

1.1.2 Skeleton and bones 13

1.1.3 Hepatic effects 14

1.1.4 Brain 15

1.1.5 Adipose tissue 16

1.1.6 Cardiovascular system 17

1.1.7 Gastrointestinal tract 17

1.1.8 Immune system 18

1.2 Pathophysiological perturbations 18

1.3 Metabolomics 21

1.3.1 Approaches to metabolome analysis 22

1.4 Analytical platforms 24

1.5 Univariate analysis 24

1.6 Multivariate analysis 25

1.6.1 Data pre-processing. 26

1.6.2 Scaling 28

1.7 Data visualisation 29

1.7.1 Unsupervised Techniques 29

1.7.2 Principal Component Analysis (PCA) 30

1.7.3 Detecting outliers: (DModX and Hotelling's T^2) 31

1.7.4 Supervised Techniques 33

1.7.5 Model validation 35

1.7.6 Cross validated ANOVA (CV-ANOVA) 38

1.7.7 Receiver Operating Characteristic (ROC) 38

1.8 Biomarkers identification using an S-plot 40

1.8.1 Variable importance in the projection (VIP) 41

1.8.2 Corrected p values 42

1.8.3 Jack-knifing (JK) uncertainties 43

1.9 Aims and objectives 44

1.9.1 First objective 44

1.9.2 Second objective 44

1.9.3 Third objective 45

1.9.4 Fourth objective 45

2 Materials and Methods 47

2.1 Chemicals and Solvents 47

2.2 Sample Preparation 47

2.3 HPLC conditions 47

2.3.1 Mobile phase solutions for ZIC-pHILIC chromatography 47

2.3.2 Mobile Phase for C18 Chromatography 48

2.3.3 HPLC setup 48

2.3.4 Orbitrap Exactive MS setup 50

2.4 Data extraction methods used in processing the files obtained from LC-MS analysis of plasma samples. 51

2.4.1 mzMatch and IDEOM 51

2.4.2 Data bases used for identification 54

2.5 Metabolomics profiling 54

2.5.1 Statistical softwares used 54

2.5.2 Pre-treatment 54

2.5.3 Pooled samples 55

2.5.4 Data visualisation and biomarkers identification 55

2.5.5 Diagnostics and validation 57

2.5.6 Putative biomarker selection workflow was as follow: 58

3 Effect of acute GC blockade on metabolic dysfunction in patients with T2D using metabolomics 60

3.1 Abstract 60

3.2 Introduction 61

3.3 Methodology 65

3.3.1 Participants and sample collection 65

3.3.2 Study design and protocol 65

3.3.3 LC-MS analysis 67

3.3.4 Data extraction and processing 67

3.3.5 Data analysis 67
3.4 Results 68
3.4.1 Data visualisation 70
3.4.2 Biomarker identification 73
3.5 Discussion 85
4 A metabolomic study of the interaction between HC and insulin 93
4.1 Abstract 93
4.2 Introduction 95
4.3 Methodology 99
4.3.1 Sample collection 99
4.3.2 LC-MS analysis 100
4.3.3 Data extraction and processing 100
4.3.4 Data analysis 100
4.4 Results 101
4.4.1 Data visualisation 103
4.4.2 Biomarker identification 106
4.5 Discussion 123
5 Metabolomic profiling of patients with congenital adrenal hyperplasia uncovers significant biomarkers associated with the disease progress. 130

5.1 Abstract 130
5.2 Introduction 132
5.3 Methodology 135
5.3.1 Anthropometric data collection 135
5.3.2 LC-MS analysis 135
5.3.3 Data extraction and processing 135
5.3.4 Data analysis 135
5.4 Results 136
5.4.1 Anthropometrics and clinical measurements 136
5.4.2 Study the metabolomics difference between the groups 142
5.4.3 Biomarkers identification 143
5.5 Discussion 147
6 Exploration of different cut offs of GC dose using metabolomics 152
6.1 Abstract 152
6.2 Introduction 154
6.3 Methodology 158
6.3.1 Patient recruitment 158
6.3.2 Procedure for collection of anthropometric data 158
6.3.3 LC-MS analysis 159

6.3.4 Data extraction and processing 159

6.3.5 Data analysis 160

6.4 Results 160

6.4.1 Metabolomics profiling of different GC cutoffs 160

6.4.2 Metabolomics difference between patients receiving 1-5 mg and those receiving >5-15 mg prednisolone equivalent. 165

6.5 Discussion 172

7 General discussion 177

7.1 Conclusion 183

7.2 Strengths and limitations 183

7.3 Future work 184

References 186

Appendices 207

Appendices for Chapter 3 207

Appendices for Chapter 4 210

Appendices for Chapter 5 212

Appendices for Chapter 6 214

List of Figures

Figure 1.1 Steroidogenesis. 6

Figure 1.2 Hypothalamic Pituitary Adrenal-Axis (HPA-Axis). 8

Figure 1.3 Physiological conversion between cortisone and cortisol. 9

Figure 1.4 Normal probability plot of residuals. 28

Figure 1.5 Distance to model (DModX) vs Hotellings T^2 plot. 32

Figure 1.6 Hierarchical Clustering Analysis (HCA) plot. 33

Figure 1.7 Orthogonal Partial Least Square Discriminant Analysis (OPLS-DA) score plot. 34

Figure 1.8 Observed vs Predicted plot. 36

Figure 1.9 Permutations test. 37

Figure 1.10 Area Under the Reciever Operating Characterestics Curve (AUC). 39

Figure 1.11 S-plot. 41

Figure 3.1 2D PCA score plot for QC (pooled) plasma samples of patients with T2D. 68

Figure 3.2 Hierarchical Clustering Analysis (HCA) plot for patients with T2D having placebo and GC blockade. 70

Figure 3.3 (A) PCA vs (B) OPLS-DA score plots for pstients with T2D. 72

Figure 3.4 OPLS-DA score plot of placebo vs GC blockade samples of patients with T2D based on 18 putative metabolites. 73

Figure 3.5 (A)OPLS-DA score plot and (B) ROC curve of placebo vs GC blockade treatment in patients with T2D based on readings of bile acids metabolites and their conjugates. 77

Figure 3.6 OPLS-DA score plots of the effect of insulin on (A) 537 and (B) 2 putative metabolites. 79

Figure 3.7 OPLS-DA score plots of the effect of insulin on (A) 537 and (B) 8 putative metabolites following GC blockade treatment. 82

Figure 3.8 Heat map showing the putative metabolites that are significantly affected by insulin following GC blockade treatment. 84

Figure 4.1 2D PCA score plot for QC (pooled) samples in healthy individuals. 101

Figure 4.2 Hierarchical Clustering Analysis (HCA) for healthy subjects having different doses of HC and insulin. 103

Figure 4.3 (A) PCA vs (B) OPLS-DA score plots for healthy individuals recieving different doses of HC and insulin. 105

Figure 4.4 OPLS-DA score plot for for healthy individuals having either high or low insulin dose. 107

Figure 4.5 OPLS-DA score plot for the effect of insulin on 10 selected metabolites. 111

Figure 4.6 OPLS-DA score plot for the effect of HC dose on 23 significant puatative metabolites in plasma of healthy individuals. 114

Figure 4.7 OPLS-DA score plot for the effect of HC dose on selected 10 significant putative metabolites with highest AUC valuse in plasma of healthy individuals. 117

Figure 4.8 Heat map shows putative biomarkers that significantly affected by both interventions insulin and HC. 121

Figure 5.1 Hierarchical Clustering Analysis (HCA) of patients with CAH based on anthropometrics and clinical measurements. 137

Figure 5.2 (A) OPLS-DA score plot of 119 patients with CAH based on anthropometrics and clinical measurements, and (B) Pie chart showing the contribution of each anthropometric and clinical parameter in the classification. 138

Figure 5.3 Error plots (means and 95% confidence intervals), comparing the anthropometrics and clinical measurements among the three groups using one-way ANOVA..... 140

Figure 5.4 2D PCA score plot shows 119 observations for patients with CAH (grey-No class) plus 5 pooled samples (plum-QC). 142

Figure 5.5 The ROC curves of low risk vs high risk groups, (A) for anthropometrics measurements and (B) for corresponding metabolomics difference. 146

Figure 6.1 OPLS-DA score plots shows 4 comparisons of 117 samples of patients with CAH grouped based on their daily doses of GC. 162

Figure 6.2 OPLS-DA score plot shows samples of patients with CAH receiving either 1-5 mg or >5-15 mg prednisolone equivalent. 166

Figure 6.3 Bar chart of the most significant metabolites. 169

Figure 6.4 (A) OPLS-DA score plot and (B) Area under the ROC, both built up on readings of 7 putative biomarkers (Table 6.4) in 117 patients..... 170

List of Tables

Table 1.1 Indication of GC treatments and their side effects. 3

Table 1.2 Enzymes associated with GC biosynthesis and their dysfunctions. 6

Table 2.1 Gradient elution programme applied for ZICpHILIC in LC-MS analysis..... 49

Table 2.2 Gradient elution programme applied for C18-AR in LC-MS analysis. 50

Table 3.1 Shows proportions (%) of HC and insulin doses based on the HCA grouping. 71

Table 3.2 Shows list of putative biomarkers that significantly changed following GC blockade treatment..... 75

Table 3.3 List of bile acids and their conjugates that increased following treatment with GC blockade. 76

Table 3.4 Putative biomarkers which significantly increased following insulin dose. 81

Table 3.5 Putative biomarkers that significantly affected by the insulin dose following GC blockade..... 81

Table 4.1 Shows proportions (%) of samples with different HC and insulin doses based on the HCA grouping. 104

Table 4.2 Metabolites that change significantly following insulin dose. 109

Table 4.3 The 10 putative metabolites with highest AUC values and their correlations (r) to insulin dose. 112

Table 4.4 Misclassification table showing the proportions of correctly classified observations using on Fisher's probability. 113

Table 4.5 Putative metabolites that were significantly affected in plasma of healthy individuals following HC dose. 116

Table 4.6 The 10 metabolites with highest AUC values and their correlations (r) to HC dose. 119

Table 4.7 Putative biomarkers significantly affected by both interventions (Split plot ANOVA). 120

Table 4.8 Putative metabolites that show significant interaction in both interventions. 122

Table 5.1 Shows values of the anthropometrics and clinical measurements among the three groups. 141

Table 5.2 List of putative biomarkers that show significant differences among the three groups using one way ANOVA. 144

Table 6.1 Data corresponding to (Figure 6.1) regarding group assignment plus AUC for classification. 164

Table 6.2 Comparison of anthropometric and clinical measurements between the low (L) and high (H) dose GC exposed groups. All measurements were similar between the two groups except for GC dose. 165

Table 6.3 Putative biomarkers significantly affected by the difference in GC dose between the low (L) and high (H) GC dose groups. 168

Table 6.4 List of significant putative biomarkers used to build up the OPLS-DA model in Figure 6.4. 171

List of Abbreviations

ACTH	Adrenocorticotrophic Hormone
ANOVA	Analysis of Variance
ATP	Adenosine Triphosphate
AUROCC	Area Under the ROC Curve
BCAA	Branched Chain Amino Acids
BMI	Body Mass Index
BNF	British National Formulary
BP	British Pharmacopoeia
CAH	Congenital Adrenal Hyperplasia
CRH	Corticotrophin Releasing Hormone
CV	Cross Validation
CV-ANOVA	Cross Validated ANOVA
DM	Diabetes Mellitus
ESI	Electrospray Ionisation
ESI-MS	Electrospray Ionisation-Mass Spectrometry
FDR	False Discovery Rate
FFAs	Free Fatty Acids
FT	Fourier Transformation
FTIR	Fourier Transform Infra-Red
GC	Glucocorticoid
GC-MS	Gas Chromatography Mass Spectrometry

GLUT	Glucose Transporter
HC	Hydrocortisone
HCA	Hierarchical Cluster Analysis
HILIC	Hydrophilic Interaction Liquid Chromatography
HPA	Hypothalamic Pituitary Adrenal
HPLC	High Performance Liquid Chromatography
HRMS	High Resolution Mass Spectrometry
LC	Liquid Chromatography
LC-MS	Liquid Chromatography-Mass Spectrometry
m/z	Mass to Charge Ratio
MRI	Magnetic Resonance Imaging
MS	Mass Spectrometry
MS/MS	Tandem Mass Spectrometry
MVA	Multivariate Analysis
NAD+	Nicotinamide Adenine Dinucleotide (oxidised)
NADH	Nicotinamide Adenine Dinucleotide (reduced)
NAFLD	Non Alcoholic Fatty Liver Disease
NIESI	Negative Ionisation Electrospray Ionisation Mode
nm	nmol/L
NMR	Nuclear Magnetic Resonance
NSAIDs	Non-Steroidal Anti-Inflammatory Drugs
OPLS	Orthogonal Partial Least Squares

OPLS-DA	Orthogonal Partial Least Squares Discriminant Analysis
PCA	Principal Component Analysis
PIESI	Positive Ionisation Electrospray Ionisation Mode
PLS	Partial Least Squares
PNMT	Phenylethanolamine-N-Methyltransferase
PreDEqBNF	Prednisolone DosenEquivalent British National Formulary
QSRR	Quantitative Structure Retention Relationships
RMSECV	Root-Mean-Square Error of Cross Validation
ROC	eceiver Operator Characteristic
RP	Reversed Phase
RPLC	Reversed Phase Liquid Chromatography
RSD	Relative Standard Deviation
RT	Retention Time
SIMCA	Soft-Independent Modelling of Class Analogy
SPSS	Statistical Package for Social Scientists
T2D	Type 2 Diabetes
VIP	Variable Importance in the Projection
ZIC	Zwitterionic

Terms used interchangeably

Metabolic profiling = untargeted metabolomics

Metabolome = metabolomic profile

Samples = observations

Subjects = individuals

Putative metabolites = putative biomarkers = variables

Papers published/submitted and posters presented

Papers

1. MacRitchie N, Volpert G, Alwashih MA, Watson DG, Futerman AH, Kennedy S, et al. Effect of the sphingosine kinase 1 selective inhibitor, PF-543 on arterial and cardiac remodelling in a hypoxic model of pulmonary arterial hypertension. Cell Signal. 2016;28(8):946-55.
2. Zhang R, Zhang T, Ali AM, Al Washih M, Pickard B, Watson DG. Metabolomic Profiling of Post-mortem brain reveals changes in amino acid and glucose metabolism in mental illness compared with controls. Comput Struct Biotechnol J. 2016;14:106-16.
3. Alwashih MA, Andrew R, Stimson RH, Alossimi M, Blackburn G, Watson DG, Walker BR. The exploration of different cut offs of glucocorticoid dose using metabolomics (submitted to Journal of Clinical Endocrinology and Metabolism).

Posters

1. Alwashih MA, Henderson C, Grant H, Watson DG, editors. Investigating the effect of Mephedrone on rat hepatocytes using metabolomics. ISSX meeting; 2015; Glasgow.
2. Alwashih MA, MacFarlane DP, Walker BR, Andrew R, Stimson RH, Gavin B, et al., editors. Chemometrics uncovers significant anthropometric and biochemical differences in 119 patients with Congenital Adrenal Hyperplasia (CAH):Analysis of the United Kingdom Adult CAH Study Executive (CaHASE) Cohort. Inaugural Metabolomics Inaugural Meeting; 2015; Edinburgh.
3. Alwashih MA, Walker BR, Andrew R, Stimson RH, Watson DG, editors. A metabolomics study of the interaction between hydrocortisone and insulin. 8th Saudi Conference; 2014; London (Imperial College).

Abstract

Background: Glucocorticoid deficiency and excess are difficult to identify because of the non-specificity of their clinical and biochemical features which are also poorly correlated with levels of circulating steroids. The lack of reliable biomarkers for glucocorticoid action makes it challenging to determine precise therapeutic needs of patients with GC-deficient or excessive conditions such as congenital adrenal hyperplasia and Cushing's syndrome, respectively.

Aim: To identify the main biomarkers indicative of changes in cortisol action in healthy individuals and those with different metabolic diseases.

Study design and methodology: Plasma samples were collected from three separate studies. The first study was a randomised double-blind crossover design involving 8 men with type 2 diabetes given either placebo or metyrapone + mifepristone ('glucocorticoid blockade') for 12 hours. In the second study, 20 healthy men were given metyrapone with either low or high doses of insulin, plus such a dose of hydrocortisone as to achieve low, medium or high plasma cortisol levels. Finally, plasma samples were also obtained from 119 patients with CAH receiving standard clinical care. Liquid chromatography-mass spectrometry was then employed for the metabolomic profiling of all the plasma samples, and MzMatch software was used to identify the metabolites present. Multivariate and univariate analyses were employed to determine the most reliable metabolites as biomarkers for glucocorticoid action.

Results: Branched chain amino acids, bile acids and their conjugates, and free fatty acids were the main metabolite groups that were significantly altered by at least two of the three interventions. Compared to placebo, bile acids and their conjugates were significantly ($p < 0.05$)elevated following glucocorticoid blockade, but subsequent insulin administration significantly lowered their levels. On the other hand, high glucocorticoid dose significantly ($p < 0.05$) increased the levels of chenodeoxyglycocholate in patients with conginetal adrenal hyperplasia, but no effects on bile acids were observed in similarly treated healthy men. Branched chain amino acids were significantly lowered in healthy men following high insulin dose, but were significantly ($p < 0.05$) increased upon high hydrocortisone infusion. High BCAs levels were associated with high body mass index , and high systolic and diastolic blood pressure in pateints with conginetal adrenal hyperplasia. In contrast, L-valine, was significantly elevated following glucocorticoid blockade in patients with type 2 diabetes. A number of saturated and unsaturated fatty acids were significantly ($p < 0.05$) elevated following hydrocortisone infusion in healthy men, but insulin reduced their levels significantly ($p < 0.05$). High glucocorticoid dose in patients with conginetal adrenal hyperplasia significantly increased C15:0, C16:0 and C20:0 while C16:1 reduced. In contrast, use of insulin following glucocorticoid blockade in patients with type 2 diabetes significantly ($p < 0.05$) reduced levels of C12:0, C18:0 and C18:3.

Conclusion: These hypothesis-free metabolomics screening studies have identified metabolites in plasma which are differentially sensitive to glucocorticoid deficiency or excess and may be useful in clinical assessment of glucocorticoid therapy.

Chapter 1:

General Introduction

1 Introduction

1.1 General background

Glucocorticoids (GC) such as cortisol have diverse physiological actions. Intracellular GC receptors are widely expressed and affect energy metabolism (e.g. interacting with insulin and inducing gluconeogenesis, stimulating lipolysis and fatty acid turnover, inducing proteolysis) (Andrews and Walker, 1999a, Macfarlane *et al.*, 2008), cardiovascular control (Walker, 2007) (inducing sodium and water retention, potentiating vasoconstriction, increasing blood pressure), cellular proliferation, central nervous system function (impairing short-term memory, altering mood) (Seckl and Olsson, 1995) and innate immunity (enhancing macrophage apoptosis, inhibiting pro-inflammatory cytokine signalling) (Sapolsky *et al.*, 2000) (Table 1.1). Most actions of GC are mediated slowly by altered gene transcription in response to altered intracellular cortisol concentrations, whereas plasma levels of cortisol exhibit marked circadian and ultradian variation, thus there is a poor correlation between plasma cortisol levels and the clinical and biochemical actions of cortisol.

Table 1.1 Indication of GC treatments and their side effects.

Indication	Side effects
Endocrine disorders such as congenital adrenal hyperplasia	Obesity, T2D
Rheumatic disorders such as arthritis	hypertension
Collagen diseases such as systemic lupus erythematosus	Immunosuppression
Dermatologic diseases such as severe psoriasis	Muscle weakness
Ophthalmic diseases such as allergic conjunctivitis	Pancreatitis and peptic ulcer
Respiratory diseases such as aspiration pneumonitis	Anaemia
Neoplastic diseases that require palliative management	Short- and long-term memory loss

Acute elevation in cortisol is a crucial component of the stress response, but chronic excess of GC results in Cushing's syndrome, characterised by non-specific features including obesity, type 2 diabetes (T2D), hypertension, impaired immunity, depression and cognitive dysfunction. Subtle GC excess may be important in diverse conditions, ranging from metabolic syndrome (Walker, 2007) to neuropsychiatric disease (Seckl and Olsson, 1995). This excess may involve increased circulating levels of cortisol or increased local regeneration of cortisol within target tissues by the enzyme 11β-hydroxysteroid dehydrogenase type 1 (11β-HSD1) (Rask *et al.*, 2001). GC deficiency is potentially life threatening during stress, but is characterised by non-specific clinical features such as lethargy, hypotension and weight loss. The deficiency is especially difficult to diagnose during critical illness when conventional tests of cortisol production, such as adrenocorticotropic hormone (ACTH) stimulation tests, may be unreliable (Boonen *et al.*, 2013). However, it is crucial to identify patients at risk of serious complications or those most likely to have a disease. Metabolomics has been introduced as a new tool for diagnosing and

predicting diseases via discovery of reliable biomarkers; for instance, elevated amino acids are associated with 60 to 100% risk of having diabetes compared to the 5–37% risk associated with known polymorphisms (Wang *et al.*, 2011).

In the current work, the aim was to identify biomarkers that reflect GC action. To investigate GC deficiency, metabolomic analysis was performed on plasma samples obtained from healthy men and patients with T2D after administration of the GC antagonist RU38486 (mifepristone) together with the inhibitor of cortisol biosynthesis, metyrapone, a combination which has been termed 'glucocorticoid blockade' (Wake *et al.*, 2007, Macfarlane *et al.*, 2014). To investigate GC dose effects, samples from healthy men treated with metyrapone were obtained and this was followed by hydrocortisone (HC) replacement to induce low, medium and high (supra-physiological) circulating cortisol levels. In each study, the specificity of the response to GC was tested by taking measurements before and after insulin infusion. The metabolomic features of GC excess in plasma samples of patients with congenital adrenal hyperplasia (CAH) receiving GC replacement therapy from the UK Congenital adrenal Hyperplasia Adult Study (CaHASE) (Arlt *et al.*, 2010) were also investigated.

1.2 Glucocorticoids

GC are steroid hormones manufactured from cholesterol via a process called steroidogenesis (Figure 1.1). Major classes of steroid hormones include:

(A) Progestagens, which are divided into progesterones (which maintain pregnancy via suppressing uterine contractility and prevent spontaneous abortion) and corticosteroids (which are divided into i) mineralocorticoids such as aldosterone, which induces reabsorption of sodium and water and secretion of potassium via the kidneys and ii) GC such as cortisol, which have various physiological activities, for instance, suppression of the immune system and glucose metabolism).

(B) Androstagens, which are divided into androgens such as testosterone (which contributes to the development of male characteristics) and oestrogen (which contributes to the development of female characteristics) (Miller and Auchus, 2011) (Table 1.2).

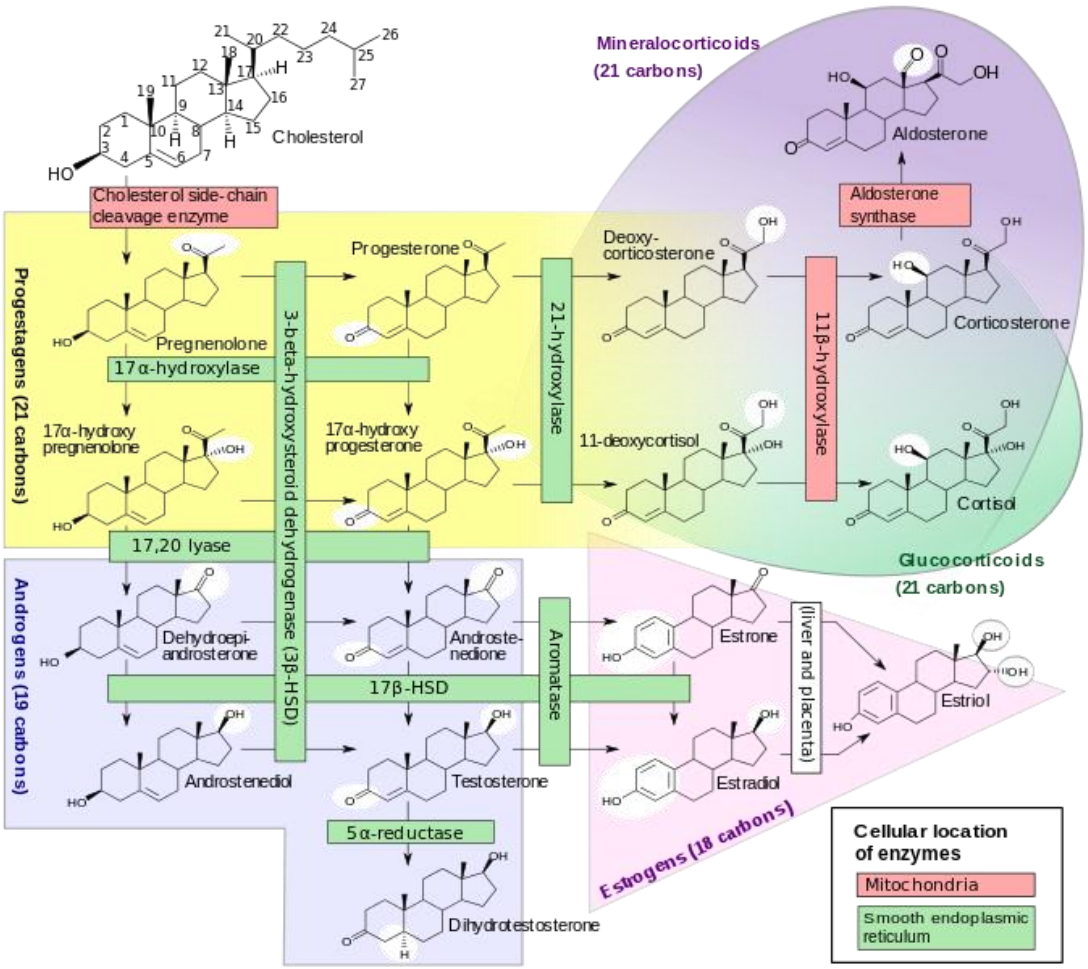

Figure 1.1 Steroidogenesis.
Conversion of cholesterol into steroid hormones. Enzymes involved in the process are coloured according to their cellular location. Metabolites shaded in yellow represent progestogens (21 carbons), while those shaded in light blue represent androgens (19 carbons).

Table 1.2 Enzymes associated with GC biosynthesis and their dysfunctions.

Enzyme	Physiological function	Dysfunction
17α-hydroxylase	Converts pregnenolone to 17 hydroxy pregnenolone	Congenital adrenal hyperplasia*
3β-hydroxysteroid dehydrogenase	Converts 17 hydroxy pregnenolone to 17 hydroxy progesterone	Congenital adrenal hyperplasia*
21-hydroxylase	Converts 17 hydroxy progesterone to 11 deoxycortisol	Congenital adrenal hyperplasia (95% of the cases)
11β-hydroxylase	Converts 11 deoxycortisol to cortisol	Congenital adrenal hyperplasia*
11β-hydroxysteroid dehydrogenase	Converts corticosterone to cortisol	Cushing's syndrome

*Uncommon, the table shows enzymes contribute to steroidogenesis and their physiological and pathophysiological effect.

1.3 Physiological role of GC

Research regarding the role of GCs has been on-going over the past century and a half, during which time it has led to various key advancements in many aspects of molecular biology. GC are steroid hormones that play multiple roles in the body by regulating various processes involved in the metabolism of carbohydrates, lipids and proteins, as well as playing key roles in the regulation of the immune and cardiovascular systems, and in coping with stress. In this way, these hormones regulate various aspects of the body's homeostasis. For this reason, a deficiency of GCs results in postural hypotension, hypoglycaemia and weight loss, while excess GCs leads to hypertension, glucose intolerance and obesity (Andrews *et al.*, 1999). Cortisol is the most physiologically important GC in the body and is produced by the adrenal glands, which are the small bodies that sit on top of each of the kidneys. The secretion of GCs is regulated by the hypothalamic-pituitary-adrenal (HPA) axis. The adrenal glands are stimulated to release GC by ACTH, or corticotropin, which is released from the anterior pituitary gland. This corticotropin, whose release is also controlled by another hormone—corticotropin releasing hormone (CRH), from the hypothalamus—acts to keep the amount of cortisol released by the adrenal gland within the normal range according to the needs of the body. The hypothalamus, in turn, releases a stimulating hormone in response to certain signals in the blood, or from stress (e.g. injury, infection or surgery), but mainly through a negative feedback mechanism. If the level of cortisol in the blood is high, CRH release from the hypothalamus is suppressed, meaning that the anterior pituitary is not

stimulated to release ACTH, thus causing the adrenal glands to stop producing cortisol, and vice versa (Figure 1.2).

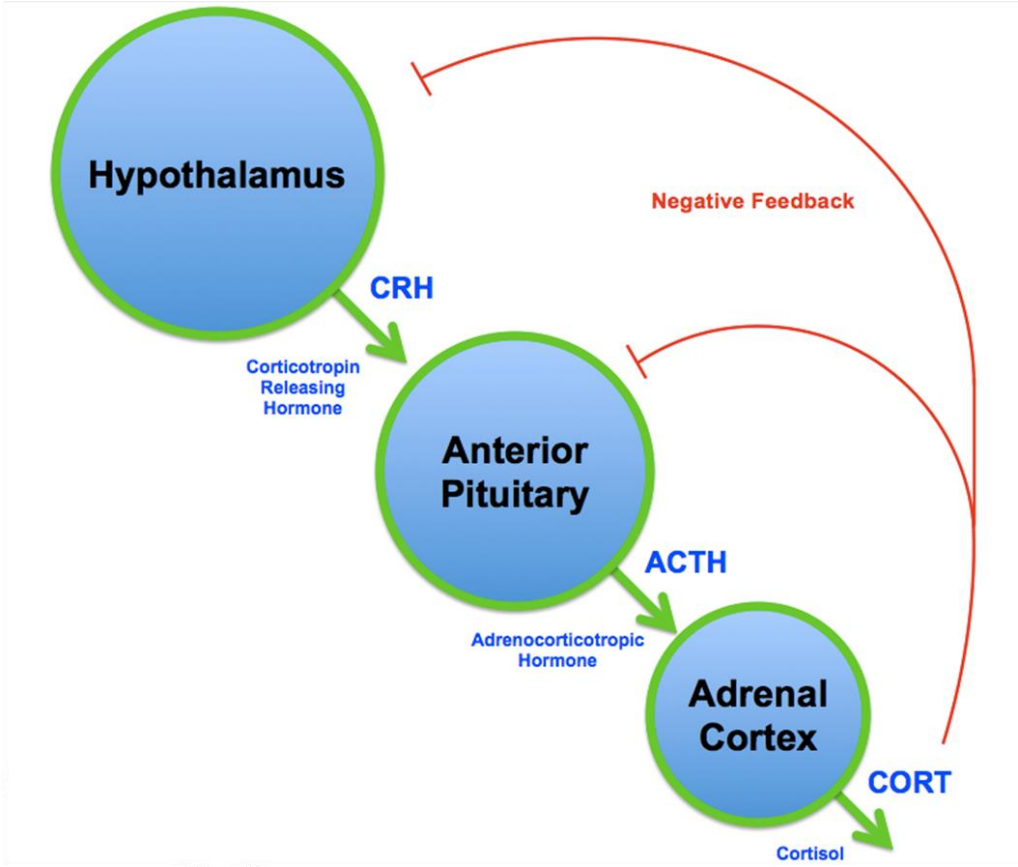

Figure 1.2 Hypothalamic Pituitary Adrenal-Axis (HPA-Axis).
HPA axis regulation of the secretion of cortisol. The hypothalamus releases CRH into the pituitary gland, which in turn releases ACTH from its anterior lobe. The ACTH induces the adrenal cortex in the adrenal gland to release GC.

Cortisol is the active circulating GC, while its precursor is cortisone (Figure 1.3), the inactive form of cortisol found mainly in the kidneys (Joels *et al.*, 2011). The tissue-specific inter-conversion of cortisone and cortisol occurs in the endoplasmic reticulum under the action of two isozymes of 11β-HSD1 and 11β-HSD2 (Campino *et al.*, 2010, Walker, 2006a).

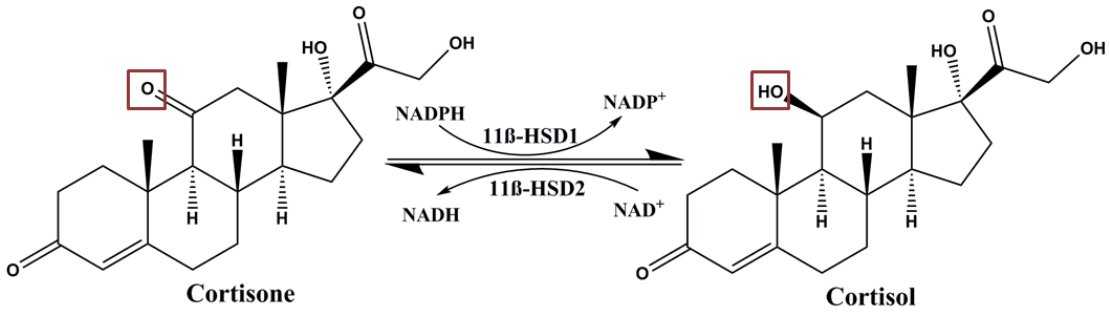

Figure 1.3 Physiological conversion between cortisone and cortisol.
Conversion of cortisone (inactive) to cortisol (active) by the enzyme 11β-hydroxysteroid dehydrogenase 1 (11βHD1), while 11βHD2 converts cortisol to cortisone.

The two isozymes are coded by two distinct genes present in different tissues. The 11β-HSD1 isozyme is present mainly in the liver, kidney, adipose tissue and brain, while the 11β-HSD2 isozyme is mostly present in the kidney and salivary glands (Campino et al., 2010). The inert cortisone is converted to cortisol in humans by 11β-HSD1, while the opposite reaction takes place through the action of 11β-HSD2. A restricted concentration of cortisol is what brings about the activation of the GC receptor (GR), as it is the ligand-induced activation of the GR that mostly produces GC activity. The presence of 11β-HSD1 in tissues like liver and adipose tissue leads to cortisol accumulation due to reduced cortisone and diffusion from circulating levels in the plasma. In the kidney, the level of cortisol is decreased by 11β-HSD2 (Ferrari, 2010). The tissue-specific concentration of cortisol is also maintained by cortisol metabolism in the liver.

1.1 Actions of GC in peripheral tissues

The effects of GC vary from one tissue to another, depending on the activity of glucose transporters and enzymes that regulate the processes of glycogenesis, glycolysis and gluconeogenesis. GC promote hepatic gluconeogenesis and inhibit peripheral utilisation of glucose. Additionally, they promote glycogen synthesis, which is needed for an acute stress response. High levels of GCs also increase the catabolism of proteins (proteolysis) and lipids (lipolysis), thus supplying the resulting amino acids and free fatty acids as substrates for gluconeogenesis in the liver. These effects will be discussed in more detail below.

1.1.1 Muscle

GC modulate protein and glucose metabolism in the skeletal muscle by antagonising the actions of insulin mediated via the insulin/insulin-like growth factor 1 (IGF-1) signalling pathway (Heszele and Price, 2004). Excessive GC activity within skeletal muscles leads to increased catabolism of proteins and reduced protein synthesis, leading to a severe loss of muscle mass known as muscle atrophy or steroid myopathy. Steroid myopathy is recognised as a common feature of Cushing's syndrome and long-term steroid therapy, and is clear proof that excess GCs directly or indirectly promote increased catabolism of skeletal muscle (Vegiopoulos and Herzig, 2007). Patients with steroid myopathy exhibit symmetric weakness in the proximal lower extremities (Batchelor *et al.*, 1997, Weiner *et al.*, 1993).

The breakdown of muscle mass leads to the production of amino acids, which are mobilised by the body to serve as an alternative source of energy as well as precursors for gluconeogenesis and protein synthesis. This occurs due to the increased energy demands of the body under stress and can lead to muscle wasting. This condition has been observed in cancer cachexia, a severe wasting syndrome in the tumour bearing state, which is associated with chronically elevated GC levels. In this condition, the prolonged action of the GC leads to life-threatening weakening of the patients, thereby substantially decreasing their prognosis, quality of life and tolerance to medications and other therapeutic interventions (Tisdale, 2002). Similar effects are observed in other stressful conditions, such as sepsis and starvation, where the chronically elevated GC-induced catabolic effect causes muscle wasting and the resulting body weakness. In some disease states, such as asthma, rheumatoid arthritis and chronic obstructive pulmonary disease, prolonged use of exogenous GC such as HC, dexamethasone and prednisolone can lead to muscle atrophy as a result of increased muscle protein breakdown (Wang and Harris, 2015).

In addition, GC inhibit glucose uptake and oxidation in the muscle and reduce its storage as glycogen. This effect may be mediated via blockade of the insulin/IGF-1 signalling cascade (Heszele and Price, 2004) or suppression of insulin secretion by pancreatic β-cells (Lambillotte *et al.*, 1997). The inhibition of glucose uptake in the muscle increases its availability for other tissues, such as the brain, immune system and, in the case of cancer patients, the tumour (Vegiopoulos and Herzig, 2007).

GC have direct catabolic effects on skeletal muscles through interactions with intracellular receptors to increase glutamine synthase expression, leading to conversion of free muscle amino acids into glutamine for export; and the degree of muscle atrophy correlates with the level of expression of glutamine synthase, a mobiliser of amino acids (Kanda *et al.*, 2001). These effects can be reversed by administration of growth hormone and recombinant number 1 (IGF-1), both of which reduce expression of glutamine synthase (Kanda *et al.*, 1999, Kimura *et al.*, 2001). Also, IGF-1increases signalling by Akt1 (RAC-α serine/threonine protein kinase), resulting in suppression of catabolic pathways, thus inducing muscle hypertrophy (Stitt *et al.*, 2004). GC also decrease the translocation of glucose transporter type 4 (GLUT 4) glucose transporters to the cell surface. The GLUT 4 receptor's role is the insulin-dependent uptake of glucose in the skeletal muscle. Thus, by inhibiting the receptor's translocation to the cell's surface, glucose uptake is prevented in the presence of GCs. These hormones also enhance lipolysis, probably through increased local synthesis of adrenaline (Andrews and Walker, 1999b). By suppressing IGF-1 activity, GC also reduce the synthesis of type I collagen. Additionally, GCs indirectly induce osteopenia by causing a decrease in intestinal Ca^{2+} absorption coupled with increased renal excretion, as well as decreased production of the hormones oestrogen and testosterone (van Staa, 2006, Canalis *et al.*, 2007). The resulting steroid-induced weakness of the muscle makes the patient susceptible to increased falls (Trikudanathan and McMahon, 2008).

1.1.2 Skeleton and bones

GC exert significant effects on the skeleton by inducing increased bone resorption and a progressive decline in bone formation, which particularly affects the trabecular bone (van Staa *et al.*, 2002, McDougall *et al.*, 1994). The resulting decline in bone density results in increased likelihood of bone fractures, which are GC dose dependent. GC also impair the replication, differentiation and function of osteoblasts (Canalis, 2005). There is also an increased rate of apoptosis of osteoblasts and osteocytes because the GCs activate caspase 3, which acts as a key mediator of apoptosis (Liu *et al.*, 2004, O'Brien *et al.*, 2004). This increased apoptotic activity substantially reduces bone formation and makes the bones more fragile. In fact, increased risk of vertebral bone fractures has been observed in post-menopausal women receiving long-term GC therapy (Angeli *et al.*, 2006), but it is not clear whether the risk varies between sexes (van Staa *et al*., 2002). Thus, as a precaution, patients on long-term GC therapy are given prophylactic doses of bone-protection treatment with daily calcium and vitamin D3 supplements; they are also advised not to smoke, to reduce their weight and to avoid alcohol consumption (Eastell *et al.*, 1998). Patients on long-term GC therapy who have additional bone-density risk factors, such as postmenopausal women, are also given bisphosphonate therapy as a preventive strategy against osteoporosis. The bisphosphonate acts to inhibit bone resorption mediated by osteoclasts and to prevent osteocyte and osteoblast apoptosis via the activation of extracellular kinases (Plotkin *et al.*, 1999, Eastell et al., 1998). Risedronate (Wallach *et al.*, 2000, Reid *et al.*, 2000), alfacalcidol and alendronate (de Nijs *et al.*, 2006, Kishimoto *et al.*, 2006, Minisola *et al.*, 2006)

and teriparatide (Saag *et al.*, 2007) are prescribed as preventive therapy for osteoporosis caused by GCs.

1.1.3 Hepatic effects

In addition to promotion of gluconeogenesis and glycogenesis, high levels of GCs have also been associated with the development of non-alcoholic fatty liver disease (NAFLD) as occurs in insulin resistance (Marchesini *et al.*, 2001). This effect might contribute to the condition of hepatic steatosis that is observed in metabolic syndrome (Andrews and Walker, 1999a). In fact, fat accumulation in the liver has been demonstrated in patients suffering from Cushing's syndrome, and various animal models of obesity, dyslipidemia and hepatic steatosis have demonstrated dramatically increased GC levels (Anstee and Goldin, 2006, Alberts *et al.*, 2005). GC treatment also leads to increased hepatic synthesis of triglycerides and decreased oxidation of fatty acids, both of which result in increased accumulation of hepatic lipids, as has been demonstrated in rats (Cole *et al.*, 1982) and in isolated hepatocytes exposed to GC (Mendoza-Figueroa *et al.*, 1988). For this reason, hepatic triglyceride accumulation is inhibited in adrenalectomised rats, particularly in response to high dietary fat intake, an effect that is reversed by replacement therapy with GC (Mantha *et al.*, 1999). Although the mechanisms involved in the development of GC-dependent fatty liver are largely unknown, the increased hepatic lipogenesis and associated increase in very low density lipoprotein (VLDL) production have been attributed to the induction of lipogenic enzymes such as acetyl-CoA-carboxylase or fatty acid synthase (Mangiapane and Brindley, 1986). The

inhibition of mitochondrial fatty acid β-oxidation by GC also promotes the accumulation of lipids intracellularly, which exacerbates the pro-steatotic effect (Letteron *et al.*, 1997). In adipose tissues, NAFLD causes enhanced breakdown of fats to release free fatty acids (FFAs) and glycerol into the blood, as has been confirmed in non-diabetic people with NAFLD using tracer studies (Fabbrini *et al.*, 2008, Bugianesi *et al.*, 2005). The FFAs released into circulation in turn contribute a significant proportion of the total fat deposits in the liver (Donnelly *et al.*, 2005). Insulin resistance as a feature of NAFLD (Gastaldelli *et al.*, 2007) may occur either as a primary outcome or as secondary to enhanced gluconeogenesis induced by increased levels of FFAs and glycerol in the liver (Chen *et al.*, 1999). The condition might be exaggerated in individuals with obesity-induced insulin resistance, a situation that results in the high presence of NAFLD in patients with T2D.

1.1.4 Brain

GC regulate the brain and behaviour, leading to modifications in learning and memory. Regulation of the HPA axis can be a self-repeating process, given that GCs moderate both the initiators and the terminators of the stress response. Thus, stress is necessary for the optimisation of behaviour in response to environmental pressures. Dysregulation of the HPA axis is implicated in the pathogenesis of many diseases, including anxiety and depression (McEwen, 1998). It is of paramount importance to efficiently initiate a stress response, as it promotes survival, while it is equally important to terminate the stress response, as GC are metabolically demanding and can lead to disease. Adverse effects of GC therapy in the brain

include manifestations of emotional lability, psychosis, gain or loss of appetite, insomnia and memory impairments (Wang and Harris, 2015).

1.1.5 Adipose tissue

The adipose tissue is a key endocrine organ in the maintenance of glucose homeostasis and energy balance in the body, and for this reason it plays a key role in the pathophysiology of metabolic syndrome (Minokoshi *et al.*, 2003). The excessive levels of GC observed in patients with Cushing's syndrome are held to be responsible for the obesity observed in these patients (Walker, 2006b). It has also been suggested that hyperactivity of the HPA axis, which leads to high levels of GC in the body, positively correlates with metabolic syndrome, as demonstrated in patients suffering from insulin resistance, hypertension and glucose intolerance (Reynolds *et al.*, 2001). This observation further suggests that GC play a causative role in the obese phenotype. Similarly, treatment with RU38486, a GR antagonist or adrenalectomy, reversed the obese condition in rats (Livingstone *et al.*, 2000). The induction of hepatic gluconeogenesis by GCs necessitates the availability of gluconeogenic substrates such as FFA and amino acids, which can be oxidised to two carbon (2C) acetyl units or other intermediates such as oxaloacetate that can eventually enter the gluconeogenesis pathway to produce glucose. Thus, in order to produce the required free fatty acids for this purpose, GC promote fat catabolism in adipose tissues (Johannsson *et al.*, 2015, Wang and Harris, 2015). The resulting free fatty acids cause hyperlipidaemia, which contributes to risks of adverse cardiovascular effects and impaired lipid homeostasis (Dallman *et al.*, 2000,

Lightman *et al.*, 2008). However, GC exert differential effects in distinct fat deposits. Thus, whereas lipolysis is increased by GC through activation of hormone-sensitive lipase (HSL) and decreased activity of lipoprotein lipase (LPL) in peripheral fat deposits (Slavin *et al.*, 1994), in some sites, such as the face and trunk, higher than physiologic levels of GC promote lipogenesis. This altered fat distribution is observed in Cushing's disease as 'buffalo hump' and round face (Kirk *et al.*, 2000).

1.1.6 Cardiovascular system

Treatment with GCs is associated with increased risk of hypertension, dyslipidaemia, atherosclerosis and cardiovascular disease. It has been suggested that these conditions are partly mediated by the insulin resistance caused by the opposing effects of GCs on carbohydrate metabolism (Andrews and Walker, 1999b).

1.1.7 Gastrointestinal tract

GC increase the risk of gastritis, ulcer formation and gastro-intestinal (GI) bleeding in peptic ulcer disease (PUD). These effects probably arise from an increase in gastric acid secretion induced by the GCs. GC also suppress the protective functions of prostaglandins by inhibiting phospholipase A_2 (PLA_2) in the arachidonic acid pathway through a mechanism similar to that of non-steroidal anti-inflammatory drugs (NSAIDs). For this reason, the risk of GC-induced ulcers is increased in patients who are taking NSAIDS because of their similar effects on PLA_2 (Trikudanathan and McMahon, 2008). There is also increased risk of pancreatitis.

1.1.8 Immune system

In the immune system, GC act as potent suppressors of immune response and thus possess potent anti-inflammatory effects, particularly in pharmacological treatment. Once released into the blood stream, GC induce the proliferation of regulatory T-cells (Tregs) while suppressing helper T-cells (Th cells). Tregs modulate the immune system by maintaining tolerance to self-antigens and preventing autoimmune diseases, while Th cells mediate the activity of other immune cells by releasing T-cell cytokines. The inhibition of Th-cell proliferation can also result from prevention of T-cell recognition of stimulating interleukin signals. GC also impair inflammation by inhibiting the secretion of histamine. Thus, the overall effect of GC on the immune system is immunosuppression, which removes the body's immune protection and leaves it susceptible to infection and disease. These effects render patients suffering from chronic stress who are exposed to high levels of GC highly vulnerable to infections.

1.2 Pathophysiological perturbations

Much of the early work on the role of GC in disease pathogenesis was inspired by two highly insightful observations, one by Dr Thomas Addison, who described a condition of adrenal hormone insufficiency, now known as Addison's disease; and the other by Dr Harvey Cushing, who described an opposite condition associated with excess GC hormone, known as Cushing's syndrome. The fact that adrenal over- or under-performance, which leads to excess or insufficient GC, respectively, are both pathological, contributed to the subsequent development and understanding

of the concept of homeostasis. GC deficiency is characterised by postural hypotension, weight loss and hypoglycaemia, while GC excess is characterised by hypertension, central obesity and glucose intolerance (Andrews and Walker, 1999b) (Table 1.1Table 1.2).

In the normal physiological state, GCs are released according to a circadian rhythm; the highest levels are present in the blood in the morning, while the levels lowest are at night, but under stress, they are produced in quantities of up to ten times the normal amount. Through this controlled release mechanism, the body manages to maintain the levels of cortisol within a physiological range, which is in serum : 09.00 h, 171-536 nmol/L and 00.00h < 50 nmol/L (Addison, 2012), which is required for the body to function properly. In Addison's disease, also known as primary adrenal insufficiency (PAI), the adrenal glands fail to produce sufficient steroid hormones, including cortisol, due to an autoimmune condition such as congenital adrenal hyperplasia (CAH), but it may also arise from tuberculosis infection, especially in the developing world (Arlt and Allolio, 2003). Other causes of PAI may include sepsis, bleeding into both adrenal glands and certain medications. Secondary adrenal insufficiency is associated with a loss of stimulation of the adrenal or anterior pituitary glands due to lack of ACTH from the anterior pituitary gland or corticotropic hormone (CRH) from the hypothalamus, respectively.

On the other hand, GC excess arises from over-stimulation of the adrenal gland as a result of a tumour in the pituitary gland, usually an adenoma, which constantly

releases ACTH into the blood stream even in the absence of stimulation from the hypothalamus (Addison, 2012). This continuous stimulation of the adrenal gland leads to over-production of cortisol. The excessive cortisol in turn causes Cushing's disease. An alternative mechanism for Cushing's disease may be a tumour in the adrenal gland itself, which causes overproduction of cortisol even in the absence of ACTH stimulation.

The lack of specific biomarkers makes clinical management of patients who require GC replacement therapy particularly challenging, and may contribute to well-documented excessive morbidity and mortality in patients with hypopituitarism or adrenocortical failure (Arlt *et al*., 2010, Filipsson *et al.*, 2006, Bergthorsdottir *et al.*, 2006). Moreover, several therapeutic strategies have been proposed to reduce cortisol secretion or action in metabolic and psychiatric diseases. These include inhibitors of cortisol biosynthesis in the adrenal cortex (such as metyrapone), GR antagonists (such as RU38486) (Jacobson *et al.*, 2005) and inhibitors of 11β-HSD1 (Hughes *et al.*, 2008). The complexity of GC action imposes a major limitation on the development of such compounds because of the lack of simple indicators for successful reduction of the cortisol effect. Thus, for example, the efficacy of early 11β-HSD1 inhibitors was not apparent until completion of a Phase IIa study (Hughes *et al*., 2008). For this reason, novel biomarkers for GC action are urgently needed. These may emerge from hypothesis-free screening technologies, including metabolomics.

1.3 Metabolomics

The term ‘metabolomics’ is defined as analytical technique is the ‘un-biased comprehensive identification and quantification of the entire metabolome under a given set of conditions with high selectivity and sensitivity’ (Dunn *et al.*, 2005). The term is derived from the word ‘metabolism’, which itself comes from the Greek word *metabolé*, which means ‘change’. Different researchers have discussed to a great extent the precise definition of metabolomics, but the common theme of these definitions is that metabolomics is concerned with the study of the low molecular weight molecules found in a cell or organism that participate in the biological metabolic functions necessary for the normal functioning of the cell, such as growth and maintenance (Oliver *et al.*, 1998, Harrigan and Goodacre, 2012). These metabolites are themselves end-products of gene and protein expression in cells based on the interaction of the cells with the immediate environment (Fiehn, 2002).

The successful study and application of metabolomics involves various fields in different disciplines, including organic chemistry, analytical chemistry, chemometrics, bioinformatics and bioscience (Fukusaki and Kobayashi, 2005). It can be applied in fields such as medical sciences (diagnosis and treatment evaluation), pharmaceutical research (mechanism of drug actions), microbiology, plant science and food and plant nutrition, among other applications (Kim *et al.*, 2013, Kondo *et al.*, 2011, Al Zweiri *et al.*, 2010, Bundy *et al.*, 2005, Hirai *et al.*, 2004).

1.3.1 Approaches to metabolome analysis

The study of metabolic perturbations associated with different disease states or treatments can be undertaken based on untargeted, semi-targeted or targeted metabolomic profiling (Dunn, 2013). These approaches differ in various aspects, including their quantitative ability (whether absolute or relative), level of experimental precision and accuracy, sample complexity in terms of the number of metabolites involved and the objective of the study.

1.3.1.1 Targeted approach (hypothesis testing)

Targeted approaches already know the identity of one or a few metabolites, in a pathway such as glycolysis, prior to sampling, and the technique is optimised to give high precision, accuracy and selectivity for the targeted analytes, making this approach highly quantitative. Thus, the targeted method utilises the results from preliminary hypothesis-generating untargeted or semi-targeted studies in order to test the hypothesis using robust techniques involving authentic standards. Definitive identification of the significant metabolites allows deductions to be made about their biological relevance in relation to the hypothesis.

1.3.1.2 Semi-targeted approach

The semi-targeted approach, also known as large-scale targeted metabolomics, has the capability to conduct measurements of hundreds of predefined biomarkers. Unlike the targeted approach, the semi-targeted approach applies one calibration curve for a set of biomarkers with a similar chemical structure. Recent

advancements in analytical techniques have narrowed the gap between targeted and untargeted metabolomic profiling.

1.3.1.3 Untargeted approach (hypothesis generating)

Also known as global metabolomics, untargeted methods of profiling provide a means of detecting hundreds to thousands of metabolites with limited or no prior knowledge of the metabolite profile expected in a given sample, for instance, the metabolomic difference between healthy patients and patients with metabolic syndrome. During this procedure, samples are analysed and the resulting data are processed using available tools. The results obtained in turn enable the researcher to derive hypotheses based on the significant observations obtained from the data. This approach involves a lot of metabolites, some of which might not be identifiable, and certainly even those that are identified cannot all be confirmed, as this would require a large number of standards, which is expensive and some standards may not be available.

As a relatively new and emerging field, metabolomics studies have been made possible by advances in analytical techniques and informatics tools, which have enabled rapid analysis of complex samples to generate vast amounts of data that can be analysed and modelled using various software and online-based tools. These technologies have been recently applied in plant, environmental and mammalian systems with the aim of identifying novel biomarkers and understanding possible biological mechanisms resulting from different treatments or genetic alterations (Dunn, 2013).

1.4 Analytical platforms

Early development of metabolomics relied on nuclear magnetic resonance spectroscopy (NMR), which is limited by low resolution for individual metabolites and the limited diversity of analytes detected. However, mass spectrometry has become increasingly applied in this area (van Ginneken *et al.*, 2007, Fardet *et al.*, 2008, Zhen *et al.*, 2007). A major technological breakthrough was the invention of the LTQ Orbitrap Fourier Transform mass spectrometer (FTMS) (Makarov *et al.*, 2006), which offers very high and consistent mass accuracy in combination with the rapid scanning required for compatibility with chromatographic systems (Kamleh *et al.*, 2008). Although a previous study using conventional liquid and gas chromatography with mass spectrometry included limited metabolomic profiling in the urine and plasma of subjects treated with anti-inflammatory synthetic GC (Ellero-Simatos *et al.*, 2012), Orbitrap FTMS had not been applied previously in studies of GC action. With the advancement in analytical techniques, hundreds of metabolite peaks are generated from a biological sample. Visualising and interpreting a metabolomic change is challenging and needs a robust multi- and univariate statistical approach to identify reliable biomarkers.

1.5 Univariate analysis

Statistical analysis deals with one variable and is considered the simplest step in analysing a single variable. Univariate analysis can be inferential or descriptive, but it does not deal with relationships and causation like regression analysis. In metabolomics, a huge number of variables are produced, and one of the aims is to

examine the relationship between the metabolomic change and the intervention. Unlike multivariate analysis, univariate analysis does not provide this important information.

1.6 Multivariate analysis

Recent advances in high data-density analytical techniques offer unrivalled promise for improved medical diagnostics in the coming decade. Genomics, proteomics and metabolomics provide a detailed descriptor of the biology of each individual. Relating the large quantity of data on many different individuals to their current (and possibly even future) phenotype is a task not well suited to classical multivariate statistics. The datasets generated by metabolomics techniques very often violate the requirements for classical multivariate analysis (MVA) (such as multiple regression, samples (N) must be greater than variables (K), the K variables should be noise-free and uncorrelated and the X-matrix should be complete i.e no missing values. For MVA, K can be much larger than N, the K variables can be multicollinear and the X-matrix noisy and incomplete i.e with missing values. However, another statistical approach exists as an alternative to classical statistical treatments that was developed in the early part of this century by Hermann Wold and colleagues and that can overcome these problems. This approach, called multivariate analysis (MVA), has the potential to revolutionise medical diagnostics in a broad range of diseases. It opens up the possibility of expert systems that can diagnose the presence of many different diseases simultaneously, and even make

predictions about the future diseases an individual is likely to suffer from (Grainger, 2003).

Data analysis is comprised of two steps, multivariate analysis followed by univariate analysis. The multivariate step contains two phases, firstly, pattern recognition using unsupervised techniques in order to get an overview of the data and to ensure that it does not contain outliers, secondly, biomarker identification followed by model validation to ensure predictive ability. Prior to starting the steps of data visualisation and biomarkers identification, data should be pre-processed.

1.6.1 Data pre-processing.

1.6.1.1 Missing values

Missing values is of a major concern in metabolomics, in which non-zero values appears in the variables matrix and it would give a misleading result. The cause of missing values may be biological and/or technical (Hrydziuszko and Viant, 2012), which can lead to [1] detection of metabolite in one sample but not in others at any concentration, [2] concentration of metabolite in a sample is below the analytical method's limit of detection, and [3] the metabolite not detected and reported by the data processing software (Di Guida *et al.*, 2016).

Different methods are employed to minimise the effect of missing values. Missing values in each detected metabolite are either replaced with; [1] Small value (SV): the half of the minimum peak intensity, [2] Mean (MN): mean of intensities, [3] Median (MD): median of intensities, [4] K-nearest neighbour imputation (KNN):

mean of nearest 10 non-missing values (Xia and Wishart, 2011), [5] Bayesian Principal Component Analysis (BPCA): employing principal component analysis regression with a Bayesian method to obtain unique replacement values (Hrydziuszko and Viant, 2012), or [6] Random Forest imputation (RF) uses the RF classification to generate adjacent matrix as a source of iterative imputation of missing values (Breiman, 2001). SIMCA-14 software, which used in multivariate analysis in this thesis, employs Non-linear Iterative Partial Least Squares (NIPALS) algorithm as a default to estimate missing values relying on slopes of least squares line that crosses the origin of observed data points.

1.6.1.2 Transformation

Transformation is used to make the data to approach normality when individual variables depart from normal distribution. Thus, transformation make the distribution of the residuals more normal which effectively helps in eliminating outliers (Eriksson *et al.*, 2013g). Many forms of data transformations are used, such as $\log_2$, $\log_{10}$, inverse, neglog, etc., depending on the data to be transformed and this can be examined using normal probability plots (Eriksson *et al*., 2013g) as shown in Figure 1.4. The observations in plot B are situated on the straight line with R^2 =0.98 after $\log_2$ transformation compared to the untransformed observations in plot A which deviate from the straight line with R^2 =0.88.

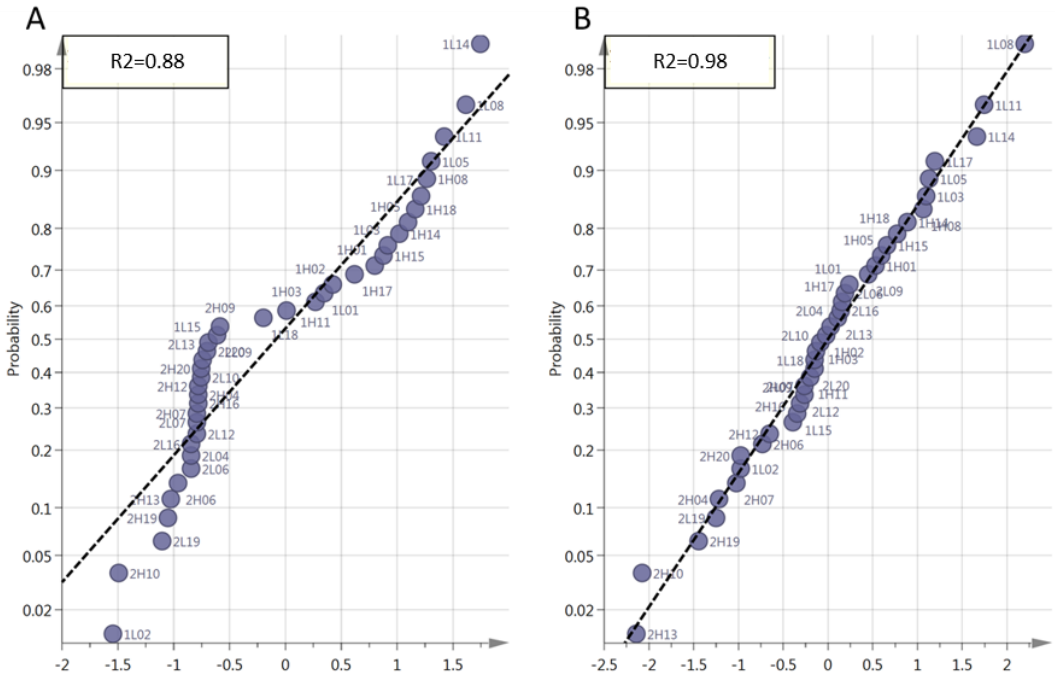

Figure 1.4 Normal probability plot of residuals.
The plot displaying the residuals standardized on a double log scale on y-axis vs standard deviation on the x-axis. Observations lying outside the –4 or +4 standard deviations are outliers. The regression line to assess the normality of the observations. (A) Untransformed variables (B) log2 transformed variables

1.6.2 Scaling

Statistical analysis focuses on metabolites with high intensities giving less weight to those with lower intensities. However,the importance of these smaller metabolites can not be neglected because they might have high biological importance. Scaling is often used in metabolomics to overcome such issues (Xi *et al.*, 2014) and can be performed by: [1] Mean centring, i.e., taking the average of each variable and subtracting it from the intensity of the variable in each row; [2] Univariate scaling, i.e., calculating standard deviation of each variable (column) and dividing it by the intensity of the variable in each row (sample); [3] Auto scaling, which is a combination of univariate scaling and mean centring. Auto-scaling is preferred

when variables have different units, but, it may increase the effect of noise variables on the analysis. To reduce such undesirable effects, [4] Pareto scaling is recommended. Pareto scaling takes the square root of each variable in a column and divides it by the intensity of the variable per row; Pareto scaling is more popular when dealing with spectroscopic data (Xi *et al*., 2014). [5] Block weighting, is another scaling technique where a variable in each row is multiplied by $1/(k_{block})^{1/2}$, where k_{block} = number of variables in that block. This technique is preferred in combination with univariate scaling when variables with different units are analysed and a block of variables with large values will dominate over smaller value blocks (Eriksson *et al.*, 2013a), for instance systolic blood pressure (mmHg) and height (m).

1.7 Data visualisation

1.7.1 Unsupervised Techniques

Due to the nature of the information contained in biological data sets (such as metabolomics data), LC-MS can generate very large amounts of data. As in this research, it is required to establish possible relationships (or correlations) among the various subjects or variables; the greater the amount of information there is to analyse, the higher the difficulty and complexity of obtaining the required results will be. It would be almost impossible to properly examine and analyse the data without appropriate statistical software. Hence, it is necessary to apply suitable statistical methods to increase the chance of identifying any potential similarities or

differences among the various samples in the data, by reducing the dimensionality of the input space of the data to a small number of dimensions.

To classify the samples into groups of similar characteristics, which can give an insight in the situation under investigation, statistical methods such as Principal Components Analysis (PCA) and Cluster Analysis such as Hierarchical Cluster Analysis (HCA) can be used. Samples classified in a group will have similar characteristics, but be different from those in other groups. No information about the groups is known beforehand and no assumptions are necessary concerning the group into which a sample may be classified. These unsupervised pattern recognition techniques aim to reduce the amount of data complexity and afterwards present in a graphical form the patterns or clusters identified in the data (Prelorendjos, 2014).

1.7.2 Principal Component Analysis (PCA)

Principal Component Analysis (PCA) is an unsupervised model employed to explore how variables cluster regardless to which class an observation belongs to (Kirwan *et al.*, 2012). It considered the main tool used by analysts for data reduction to extract meaningful information (Yamamoto *et al.*, 2009). This is achieved by combining variables that correlate with each other into few latent variables (components). The higher the correlation among variables the smaller the number of components that will be needed with components < observations, without losing an important amount of the total variation of the data (Prelorendjos, 2014). PCA is normally

employed as the first step in the analysis of metabolomics data (Kirwan *et al*., 2012, Trygg *et al.*, 2007) in order to visualise data and detect outliers.

1.7.3 Detecting outliers: (DModX and Hotelling's T^2)

Strong and moderate outliers are interesting. Strong outliers can be investigated by Hotllings' T^2 plot while moderate outlier can be found in DModX plot (Figure 1.5). The Hotelling's T^2 plot displays distance of an observation from the origin of the model plane for each observation. Values larger than the 95% confidence limit (orange horizontal dotted line in (Figure 1.5) are suspect, and values larger than the 99% confidence limit (red horizontal dotted line in (Figure 1.5,) can be considered as serious (strong outlier) as for observation P102 in (Figure 1.5A) which pulls the model in a detrimental way (Eriksson *et al.*, 2013e).

DModX is distance of an observation to the model. The critical value of DModX, denoted Dcrit (red vertical dotted line in Figure 1.5, below). Dcrit regulates the size of the area surrounding the data points. Observations with a DModX larger than the DCrit are outliers. When DModX is twice DCrit they are strong outliers. This indicates that these observations are different from the normal observations with respect to the correlation structure of the variables (Eriksson *et al*., 2013e).

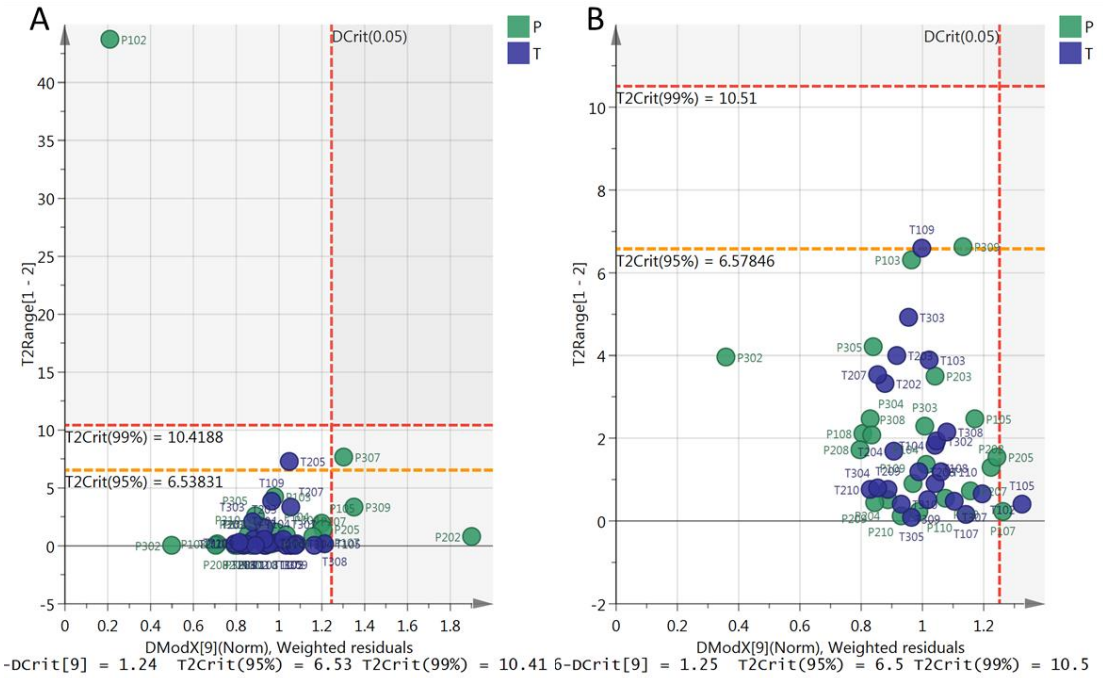

Figure 1.5 Distance to model (DModX) vs Hotellings T^2 plot.
DModX on x-axis versus Hotelling's T2 on Y-axis. Hotelling's T2 has two limits on the y-axis the first T2 Crit(95%) and called warning limit and represented by yellow dotted line, the second limit T2 Crit(99%) called action limit and represented by red dotted line. The red dotted line on the x-axis represents DModX uses critical distance DCrit at level 0.05. Observations considered strong outliers if; above the action limit or above the warning limit plus DModX critical limit. Plot **(A)** showing a model with outlier, plot **(B)** showing the same model after removing the outliers P102 and P202. (P=placebo, T=treatment).

1.7.3.1 Hierarchical Clustering Analysis (HCA)

The concept of HCA or dendrogram –both are used interchangeably- as a clustering analysis tool is to try to find a natural grouping of a data set, so that there is high similarity (low variability) of observations within clustered groups and less similarity (high variability) of observations between clustered groups (Figure 1.6). In HCA clustering, the two closest clusters or observations are merged, thereafter the two closest clusters or points are again merged, until one super cluster remains (Figure 1.6) (Lozano *et al.*, 2014). HCA is extensively used when a study is done with

no previous knowledge about grouping, and is considered a preface for a supervised multivariate techniques.

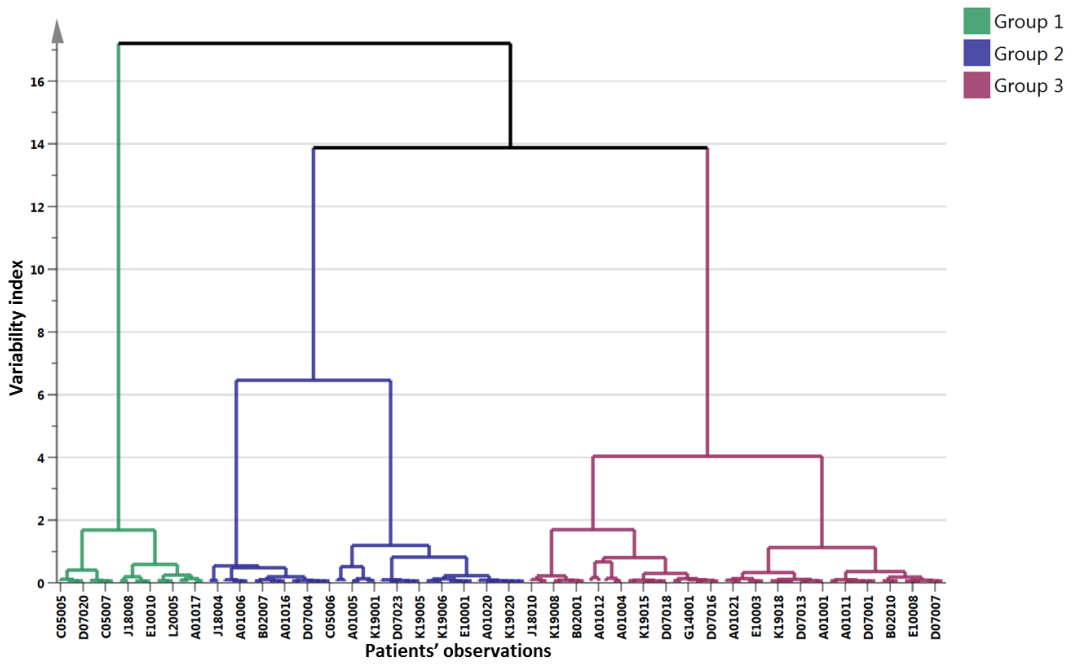

Figure 1.6 Hierarchical Clustering Analysis (HCA) plot.
The dendrogram above shows observations clustered into three groups. X-axis represents patient's observations and y-axis shows variability index. The high the variabilit index the more between groups variability, the small variability index the high within group similarity.

1.7.4 Supervised Techniques

PCA provides an overview of the dataset, but it does not relate the phenotype-disease state for instance- of an individual to the measured parameters. Partial least squares-discriminant analysis (PLS-DA) performs a PCA analysis on the Y-matrix (observations/samples) to yield a small number of latent variables, and then constructs a series of latent variables from the X-matrix (descriptors/variables/metabolites) which explain the maximum variance in these Y latent variables.

Orthogonal partial least squares - discriminant analysis (OPLS-DA) is an extension of PLS-DA model, and has an advantage over the PLS-DA that it can separate variation in *X* that correlates to *Y* (horizontally) called predictive variation, and also separate variation in *X* that is uncorrelated to *Y* (orthogonal) (Figure 1.7). OPLS-DA is a most powerful technique that is employed to examine the difference between groups (Kirwan *et al*., 2012), it can identify reliable biomarkers that have a strong association with separation between groups (Trygg *et al*., 2007) and relate disease to perturbations in metabolic pathways (Goodacre, 2007) and thus help expand our understanding of pathophysiology and future therapeutic targets.

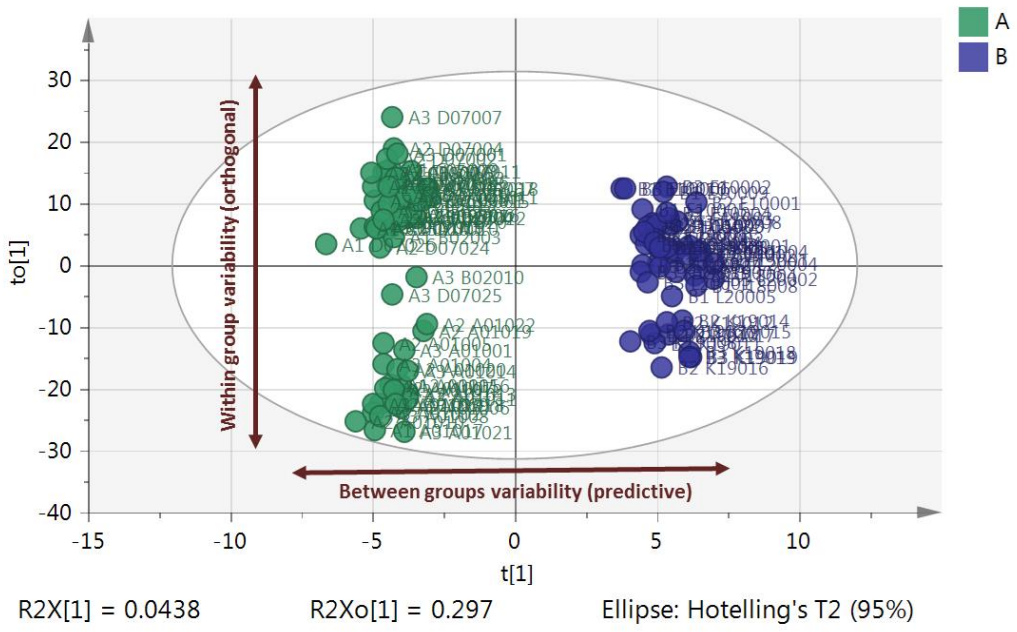

Figure 1.7 Orthogonal Partial Least Square Discriminant Analysis (OPLS-DA) score plot.
The OPLS-DA score plot shows plasma samples of patients receiving either low GC (A-green) or high GC (B-blue). The two groups clearly separated horizontally (t-predictive), within group variability (to, orthogonal) for those receiving low GC dose is higher than those receiving high GC dose. The model explains 4% of the predictive variation (between groups variability) and 29.7% of the orthogonal variation (within group variability).

The quality of a supervised model is assessed by R^2 (the goodness of fit) and Q^2 (the goodness of prediction), and *P* CV-ANOVA (the p-value of the model) from cross-validation procedures which determine the degree of significance of the model (Triba *et al.*, 2015) and are called quality parameters (Wheelock and Wheelock, 2013).

1.7.5 Model validation

During analysis, the quality parameters R^2 and Q^2 are the most powerful tools for validating any applied model. R^2 is a quantitative measure of the goodness of fit, it relates *y* (observations) to *x* (variables), by quantifying the fraction of *y* explained by the variation in *x*. The issue with such a parameter is that it can be made arbitrarily close to one, the maximal value, as long as we increase the number of components. This might lead to over-fitting the data due to the large number of variables compared to small number of observations and thus give too optimistic results. However, this can be controlled by the goodness of prediction parameter Q^2, obtained via cross validation (CV) (Kirwan *et al*., 2012) by which predefined number of observations should be left out and followed by refitting the model. This process, applied to all the data until all have been kept out only once (Eriksson *et al.*, 2013b). Then the average value of the refitted models Q^2 are compared to the R^2 of that model which provides an indication that it predicts much better than chance .

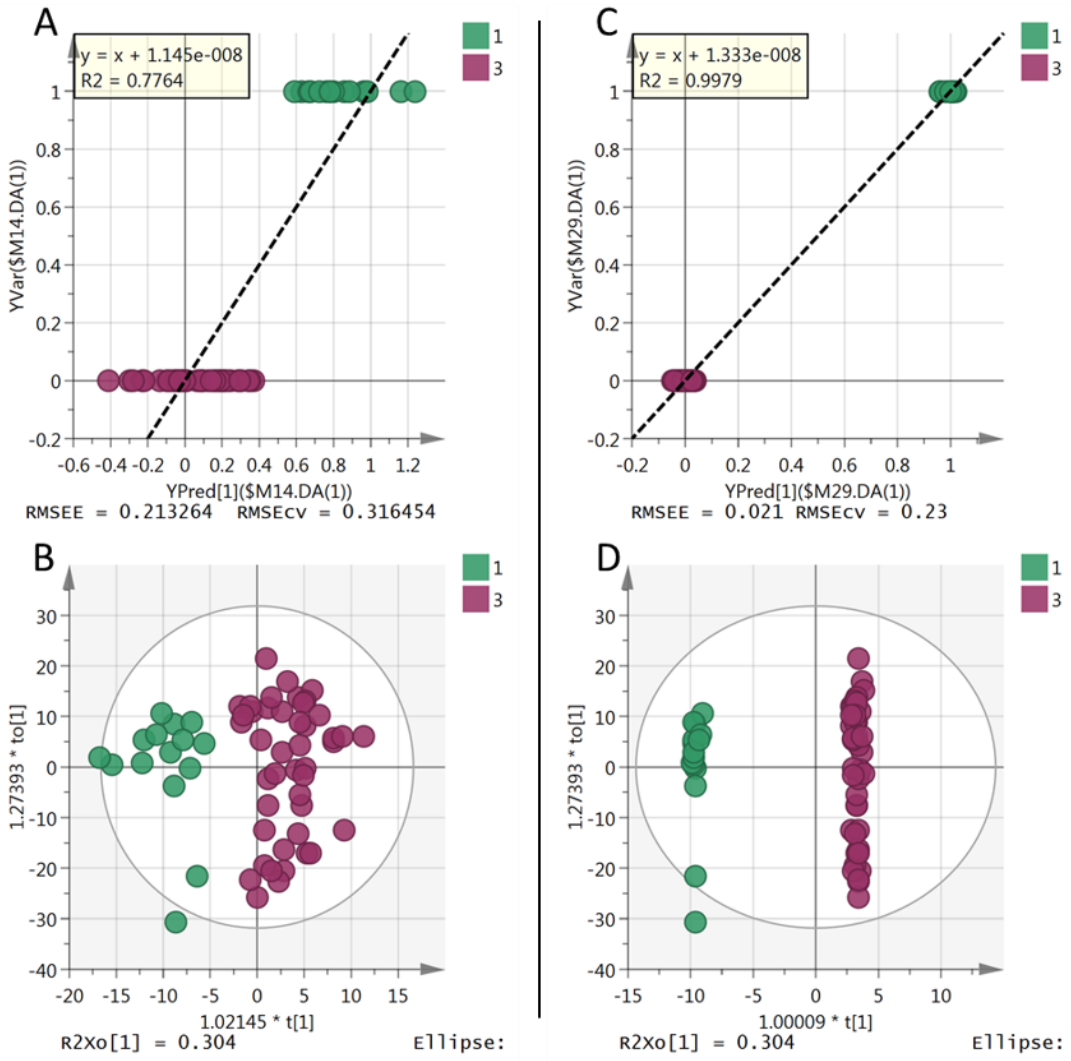

Figure 1.8 Observed vs Predicted plot.
The figure shows (A) Observed vs predicted plot with R^2 = 0.77 based on 7 CV groups (the default) compared to R^2 = 0.99 in plot with C20 CV groups. (B) OPLS-DA score plot showing two groups of observations based on 7 CV groups compared to plot D which showed tighter clustering following to 20 CV groups.

For the purpose of cross validation SIMCA P software - by default - leaves 1/7th of the data out. An observed vs predicted plot is employed to examine the efficiency of CV, by which the R^2 of the regression line should be improved. Plot C in (Figure 1.8) shows better clustering of the observations around the regression line following 1/20th CV with R^2 = 0.99 compared plot A in the same figure in which

observation gave a model with R^2= 0.77. Plot B and D, are score plots of an OPLS-DA model following 1/7th and 1/20th CV, respectively.

Moreover, in order to examin whether a specific classification of observations into two groups is significantly better than any other random grouping in two arbitrary classes, permutations test is applied (Westerhuis *et al.*, 2008).

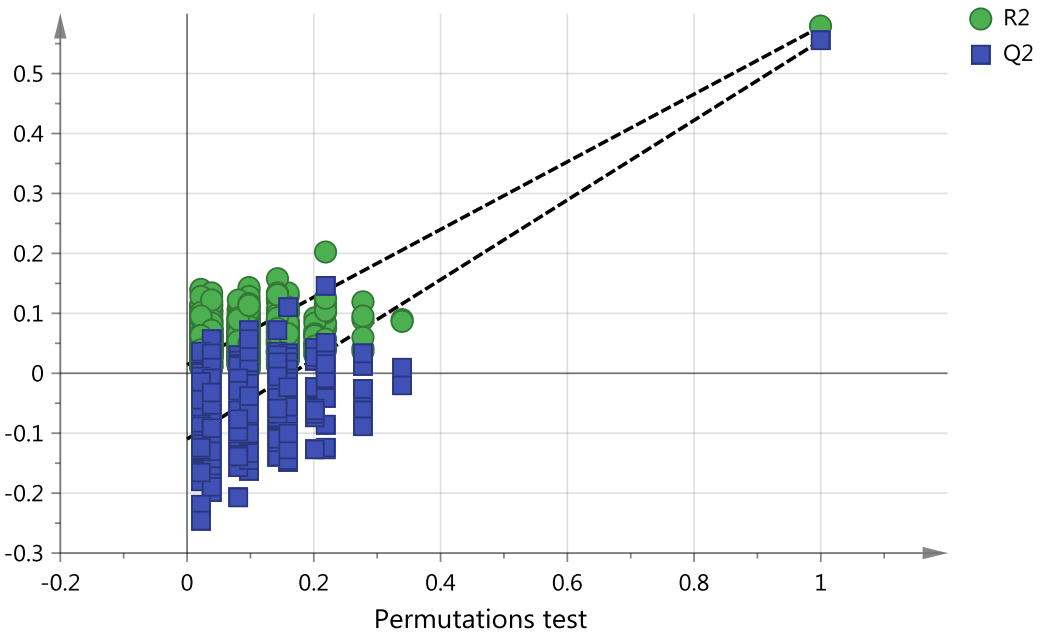

Figure 1.9 Permutations test.
The plot shows, the vertical axis gives the R^2Y and Q^2Y -values of each model. The horizontal axis represents the correlation coefficient between the original Y, which has correlation 1.0 with itself, and the permuted Y. If the supervised model has valid predictive ability, the R^2Y and Q^2Y of the real model are always larger than the corresponding values of the models fitted to the permuted responses.

In this test, the R^2 and Q^2 parameters obtained from the original model are compared to newly permuted R^2 and Q^2, this process can be repeated to generate new quality parameters. The new parameters generated from this permutation should all be lower in value than the original values. In addition to that, the

regression line of the predictive model should cross the horizontal zero line (Figure 1.9) (Eriksson *et al.*, 2013f). In order to test the significance of the variation predicted by the supervised model, Analysis of variance (ANOVA) of the cross validated residuals is employed (CV-ANOVA). Once the predictive ability of the model is validated, then the accuracy of the model in discriminating observations based on their metabolic profile should be assessed and reported using area under the receiver operating characteristic (ROC) curve.

1.7.6 Cross validated ANOVA (CV-ANOVA)

The significance of a supervised model is assessed using cross validated ANOVA (CV-ANOVA), the test examins the variation predicted by the model against H_0 hypothesis of equal cross validated predictive residuals around the mean (Eriksson *et al.*, 2008b).

1.7.7 Receiver Operating Characteristic (ROC)

Area under the ROC curve (AUROCC) is a reflection of how accurate a supervised model is at discriminating between samples/observations sharing the same metabolomics profile and those not. The greater the AUROCC, the more accurate the classifier.

The concept of an ROC is built up on two factors, sensitivity and specificity. Within metabolomics sensitivity of a biomarker is the proportion of individual for whom a biomarker is high that are correctly identified by the test, the specificity is the proportion of individuals for whom the biomarker is not high that are correctly

identified by the test (Bewick *et al.*, 2004). The ROC curve formed by several points of sensitivity and specificity in which the AUROCC is normalised to 1 and used to assess the predictability of the classifier with a rough guide as follow, 0.9–1.0 = excellent; 0.8–0.9 = good; 0.7–0.8 = fair; 0.6–0.7 = poor; 0.5–0.6 = fail (Xia *et al.*, 2013). Figure 1.10 shows an excellent classifier with AUROCC accuracy above 0.9 for all the groups which means that the model was able to determine and predict the metabolomic differences between the three groups with more than 90% accuracy.

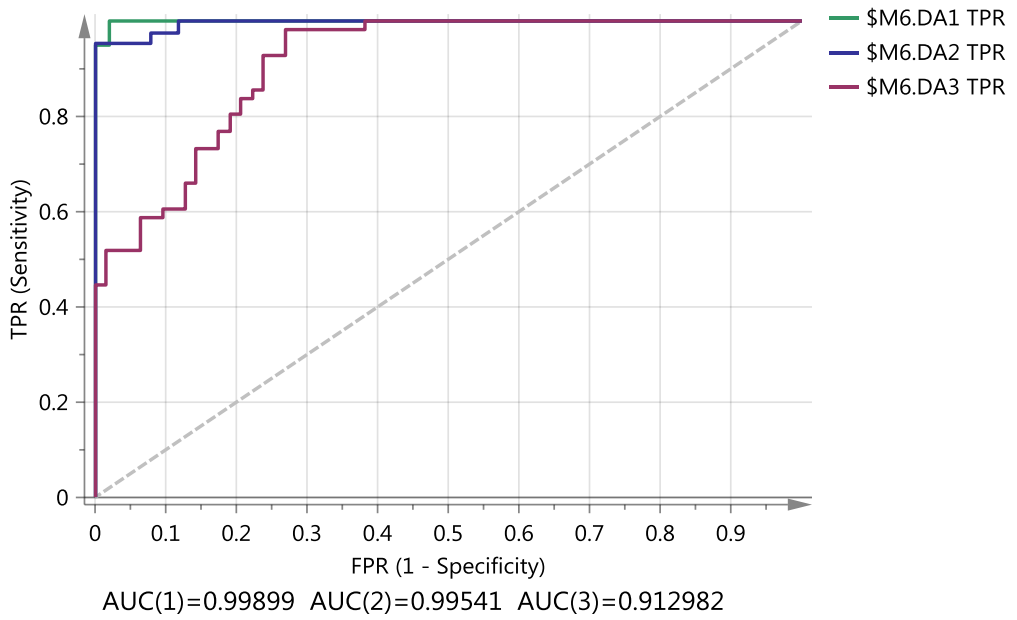

Figure 1.10 Area Under the Reciever Operating Characterestics Curve (AUC).
The ROC curve shows sensitivity (true positive rate (TPR)) on the y-axis versus (false positive rate (FPR = 1 - Specificity)) on the x-axis, the value of both normalised to 1 which represents the value of AUC for group. Three groups of patients with excellent AUC accuracy; (1-green)=0.99, (2-blue)=0.99 and (3-plum)=0.91.

1.8 Biomarkers identification using an S-plot

The S-plot is a tool used to identify biomarkers based on a supervised model. The metabolites far to the upper right and to the lower left are highly associated with difference between assigned groups. Unfortunately, there are no firm cutoffs that one can rely on when selecting metabolites using the S-plot, and also using such vague way of selecting significant metabolites could lead to neglecting other significant metabolites. For instance, L-octanoylcarnitine is a medium chain acyl carnitine which was found positively associated with arterial stiffness in obese individuals (Kim *et al.*, 2015). This significant metabolite was not picked up by the S-plot (Figure 1.11). Based on that it would be preferred to employ univariate analysis at this stage in order to guarantee equal treatment of the metabolites and then fair selection without losing potential biomarkers.

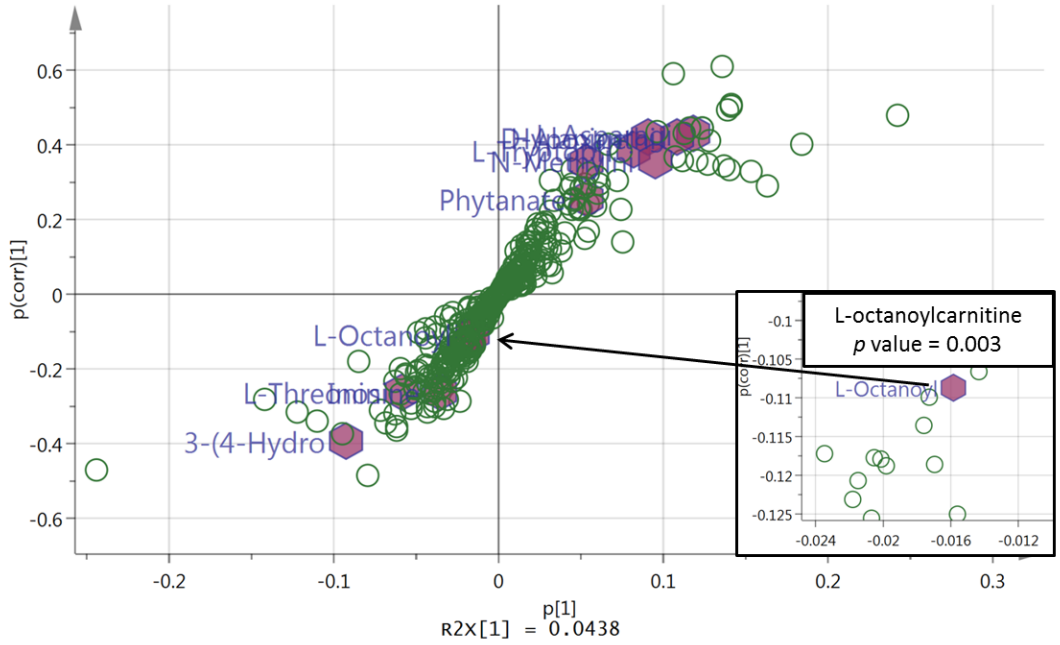

Figure 1.11 S-plot.
The plot shows metabolites distributed according to their correlation (x-axis) and magnitude of effect (y-axis) based on an intervention. Plum hexagonal symbols represent selected significant metabolites that significantly affected by the GC dose. Small box on the down right is for L-octanoylcarnitine.

1.8.1 Variable importance in the projection (VIP)

The contribution of each metabolite in a given model is examined by considering the variable importance in the projection (VIP). This parameter estimates and ranks the importance of each variable (metabolite) in the projection and it is often used for variable selection during metabolomics (Chong and Jun, 2005). Metabolites are generally considered to have a high contribution in the model if VIP > 1 (Eriksson *et al.*, 2013d, Zhang *et al.*, 2016). VIP, provides a value for each metabolite in terms of its contribution to the difference between groups (VIPpred) and its contribution to the within group variability (VIPortho). Metabolites with high VIPpred and low VIPortho values are sensitive and specific.

1.8.2 Corrected p values

The only tool in statistics used to judge the statistical significance of a variable is the p-value, α level = 0.05 is the most used level, which means that there is less than 5% risk this difference may be due to chance. Number of variable (k) has positive relation ship with increased risk of false positive discoveries, this relationship = 1-$(0.95)^k$ (Eriksson *et al.*, 2013c), where k is number of variables. For instance, k = 5 the risk of false positive = 22%, and in order to minimise this risk, bonferroni correction is employed in which the 0.05 α divided by the number of k, for instance when k = 5 the new α level of significance will be 0.01, so any variable above 0.01 will not be significant. In metabolomics variables are in the hundreds so when k = 100, α = 0.0005, this significance level might be acceptable when for example human cells lines are used as a matrix of metabolomics profiling in which almost all the conditions are under control, but in the case of human plasma which is a complex matrix (Dunn *et al.*, 2011), which renders levels of metabolites among individuals of the same group disease/control highly variable and this will affect the significance level of these variables. Based on that, a less stringent tool such as false discovery rate (FDR) (Benjamini and Hochberg, 1995) is preferred for human biological samples.

1.8.3 Jack-knifing (JK) uncertainties

A 95% confidence interval is calculated for each metabolite in the supervised model based on the jack-knife of uncertainty which estimates the prediction error rate based on the cross validation rule used (Efron and Gong, 1983). Jack-knifing is a method for finding the precision of an estimate, and is important for filtering out unreliable metabolites.

1.9 Aims and objectives

1.9.1 First objective

The first objective of this work was to determine the physiological and pathological link between GC and insulin resistance and to assess the therapeutic potential of decreasing cortisol action (via GC blockade) in patients (n=8) with T2D and NAFLDby assessing which metabolic pathways were significantly affected. The GC blockade was achieved by a combination of mifepristone (RU38486), a GC receptor antagonist, with metyrapone, an inhibitor of cortisol biosynthesis. A double blind cross over design was used in which the patients were given either placebo or GC blockade treatment followed by insulin after a 2 weeks washout period. Plasma samples were collected at the end of the treatment period and analysed for metabolite differences in order to examine the effect of insulin after the GC blockade in both groups.

1.9.2 Second objective

The second objective was to identify the biomarkers for GC and insulin action through metabolomic analysis of plasma samples from healthy men (n=20) treated with metyrapone followed by HC (HC) infusion to induce low, medium and high (supra-physiological) circulating cortisol levels. The specificity of the response to GC was assessed through measurements taken before and after insulin infusion, and the interaction between insulin and HC was also examined.

1.9.3 Third objective

To determine the categories of CAH patients at risk of having further chronic diseases through untargeted metabolomic profiling. This was performed by using liquid chromatography-high resolution mass spectrometry (LC-MS) to identify the responsible metabolites in plasma samples from these patients (n=119). The anthropometric (BMI, height, weight, age) and clinical (systolic & diastolic blood pressure and levels of androstenedione & 17-hydroxy progesterone) measurements were assessed for their contribution in patients' clustering and metabolomic differences among groups were examined .

1.9.4 Fourth objective

Another objective for this study was to explore the changes in metabolites that occur at different GC dose cut-offs in order to rationalise preventive measures against increased likelihood of GC-induced adverse effects (n=117). This was intended to also facilitate the establishment of dose cut-offs between physiological replacement required to maintain a normal metabolic state and the pharmacological therapy needed to induce specific responses.

Chapter 2:

Materials and Methods

2 Materials and Methods

2.1 Chemicals and Solvents

HPLC grade acetonitrile (ACN), chloroform and methanol were purchased from Fisher Scientific, UK. HPLC grade water was produced by a Direct-Q 3 Ultrapure Water System from Millipore, UK. AnalaR grade formic acid (98%) was obtained from Fisher Sceintific, UK. Sodium chloride (NaCl), ammonium carbonate, ammonium acetate, ammonium hydroxide solution (30-33%) and all standard compounds used to evaluate the column or develop the methods were purchased from Sigma-Aldrich, UK.

2.2 Sample Preparation

The collected samples were stored at -80°C and thawed at ambient temperature for 1-2 hours before further preparation. Metabolites were extracted by transferring 200 µl of sample to an eppendorf tube with addition of 800 µl of acetonitrile. After vortexing the samples were centrifuged at 8000 round per minute for 10 min. The supernatant was then collected into a HPLC vial as a final solution ready for LC-MS analysis.

2.3 HPLC conditions

2.3.1 Mobile phase solutions for ZIC-pHILIC chromatography

All mobile phase solutions were freshly prepared and stored at room temperature for up to 48 hours. Mobile phase A (20mM ammonium carbonate buffer, pH 9.2) was prepared by addition of 1.92g of ammonium carbonate to 800 ml of HPLC-

grade water followed by adjustment to pH 9.2 with ammonia solution and then more water was added to make the volume up to 1L. Mobile phase B was HPLC-grade acetonitrile only. The column used was a ZIC-pHILIC column (L150 × I.D. 4.6 mm, 5µm, polymeric bead support) from Hichrom Ltd, Reading, UK (Zhang *et al.*, 2013).

2.3.2 Mobile Phase for C18 Chromatography

All solutions were freshly prepared and were stored at room temperature for up to 48 hours. Mobile phase A (0.1% (v/v) formic acid in water, pH 3) was prepared by addition of 1ml of formic acid to 800 ml of HPLC-grade water followed by mixing then was completed to a volume to 1L with additional water. Mobile phase B (0.1% (v/v) formic acid in acetonitrile, pH 3) was prepared by addition of 1ml of formic acid to 800 ml of HPLC-grade acetonitrile followed mixing then was completed to a volume of 1L with more acetonitrile, pH adjusted using pH meter. The column used was an ACE C18-AR (150 × 4.6mm, particle size 5 µm, pore size 100A˚) from Hichrom Ltd., Reading UK (Zhang *et al*., 2013).

2.3.3 HPLC setup

The HPLC was fitted with the appropriate mobile phase components. The auto-sampler needle and sample syringe were flushed with the syringe wash solution (methanol: water, 1:1). The system was initially purged, successively, with 100% of each of mobile phases B followed by A at a flow at 5 ml/min for 5 min in each case. The purge valve was then closed and the selected HPLC column was conditioned

with 50% of mobile phase B at a flow rate of 0.3 ml/min for 10 min. The operating pump pressure was continuously monitored to ensure that it was below 2,000 pounds per square inch (p.s.i). injection volume is 10 ul per sample and chromatographic separations were performed on both ZIC-pHILIC and C18-AR columns by applying two separate linear gradient elutions over 30 min (excluding reequilibration, as shown in Table 2.1 and Table 2.2), column control temperature is off. The mobile phases described in sections 2.3.1 and 2.3.2 above respectively at a flow rate of 0.3ml/min. For both separations, the same operating conditions were employed for the electrospray ionization (ESI) interface which was operated in a positive/negative polarity switching mode. While on the instrument, samples were kept on a vial tray which was set to a constant temperature of 4˚C to avoid any possible degradation of samples.

Table 2.1 Gradient elution programme applied for ZICpHILIC in LC-MS analysis.

Time (min)	Mobile phase A%	Mobile phase B %	Flow rate (ml/min)
0	20	80	0.3
30	80	20	0.3
31	92	8	0.3
36	92	8	0.3
37	20	80	0.3
46	20	80	0.3

Table 2.2 Gradient elution programme applied for C18-AR in LC-MS analysis.

Time (min)	Mobile phase A%	Mobile phase B %	Flow rate (ml/min)
0	95	5	0.3
30	0	100	0.3
35	0	100	0.3
36	95	5	0.3
46	95	5	0.3

2.3.4 Orbitrap Exactive MS setup

LC-MS was performed with an Accela HPLC pump connected to an Exactive (Orbitrap) mass spectrometer from Thermo Fisher Scientific (Bremen, Germany). The quality of data acquired from an instrument has an implication on the accuracy of the deductions that can be made from a study as a whole. Instrument sensitivity was assessed weekly and any residues in the ion source chamber were removed to maintain enhanced sensitivity. This was achieved by sonicating the sample cone and the ion transfer capillaries in a 50:50 (vol/vol) methanol/water solution for 15 min.

The mass spectrometer (MS) was tuned and calibrated in accordance with the manufacturer's specifications using the Thermo Calmix standard solutions. The signals of acetonitrile dimer (2xACN+H) m/z 83.0604 and m/z 195.03765 for caffeine were used as lock masses for positive (PIESI) mode and m/z 91.0037 (2 x formate-H) was used as a lock mass for negative (NIESI) mode, during each analytical run. The MS accuracy was tested using standard analytes with intensities between 10^4 and 10^7 as calibrants. The calibrant peaks were checked to make sure that the mass deviations were less than 3 part per million (p.p.m), otherwise the

instrument was recalibrated to correct the mass errors. The spray voltage used was 4.5 kV for positive mode and -4.0 kV for negative mode. The temperature of the ion transfer capillary was 275 °C and the sheath and auxiliary gases were set at 50 and 17 arbitrary units, respectively. The full scan range was 75 to 1200 m/z for both positive and negative modes with settings of AGC target and resolution as Balanced and High ($1E^6$ and 50,000), respectively.

2.4 Data extraction methods used in processing the files obtained from LC-MS analysis of plasma samples.

2.4.1 mzMatch and IDEOM

All raw data files (Thermo-Xcalibur format) were manually sorted into folders according to study groups. Then they were converted to mzXML files using an open source software: msconvert (proteowizard.sourceforge.net), and polarity split using the mzMatch split function to separate the Exactive's positive and negative ion mass spectra. After this, XCMS was run through R and, using the centwave function, peaks were picked and each individual file converted to peakml format. The settings for the centwave function employed were: mass deviation from scan to scan (< 2) ppm, range for baseline peak width (minimum 5 seconds and maximum 100 seconds), Signal to Noise ratio (3), prefilter intensity (1000), and Mzdiff (0.001). This was followed by running mzMatch to match peaks from each sample to produce a single dataset and group individual peakml files together.

Furthermore, the noise, RSD, intensity and detection filters were run to remove irreproducible signals (Creek *et al.*, 2012). Parameter settings for the mzMatch filters were: mass deviation from sample to sample (5 ppm) and RT deviation from sample to sample (0.5 min). If there was a large shift in retention times, the signal intensities would not be comparable and the datasets would not make sense. MzMatch filtrations were: [1] RSD filter (0.5), where peak reproducibility was assessed by the RSD of peak intensities for each group of replicates; [2] noise filter (0.8), where peak shape was assessed by CoDA-DW score (0-1); [3] intensity filter (3000), where features were removed if no sample had a peak above the intensity threshold; and, [4] detection filter (3), where peaks must be present in a minimum number of samples. In addition, mzMatch fills the gap using PeakML Gap-Filler which fills gaps in the peak intensity table for peaks which may fall off during the process. Finally, IDEOM was used to filter the data further, and then the metabolites were compared and identified (Creek *et al*., 2012).

IDEOM is a Microsoft Excel template enabled for automated data processing of high resolution LC-MS data from untargeted metabolomics studies (Creek et al., 2012). In IDEOM, more noise filtration is achieved and the authentic chemical standard is matched with a sample metabolite. It is necessary to update DB with retention times using a list of retention times from authentic standards (≈180 standards) run with each experiment; this list is created using Toxid (which is an automated compound identification tool that dramatically simplifies processing of LC/MS data and identifies compounds according to retention time and chemical formula). The

retention time calculator also uses physiochemical properties (depending on the functional group and chemical formula of compounds) in the DB sheet to predict retention times based on a multiple linear regression model with the authentic standards. The retention time calculator uses the Quantitative Structure Retention Relationships (QSRR) approach to predict retention times based on the known retention times of authentic standards and the physicochemical nature of the interactions of analyte with columns that determine retention times (Creek *et al.*, 2011). In this thesis, level (2) putatively annotated compounds and level (3) putatively characterised compound classes were used to identify metabolites according to Metabolomic Standard Intiative (MSI) are level (Sumner *et al.*, 2007). Identification of more accurate putative metabolite requires more filtration of mzMatch files. The blank run with the study group to filter all intensities in a study group must be greater than that in the solvent blanks to remove contaminants. Other filters for noise, such as RSD, intensity and detection filters, are repeated. Chromatography filters, shoulder peak filter and duplicate peak filter, are also applied in IDEOM. Identification of metabolites is performed by matching the accurate mass (accurate mass error for mass identification with DB < 3ppm is suitable for formula identification from a biochemical database with unique entries in DB of 97%) and retention time (RT for identification of authentic standards is 5%) of detected metabolite peak to metabolites in the database. Final lists of identified and rejected peaks are annotated with confidence level from 0 to 10 (10 = most confident) according to the identification of each metabolite; confidence < 5 is

rejected as false identification and metabolites matched with the retention times of authentic standards are identified metabolites and highlighted yellow.

2.4.2 Data bases used for identification

- KEGG Kyoto Encyclopedia of Genes and Genomes (http://www.genome.jp/kegg/)
- HMDB Human Metabolome Data Base (http://www.hmdb.ca/)
- METACYC Metabolic Pathway Database (http://metacyc.org/)
- LIPID MAPS (http://www.lipidmaps.org/)

2.5 Metabolomics profiling

2.5.1 Statistical softwares used

All data processing, including data visualisation, biomarker identification, diagnostics and validation, was implemented using SIMCA software v.14 (Umetrics AB, Umeå, Sweden) for multivariate analysis (Zhang et al., 2016). Metaboanalyst 3.0 **(www.metaboanalyst.ca)** (Xia *et al.*, 2015) and IBM SPSS Statistics software package version 22.0 (IBM SPSS, Chicago, IL) were employed for univariate analysis**.**

2.5.2 Pre-treatment

Prior to multivariate analysis, LC-MS data was log transformed (base 2) and then Pareto scaled for variance (Par) so that the responses for each variable were centred by subtracting its mean value and then divided by the square root of its standard deviation.

2.5.3 Pooled samples

Pooled plasma samples were prepared by taking 20 µL aliquots from 10 randomly selected non-extracted plasma samples, metabolites were extracted by transferring the 200 µl to an eppendorf tube with addition of 800 µl of acetonitrile. After vortexing the samples were centrifuged at 8000 round per minute for 10 min. The supernatant was then collected into a HPLC vial as a final solution ready for LC-MS. The instrument was set to inject a pooled sample through out the run, the pooled sample had at least 4 readings. To quantify the precision of the measurements, the relative standard deviation (RSD) was calculated between the 4 pooled samples based on total intensities in each sample and an RSD must not exceeds 15%. RSD was also calculated for each of the putatively identified metabolites among the pooled samples, metabolites with RSD >15% were rejected. RSD applied as the last filter following corrected p value, 95%CI and AUC. Metabolites were removed if only detected in less than 80% of the biological samples in each defined group.

2.5.4 Data visualisation and biomarkers identification

Prior to modelling the LC-MS data, Hotelling's T^2 and DModX limits were employed to detect sample outliers which might affect the whole model. Samples were removed from the model if they were above the 99% red line (action limit) of Hotelling's T^2 or if they exceeded the 95% orange line (warning limit) of Hotelling's T^2 plus Dcrit (critical limit) of DModX (Eriksson *et al*., 2013e). Principal Component Analysis (PCA), an unsupervised model, was employed to explore how observations

clustered based on their metabolic composition regardless of their grouping (Kirwan et al., 2012, Ivosev *et al.*, 2008). On the other hand, orthogonal projections to latent structures-discriminant analysis (OPLS-DA), a supervised model, was employed to examine the differences between groups while neglecting the systemic variation (Kirwan et al., 2012). The *p* values of the biomarkers were corrected using false discovery rate (FDR)(Benjamini and Hochberg, 1995, Ruxton and Beauchamp, 2008). Variable importance in the projection (VIP) was employed to assess the contribution of each variable in the observed metabolomics change to a given model compared to the rest of variables (Eriksson *et al.*, 2013h, Chong and Jun, 2005). VIP, divided into VIPpred, which represent contribution of a metabolite to the difference between groups compared to other metabolites, and VIPortho, which indicates contribution of a metabolite to variability within group compared to other metabolites in the same model. The average VIP is equal to 1; thus a variable with VIP larger than 1 has more contribution in explaining *y* and vice versa (Eriksson et al., 2013h). The 95% confidence interval was calculated for each metabolite based on jack-knife of uncertainty which estimates the prediction error rate based on the cross validation rule used (Efron and Gong, 1983). Correlation coefficient of a metabolite to high dose of GC used to evaluate reliability of a metabolite (Wiklund *et al.*, 2008). Metabolites were then filtered based on their p-values and 95% CI so that all metabolites with p-values > 0.05 and/or 95% CIs crossing the zero point were filtered out.

2.5.5 Diagnostics and validation

R^2 and Q^2 were employed as diagnostic tools for supervised and unsupervised models. The R^2 represents the percentage of variation explained by the model while Q^2 indicates the percentage of variation in response to cross validation (Kirwan et al., 2012). In the process of cross validation SIMCA-P, by default, leaves out $1/7^{th}$ of the data, and then examines the appropriateness of the cross-validation by plotting Y observed vs Y predicted. The R^2 value of the regression line in the plot represents the strength of the association between the observed and predicted Y values; the closer to unity, the stronger is the association. The R^2 value was used to choose the number of latent variables (orthogonal axis) (Xi et al., 2014). On the other hand, permutations test was applied to both supervised models to evaluate whether the specific grouping of the observations in the two designated classes was significantly better than any other random grouping in two arbitrary classes (Westerhuis et al., 2008). Model validity was also assessed using CV-ANOVA which corresponds to H_0 hypothesis of equal cross validated predictive residual of the supervised model in comparison with the variation around the mean (Eriksson *et al.*, 2008a). The AUROCC was used to assess the accuracy of the classifier with a rough guide as follow: 0.9–1.0 = excellent; 0.8–0.9 = good; 0.7–0.8 = fair; 0.6–0.7 = poor; 0.5–0.6 = fail (Xia *et al*., 2013).

2.5.6 Putative biomarker selection workflow was as follow:

1. The metabolites were filtered based on their p-values and 95% CI of mean difference; if a metabolite had a p-value > 0.05 and/or its 95% CI crossed 0, then it was filtered out.
2. All significant metabolites were processed using Metaboanalyst in order to get corrected p-values and AUROCC; if the metabolite had an p > 0.05 and/or AUC < 0.6, it was filtered out.
3. Where there were two interventions in the study, for instance GC blockade and insulin dose, the interaction between the two interventions was examined using suitable univariate statistical tests such as Two-Way repeated mesurements ANOVA. The specific tests used in each study have been stated in the subsequent chapters wherever applicable.

Chapter 3:

Studying the effect of acute GC blockade on metabolic dysfunction in patients with T2D using metabolomics

3 Effect of acute GC blockade on metabolic dysfunction in patients with T2D using metabolomics

3.1 Abstract

Background and Aim: Supraphysiological levels of GC have a strong association with the development of metabolic syndrome which is composed of T2D and is commonly associated with dyslipidemia, obesity and often hypertension. These complications contribute to the development of cardiovascular disease. This study examined the role of acute GC blockade on metabolomic changes in patients with T2D and its role in improving insulin sensitivity.

Methodology: Untargeted metabolomics profiling, using LC-MS, of plasma samples from 8 men with T2D. The participants had been subjected to a randomised, double-blinded, placebo-controlled crossover study of acute GC blockade using the GC receptor antagonist RU38486 and a cortisol biosynthesis inhibitor.

Results: GC blockade significantly increased plasma levels of bile acids and their conjugates, and significantly decreased phosphocholines. Compared to placebo, GC blockade reduced endothelial dysfunction mediated via insulin through L-arginine metabolism, and significantly reduced some bile acids and 2-methylbutyroylcarntine. Fatty acid levels reduced significantly upon insulin injection following GC blockade compared to placebo.

Conclusion: GC blockade improves the effect of insulin in lowering plasma levels of bile acids.

3.2 Introduction

T2D is a widespread chronic disease worldwide. Half a billion people are expected to be affected by the disease by 2030 (Klein and Shearer, 2016). Chronic complications developed during progression of the disease are diverse, ranging from insulin resistance to cardiovascular diseases (Smyth and Heron, 2006). Insulin stimulates lipogenesis in liver, muscle and adipose tissues and promotes its storage. Insulin induces synthesis of protein and glycogen, and inhibits lipolysis. Insulin resistance dysregulates these functions (Saltiel and Kahn, 2001) which leads to hyperglycaemia that can result in various complications such as neuropathy, retinopathy and nephropathy (Dunn, 2013).

Metabolic syndrome can manifest itself in hepatic tissues as NAFLD which is also an indicator for insulin resistance (Marchesini *et al*., 2001). In adipose tissues, the latter causes enhanced breakdown of fats to release free fatty acids (FFAs) and glycerol into blood as has been confirmed in non-diabetic people with NAFLD using tracer studies (Fabbrini *et al*., 2008, Bugianesi *et al*., 2005). The FFAs released into circulation in turn contribute a significant proportion of the total fat deposits in the liver (Donnelly *et al*., 2005). On the other hand, insulin resistance as a feature of NAFLD (Gastaldelli *et al*., 2007) may occur either as a primary outcome or secondarily to enhanced gluconeogenesis induced by increased levels of FFAs and glycerol in the liver (Chen *et al*., 1999). The condition might be exaggerated in

individuals with obesity-induced insulin resistance, a situation that results in the high presence of NAFLD in patients with T2D.

Evidence suggests that anti-diabetic treatments which improve insulin sensitivity such as metformin and thiazolidinediones also reduce hepatic triglyceride content in patients with NAFLD (Shyangdan *et al.*, 2011), although the effect is generally modest. For this reason, new approaches with higher efficacies are urgently required. One such approach is to decrease GC activity in both the adipose tissue and liver, thus minimising lipolysis and gluconeogenesis in these two tissues, respectively (Macfarlane *et al.*, 2008a, Andrews and Walker, 1999b). As the most important GC in humans, cortisol is the key target for anti-GC therapy. However, lowering the circulating levels of cortisol in the body might be problematic since it can lead to adrenocortical crisis during periods of increased stress. This challenge can be overcome by selectively lowering cortisol in the liver and adipose tissues through inhibition of 11β-HSD1, an enzyme that amplifies local activation of GC receptors through the conversion of cortisone, which is inactive, to cortisol, an active form (Rosenstock *et al.*, 2010, Feig *et al.*, 2011). In doing so, 11β-HSD1 contributes extra-adrenal cortisol to the liver and adipose tissues, thus increasing the risk of NAFLD (Morgan and Tomlinson, 2010, Stimson *et al.*, 2009).

The activity of 11β-HSD1 has been found to be increased in adipose tissues and sustained in livers of obese patients with T2D (Stimson *et al.*, 2011, Rask *et al.*, 2002). For this reason, this enzyme has been targeted as a means to improve insulin

sensitivity in these patients. However, based on 3 months' treatment in patients with T2D, the efficacy obtained with 11β-HSD1 inhibitors towards glycaemic control was not sufficient to support their commercial viability as anti-diabetic medications. In order for these types of medications to have commercial value, new therapeutic indications need to be identified, such as NAFLD. Based on preclinical studies in transgenic mouse models, 11β-HSD1 overexpression in adipose tissues and liver leads to the development of fatty liver (Paterson *et al.*, 2004, Masuzaki *et al.*, 2001), while its inhibition decreases liver fat content (Berthiaume *et al.*, 2007). However, it is not clear if non-diabetic patients with NAFLD would benefit from 11β-HSD1 inhibition since some studies in these patients have found low levels of 11β-HSD1 in the adipose tissue and liver (Ahmed *et al.*, 2012, Konopelska *et al.*, 2009, Westerbacka *et al.*, 2003), although cortisol levels were elevated (Zoppini *et al.*, 2004).

Many metabolomics studies have been applied to uncover metabolic dysregulations associated with T2D (Guasch-Ferre *et al.*, 2016). For instance, in the Framingham Heart Study with more than 12 years of follow up, lipid profiling using LC-MS was carried out on plasma samples of 189 participants who developed T2D and 189 matched controls. The authors reported that the risk of prediabetes and diabetes increased with increase in levels of lipids with lower numbers of double bonds and lower numbers of carbon atoms (Rhee *et al.*, 2011). Metabolomics studies have also reported an association between high levels of branched chain amino acids (BCAs) and diabetes (Wang *et al*., 2011a), and also with insulin resistance (Wang et al.,

2011a, Roberts *et al.*, 2014, Newgard *et al.*, 2009). In a study of 2,422 participants followed up for 12 years, 201 of them developed diabetes, and this was associated with high levels of BCAs (Wang *et al*., 2011a). A replication study of 163 case-controls was performed and reported the association of BCAs with the incidence of diabetes.

However, no metabolomics study has been performed to assess the therapeutic potential of decreasing cortisol action on improving insulin sensitivity. In the current study the metabolomic effects of different doses of cortisol were evaluated in 8 patients with T2D and NAFLD to determine which metabolic pathways were significantly affected. This group of patients was selected based on the fact that they are a potential target for longer term interventions to decrease cortisol activity. A GC blockade approach (Wake *et al*., 2007a), was employed through a combination of RU38486 and metyrapone (Wake *et al.*, 2007b). A double blind cross over design was used in which the patients were given either placebo or GC blockade treatment followed by insulin after a 2 weeks' washout period, in order to examine the effect of insulin after the GC blockade treatment in both groups. Plasma samples were collected at the end of the treatment period and analysed for metabolite differences.

3.3 Methodology

3.3.1 Participants and sample collection

Fourteen male patients with T2D were recruited from Edinburgh Royal Infirmary diabetes clinic. Inclusion criteria included: age 20 – 70 years; glycated haemoglobin (HbA1c) <8% (64mmol/mol); Body mass index (BMI) <40 kg/m^2; negative tests for hepatitis B and C; general health good; normal screening blood tests (full blood count, renal function, electrolytes, thyroid function, ferritin); alcohol intake <20 units/week; no medications known to increase fat deposition in the liver, e.g. nucleoside analogues, methotrexate and amiodarone; no medications known to interfere with lipolysis, e.g. beta blockers; and no GC use in the last 6 months. All patients were receiving treatment with a single oral anti-diabetic agent (metformin) and primary prevention with a statin. Importantly, neither metformin nor statins influence fatty acid turnover. Fat mass was measured by bioimpedence (Body fat Monitor BF302, OMRON Healthcare (UK) Ltd, Henfield, UK). Local ethical committee approval and written informed consent were obtained (Macfarlane *et al.*, 2014).

3.3.2 Study design and protocol

Participants entered a two phase randomised double-blind placebo controlled crossover study of GC blockade. In the active phase, subjects took 400mg RU38486 (mifepristone, Exelgyn, Henley-on-Thames, UK) and 1g of metyrapone (metopirone, Alliance Pharmaceuticals, Chipenham, UK) at 2300h the evening before and at

0800h on the morning of the study, as previously described (Wake *et al*., 2007a). Study visits were separated by a wash out period of at least two weeks.

Subjects received primed infusions of 1,1,2,3,3-$^{2}H_5$-glycerol (1.6 µmol/kg for 1 min, then 0.11 µmol/kg/min) and 6,6-$^{2}H_2$-glucose (17.6 µmol/kg for 1 min, then 0.22 µmol/kg/min), as well as $^{13}C_1$-palmitate infused at 0.04µmol/kg/min. Given the short time required to reach steady state with the palmitate tracer, the palmitate infusion was interrupted during the study to reduce the volume of 20% (w/v) albumin infused. Blood samples were taken at baseline (1), between 60-90mins (2), and at 210-240mins (3), the latter during the final 30mins of a low dose (10mU/m^2/min) hyperinsulinaemic-euglycaemic clamp to investigate suppression of lipolysis and endogenous glucose production. Euglycaemia was maintained by a variable rate infusion of 20% (w/v) dextrose if necessary.

3.3.2.1 Patients numbering

Each patient had a number of 4 characters, first character was either placebo (P) or GC blockade treatment (T) phase, the seconed character was either (1) baseline, (2) pre-insulin or (3) post-insulin. The last two characters represented the patients' number. For instance P302= first character (P) represent placebo, second character (3) represents the time point of sample collection which here represents post-insulin. The last two characters (02) represents the patient's number.

3.3.3 LC-MS analysis

- LC-MS conditions and sample preparation are reported in detail in sections 2.1-2.3 (pages: 47-51).
- Columns used in this project were ZICpHILIC and C18-AR.

3.3.4 Data extraction and processing

These details have been reported in section 2.4 (pages: 51-54).

3.3.5 Data analysis

Most of the details of data analysis are reported in section 2.5 (pages: 54-58). Two-way repeated measurements ANOVA was employed on putative metabolites that showed significant changes following administration of insulin, GC blockade, or both. The test was conducted to examine the difference between baseline, pre-insulin and post-insulin as repeated measurements in each intervention (placebo or GC blockade) separately. In addition, it tested the difference between GC blockade and placebo as paired plus the interaction between GC blockade and insulin dose.

3.4 Results

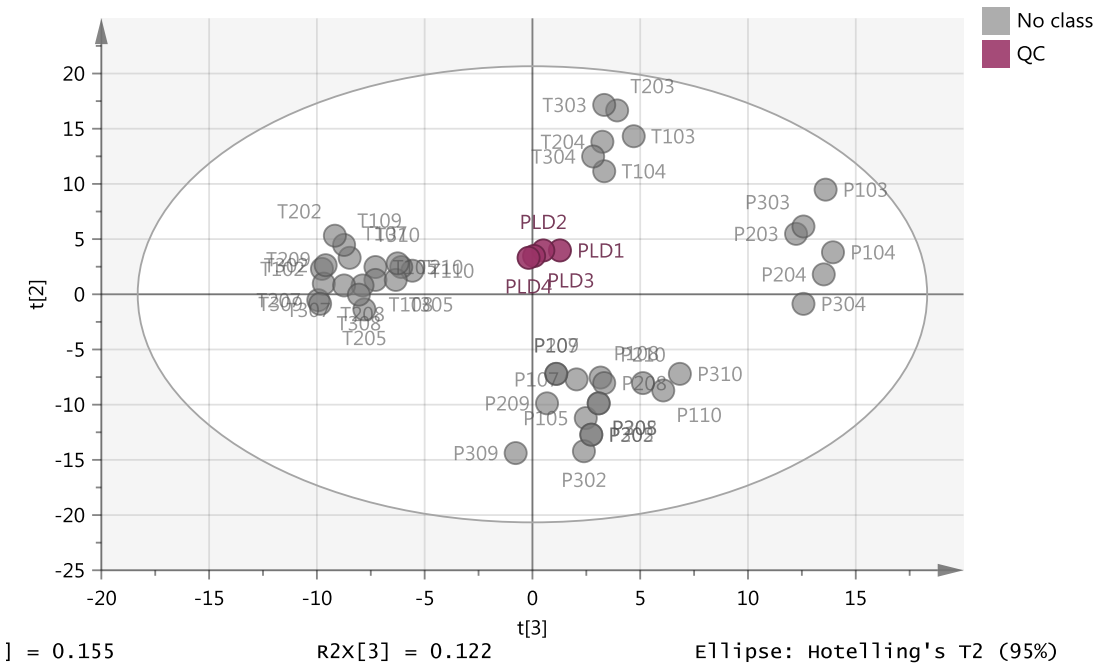

Figure 3.1 2D PCA score plot for QC (pooled) plasma samples of patients with T2D.
The plot shows the clustering of pooled samples (plum-QC) compared to the rest of plasma samples (grey-No class) of patients with T2D. Samples numbering are (P) placebo, (T) GC blockade treatment phase, the seconed character (1) baseline, (2) pre-insulin or (3) post-insulin, The last two characters represents the patients' number..

The instrument was set to inject a pooled sample after every 15 plasma samples, thus the pooled sample had 4 readings (Figure 3.1, above). To quantify the precision of the measurements, the relative standard deviation (RSD) was calculated between the 4 pooled samples based on total intensities in each sample and an RSD of 0.2% was obtained. RSD was also calculated for each of the putative biomarkers in the pooled samples and the highest RSD was for N-(tetracosanoyl)-sphing-4-enine (66.68%) followed by S-(3-oxo-3-carboxy-n-propyl)cysteine (13%) while the lowest RSD was for dihydroxyoctadecanoic acid (0.04%). The precision of these values clearly indicates that any metabolomic differences between groups cannot be due to instrumental factors alone. None of the metabolites were removed based on the RSD.

3.4.1 *Data visualisation*

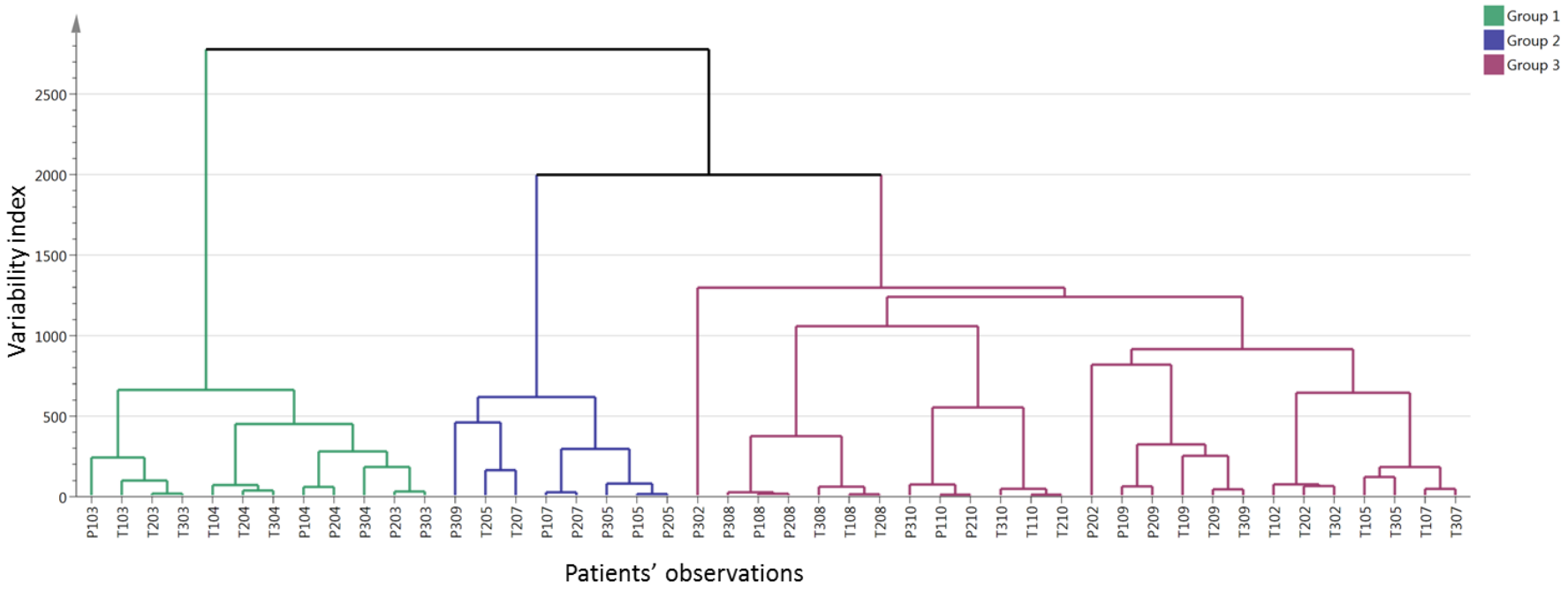

Figure 3.2 Hierarchical Clustering Analysis (HCA) plot for patients with T2D having placebo and GC blockade.
The dendrogram shows observations clustered into three groups. X-axis represents the samples and y-axis shows the variability index. The higher the variability index the larger the between group variability and the lower the similarity index, the smaller the between group variability. The plot divides samples into three groups; group 1 (green), group 2 (blue) and group 3 (plum). Characters on the x-axis are (P) placebo, (T) GC blockade treatment phase, the seconed character (1) baseline, (2) pre-insulin or (3) post-insulin, The last two characters represents the patient's number.

A hierarchical clustering analysis (Figure 3.2) shows that samples clustered into three groups. Inter-individual variability played a major role in the clustering pattern in group 1, for instance, all the samples in the groups belonged to patients number 3 and 4. Nevertheless, 75% (6 out of 8 samples) in group 2 were patients having placebo, on the other hand, 61.1% (16 out of 26 observations) in group 3 were accounted for by patients having GC blockade treatment (Table 3.1).

Table 3.1 Shows proportions (%) of HC and insulin doses based on the HCA grouping.

HCA grouping	Samples (n)	Placebo			Treatment		
		Baseline	Pre-insulin	Post-insulin	Baseline	Pre-insulin	Post-insulin
1 (Green)	12	16.67	16.67	16.67	16.67	16.67	16.67
2 (Blue)	8	25	25	25	0	25	0
3 (Plum)	26	11.54	15.38	11.54	23.08	15.38	23.08

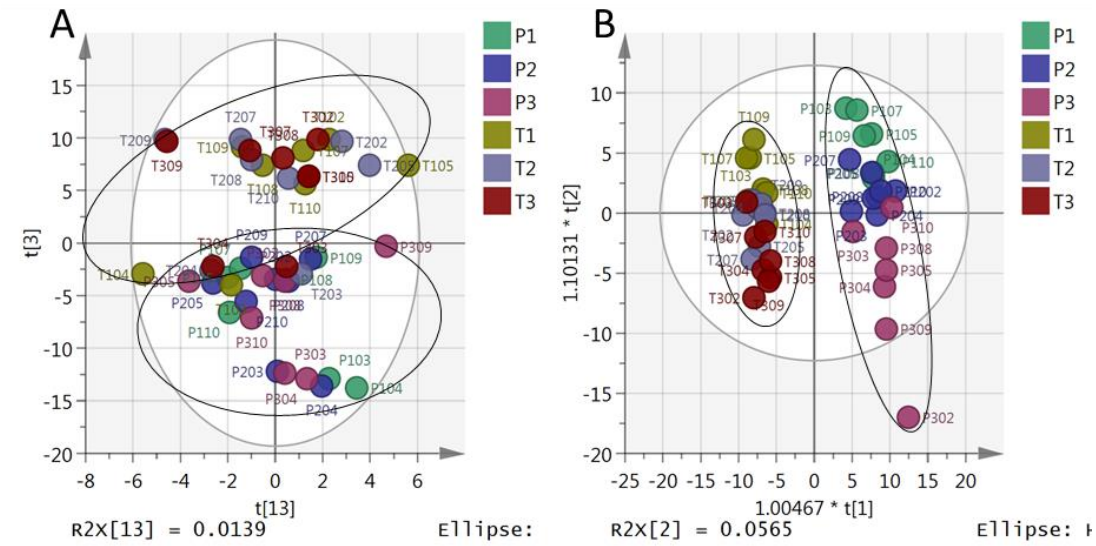

Figure 3.3 (A) PCA vs (B) OPLS-DA score plots for pstients with T2D.
The figure shows distribution of 48 samples based on readings of 537 putative biomarkers in 8 patients with T2D. (P) denotes placebo and (T) denotes GC blockade treatment, samples collected at 1 = baseline, 2 = pre-insulin and 3 = post-insulin. Plot (A) PCA has R^2 = 0.909, Q^2=0.565. Plot (B) OPLS-DA has R^2 = 0.749, Q^2=0.618.

A principal components analysis (PCA) score plot (Figure 3.3A) shows no clear clustering pattern. Separation between groups based on type of intervention can be seen clearly in the OPLS-DA score plot (Figure 3.3B) although observations in pre-insulin and baseline showed some overlap when placebo had been given.

To study the effect of GC blockade in patients with metabolic syndrome, an OPLS-DA model was built on 537 putative biomarkers which were measured in 48 samples from 8 patients with T2D. In a comparison of placebo to GC blockade, 18 putative biomarkers (Table 3.2) passed the 95% CI filter and showed a significant change based on the corrected p-value and had an AUC above 0.7. These markers were then used to rebuild an OPLS-DA model (Figure 3.4) in order to examine its ability to separate subjects based on the intervention.

3.4.2 Biomarker identification

3.4.2.1 Effect of GC blockade treatment on plasma metabolome of patients with T2D.

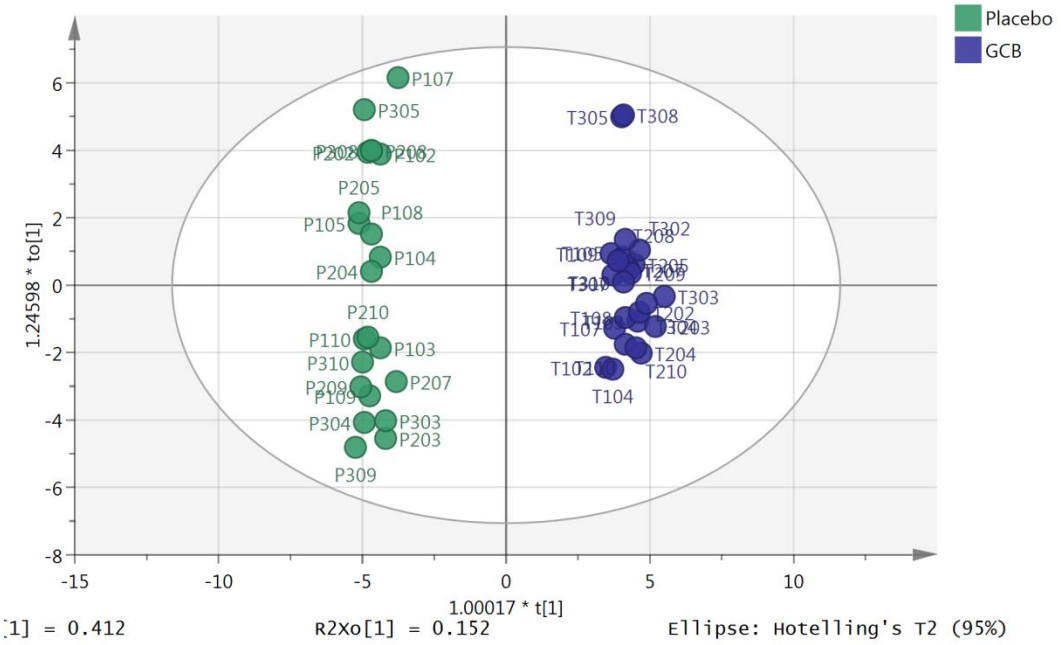

Figure 3.4 OPLS-DA score plot of placebo vs GC blockade samples of patients with T2D based on 18 putative metabolites.
The plot shows distribution of 46 observations based on readings of 18 putative biomarkers. The model includes two groups, subjects treated with placebo (22 samples-green) and subjects treated with GC blockade (24 samples-blue).The model consists of one predictive x-score component; component t[1] and two orthogonal x-score components to[1-2]. t[1] explaining 41.2% of the predictive variation in x, to[1] explaining 15.2% of the orthogonal variation in x, R^2X (cum) = 0.673, R^2Y (cum) = 1, R^2 (cum) = 0.99, Goodness of prediction Q^2 (cum) = 0.981.

The OPLS-DA score plot (Figure 3.4, above) was built on 18 putative biomarkers (Table 3.2) that significantly changed based on the treatment. Two observations (P302 and P307) were excluded as they were considered outliers based on Hotelling's T^2 vs DModX plot. The plot clearly shows significant separation between the two groups with *P* CV-ANOVA = 8.8E-32. 67% of the change in metabolites was explained by the model, 41% out of this variability was due to GC blockade

treatment, while 26% of the variability in metabolites had no relation to the type of intervention. 99% of the variability between the subjects was explained by the variability in the metabolites, around 98% of this variability was predicted by the model based on cross-validation. The validity of the number of orthogonal components in the model was examined using observed versus predicted plot, the regression line in the plot was R^2 = 0.99 (Figure S3.1B, appendix), indicating validity of the cross validation of the model. Based on the permutations test plot (Figure S3.1A, appendix), the original model has valid predictive ability compared to the newly permuted Q^2. Thus, 18 putative biomarkers that were significantly changed by the GC blockade treatment constitute a unique metabolomics classifier with excellent accuracy AUROCC=1 for each group (Figure S3.1C, appendix).

Table 3.2 Shows list of putative biomarkers that significantly changed following GC blockade treatment.

Putative biomarkers	AUC	Placebo : GC blockade	FDR
Bile acids and their conjugates			
Chenodeoxyglycocholate ^{C18}	0.9	1 : 10.62	6.6E-06
Glycocholate ^{C18}	0.85	1 : 180.93	0.0001
Taurodeoxycholate *	0.87	1 : 35.65	0.00003
Glycochenodeoxycholate sulphate ^{C18}	0.99	1 : 16.86	1.8E-06
Glycochenodeoxycholate glucuronide ^{C18}	0.8	1 : 19.37	0.009
Miscellaneous			
7-oxo-11E,13-Tetradecadienoic acid	0.9	1 : 3.92	0.001
Hexanoic acid (C6:0) *	0.8	1 : 1.25	0.02
D-Glucuronate *	1	1 : 13.4	3.1E-22
Androsterone sulphate	0.7	1 : 1.76	0.01
Pregnenolone sulphate	0.96	1 : 116.5	6.3E-06
L-Valine	0.6	1 : 1.5	0.03

* Retention time matches standard. ^{C18} metabolites identified using C18-AR column, the rest identified using ZICpHILIC column.

Bile acids and their conjugates (Table 3.3) are the major group of putative biomarkers that were significantly elevated following GC blockade treatment.

Table 3.3 List of bile acids and their conjugates that increased following treatment with GC blockade.

Putative metabolites	r	99% CI	VIPpred	VIPorth
Chenodeoxyglycocholate ^{C18}	0.64	(0.10, 0.44)	1.25	0.72
Glycochenodeoxycholate sulfate ^{C18}	0.98	(0.28, 0.57)	1.46	0.51
Glycochenodeoxycholate glucuronide^{C18}	0.41	(0.05, 0.30)	0.63	1.2
Glycocholate ^{C18}	0.57	(-0.04, 0.53)	0.81	1.14
Taurodeoxycholate *	0.61	(0.19, 0.33)	0.92	0.97

* Retention time matches standard. C18 metabolites identified using C18-AR column, the rest identified using ZICpHILIC column. VIPpred= variable importance in the projection (predictive value), VIPortho= variable importance in the projection (orthogonal value).

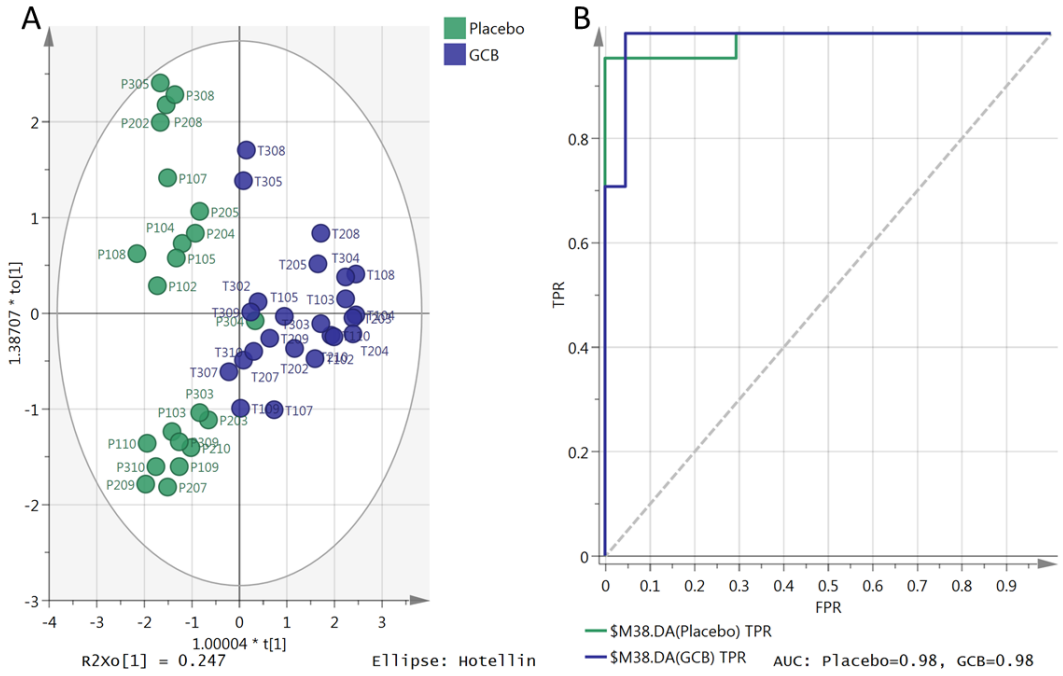

Figure 3.5 (A)OPLS-DA score plot and (B) ROC curve of placebo vs GC blockade treatment in patients with T2D based on readings of bile acids metabolites and their conjugates.
The OPLS-DA score plot 9A) shows 46 observations of placebo vs GC blockade treatment based on bile acids metabolites and their conjugates readings (Table 3.3) in two groups, subjects treated with placebo (22 samples-green) and subjects treated with GC blockade (24 samples-blue).The model consists of one predictive x-score component; component t[1] and three orthogonal x-score components to[1-3]. t[1] explains 44.8% of the predictive variation in x, to[1] explains 24.7% of the orthogonal variation in x, R^2X (cum) = 0.911, R^2Y (cum) = 1, R^2 (cum) = 0.74, Goodness of prediction Q^2 (cum) = 0.682. On the right, plot (B) shows area under the ROC curve (AUROCC) of the two groups, x-axis showing (FPR) false positive rate (1-specificity), y-axis showing true positive rate (sensitivity). AUROCC for placebo = 0.98 and GC blockade = 0.98.

An OPLS-DA score plot (Figure 3.5A) was built on 5 metabolites of bile acids and their conjugates (Table 3.3). Two observations (P302 and P307) were excluded as they were considered outliers based on Hotelling's T^2 vs DModX plot. The OPLS-DA plot shows significant separation between the two groups with *P* CV-ANOVA = 3.1E-7. Around 91% of the changes in metabolites was explained by the model, 44.8% out of this variability was due to the effect of GC blockade treatment, while 46% of the variability in metabolites had no relation to the treatment. 74% of the variability between the subjects was explained by the variability in the metabolites, around

68% of this variability was predicted by the model based on cross-validation. The validity of the number of latent variables in the model was examined using the observed versus predicted plot, the regression line of the plot was $R^2 = 0.74$ (Figure S3.2B, appendix) indicating validity of the cross validation. Based on the permutations test plot (Figure S3.2A, appendix), the original model has valid predictive ability compared to the newly permuted Q^2. The 5 putative biomarkers that were significantly elevated following GC blockade treatment have excellent classifying ability (Figure 3.5B, above) (AUROCC= 0.98) in differentiating between patients treated with placebo and those treated with GC blockade.

3.4.2.2 Study of the effect of insulin on plasma metabolome of patients with T2D regardless of GC blockade treatment or placebo.

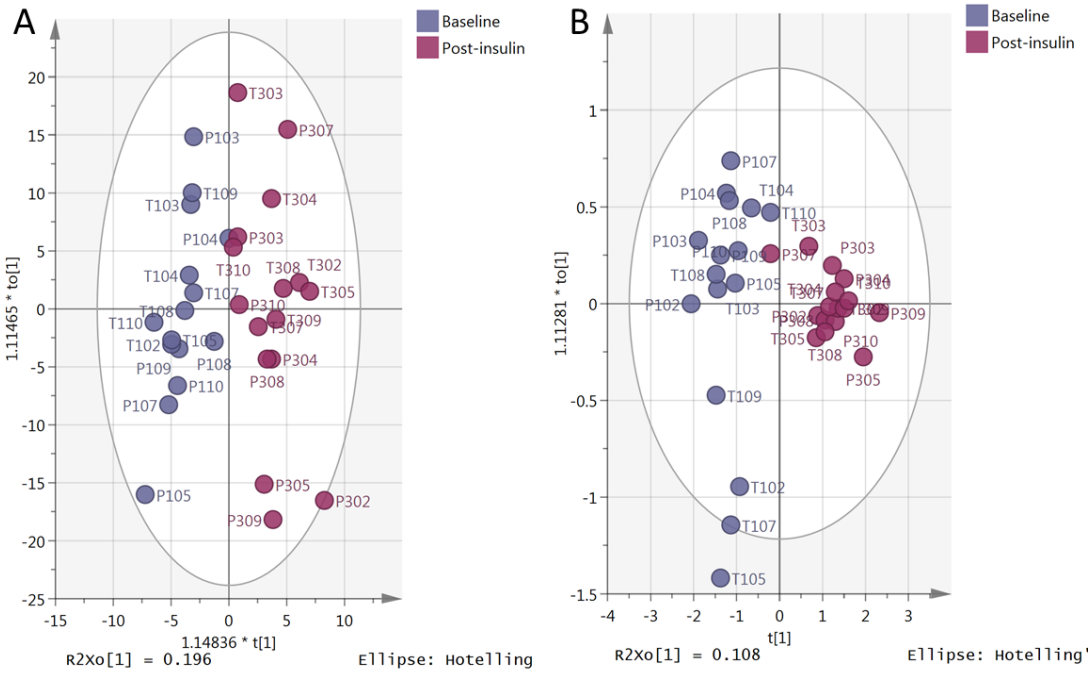

Figure 3.6 OPLS-DA score plots of the effect of insulin on (A) 537 and (B) 2 putative metabolites. Plot A shows distribution of 31 observations based on readings of 537 putative biomarkers. The observations classified into two groups; baseline (15 samples-blue/grey) and post-insulin (16 samples-plum). The model consists of one predictive x-score component; component t[1] and one orthogonal x-score components to[1]. t[1] explains 4.4% of the variability between the two groups, to[1] explains 19.6% of the variability within group, R^2X (cum) = 24%, R^2Y (cum) = 1, R^2 (cum) = 0.78, Goodness of prediction Q^2 (cum) = 0.224. **(B)** OPLS-DA score plot shows distribution of 32 observations based on readings of 2 putative biomarkers (Table 3.4, below). The observations classified into two groups; baseline (16 samples-blue/grey) and post-insulin (16 samples-plum). The model consists of one predictive x-score component; component t[1] and one orthogonal x-score components to[1]. t[1] explains 89.2% of the variability between the two groups, to[1] explains 10.8% of the orthogonal variation in (within group variability), R^2X (cum) = 1, R^2Y (cum) = 1, R^2 (cum) = 0.863, Goodness of prediction Q^2 (cum) = 0.852.

The OPLS-DA score plot (Figure 3.6A) shows separation between the two groups of observations (baseline vs post-insulin), but this separation is insignificant *P* CV-ANOVA = 0.144. The model shows that only 4.4% of the variation in the putative metabolites between the two groups was due to the insulin dose while 19.6% of the

variability had no link to the effect of insulin dose. The model explained 78% of the variability among the samples which led to the variability in the putative metabolites; only 22.4% of this variability was predicted by the model based on cross-validation of the R^2.

The supervised model (Figure 3.6A) was rebuilt (Figure 3.6B) using two putative biomarkers that significantly increased following insulin dose (N4-Acetylaminobutanal and 2,3,4,5-Tetrahydropyridine-2-carboxylate, Table 3.4) which passed the filters of FDR corrected p-value <0.05, AUC >0.8 and the 95% CI of the differences in means. The plot (Figure 3.6B) shows clear separation between the observations in the two groups (baseline vs post-insulin) with *P* CV-ANOVA = 7.6E-11. And it also shows that within group variability in the post-insulin group is smaller than those in the baseline group. The model shows that 89% of the variation in these two putative metabolites among subjects was due to the insulin dose while 11% has no link to the insulin dose. 86% of the variability between the subjects was explained by the variability in the two putative metabolites, 85% of this variability was predicted by the model based on cross-validation of the R^2. The validity of the number of orthogonal components in the model was examined using observed versus predicted plot, the regression line in the plot was $R^2 = 0.86$ (Figure S3.3B, appendix) indicating validity of the model. Based on the permutation test (Figure S3.3A, appendix) the original model has valid predictive ability compared to the newly permuted Q^2. N4-acetylaminobutanal and 2,3,4,5-tetrahydropyridine-2-

carboxylate have excellent classifying ability (AUROCC=1) of patients with T2D treated with insulin compared to baseline (Figure S3.3C, appendix).

Table 3.4 Putative biomarkers which significantly increased following insulin dose.

Putative biomarkers	Placebo		Treatment		Ratio
	FDR	AUC	FDR	AUC	P1 : P3 : T1 : T3
N4-Acetylaminobutanal	7.7E-06	1	0.0018	0.95	1 : 14.2 : 3.2 : 12
2,3,4,5-Tetrahydropyridine-2-carboxylate	7.7E-06	1	2.7E-06	1	1 : 8.64 : 1: 7.9

P1 = Baseline in placebo, P3 = Post-insulin in Placebo, T1 = Baseline in GC blockade treatment and T3 = Post-insulin in GC blockade treatment. AUC=area under the curve, FDR= false discovery rate(corrected p-value).

3.4.2.3 The effect of insulin dose on plasma metabolome of patients with T2D following GC blockade treatment compared to placebo.

Table 3.5 Putative biomarkers that significantly affected by the insulin dose following GC blockade.

Putative biomarkers	AUC	P1 : P3 : T1 : T3	FDR(T)	r	99% CI
2,3,4,5-Tetrahydropyridine-2-Carboxylate	1	1: 8.6: 1: 7.9	1E-6	0.93	(0.11, 0.67)
N4-Acetylaminobutanal	0.95	1: 14.2: 3.2: 12	0.001	0.79	(0.07, 0.59)
2-Methylbutyroylcarnitine	0.84	1: 1.03: 1.5: 0.8	0.02	-0.64	(-0.48, -0.05)
Chenodeoxyglycocholate ^{C18}	0.91	1: 0.3: 13.2: 2.9	0.007	-0.69	(-0.50, -0.08)
Taurodeoxycholate *	0.88	1: 0.5: 117: 22	0.023	-0.61	(-0.42, -0.08)
γ-Linolenic acid(C18:3)	0.83	1: 0.7: 1.2: 0.6	0.032	-0.57	(-0.37, -0.10)
Stearic acid(C18:0)	0.84	1: 1.02: 1.2: 0.7	0.032	-0.53	(-0.51 , 0.07)
Lauric acid (C12:0)	0.78	1: 1.3: 1.7: 0.8	0.032	-0.54	(-0.63 , 0.17)

* Retention time matches standard. ^{C18} metabolites identified using C18-AR column, the rest identified using ZICpHILIC column. (P1 = Baseline in placebo, P3 = Post-insulin in Placebo, T1 = Baseline in GC blockade treatment and T3 = Post-insulin in GC blockade treatment), FDR(T)= FDR= false discovery rate(corrected p-value)for the insulin effect following GC blockade treatment, AUC=area under the curve.

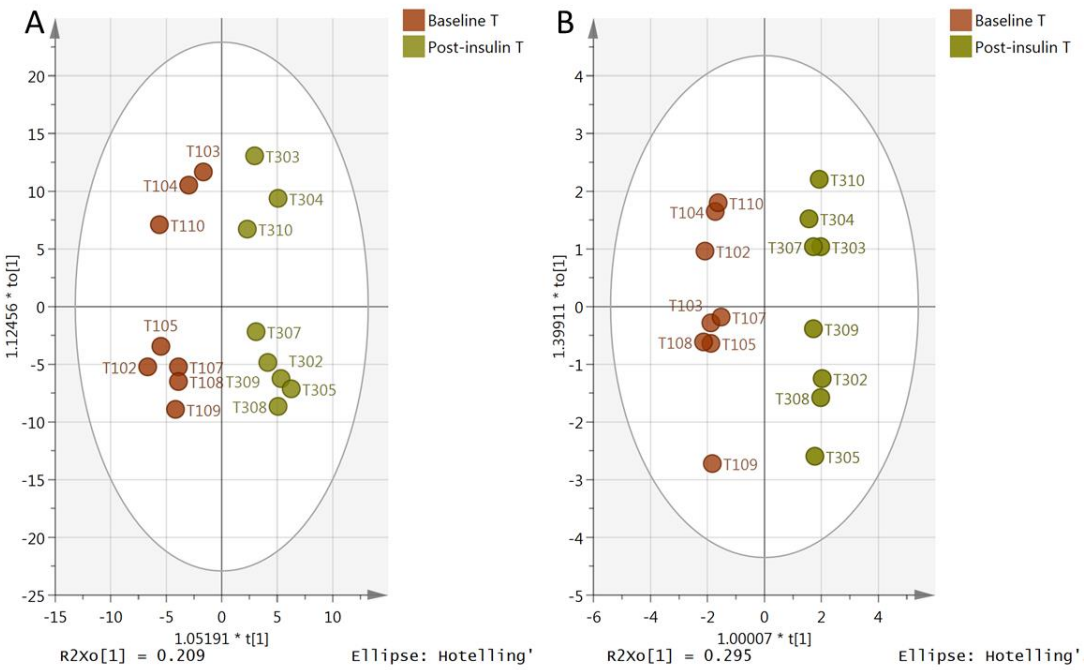

Figure 3.7 OPLS-DA score plots of the effect of insulin on (A) 537 and (B) 8 putative metabolites following GC blockade treatment.

Plot **(A)** shows distribution of 16 observations based on readings of 537 putative biomarkers following GC blockade treatment. The observations classified into two groups; baseline (8 samples-brown) and post-insulin (8 samples-dark yellow). The model consists of one predictive x-score component; component t[1] and one orthogonal x-score components to[1]. t[1] explains around 7% of the predictive variation in x, to[1] explains 21% of the orthogonal variation in x, R^2X (cum) = 27.8%, R^2Y (cum) = 1, R^2 (cum) = 0.90, Goodness of prediction Q^2 (cum) = -0.12. **(B)** shows distribution of 16 observations based on readings of 8 putative biomarkers (Table 3.5, above). The observations classified into two groups; baseline (8 samples-brown) and post-insulin (8 samples-dark yellow). The model consists of one predictive x-score component; component t[1] and three orthogonal x-score components to[1-3]. t[1] explains 45.6% of the predictive variation in x, to[1] explains 29.5% of the orthogonal variation in x, R^2X (cum) = 891, R^2Y (cum) = 1, R^2 (cum) = 0.991, Goodness of prediction Q^2 (cum) = 0.977.

The first model (Figure 3.7A) was built on readings of 537 putative biomarkers in 16 samples of patients treated with GC blockade: 8 samples at baseline and 8 samples following insulin. Although the model showed clear separation between the two groups, this separation was not statistically significant at the multivariate level (*P* CV-ANOVA = 1). The model explained only 7% of the variation in the metabolome

following insulin treatment. In order to get a better model, the putative metabolites were filtered using FDR corrected p value <0.05, AUC<0.7 and 95% CI of the difference. 8 metabolites passed these filters (Table 3.5), and a new model (Figure 3.7B) was built on these 8 metabolites. The model showed clear and significant separation between the two groups P CV-ANOVA = 6.3E-6. The model explained 89% of the variation in the metabolites and 46% of this variation were due to insulin treatment while 43.5% has no link to the intervention. 99% of the variability between the subjects was explained by the variability in the metabolites, around 97.7% of this variability was predicted by the model based on cross-validation of the R^2.

N4-acetylaminobutanal and 2,3,4,5-tetrahydropyridine-2-carboxylate showed significant elevation following insulin injection in both placebo and GC blockade treatment; this indicates that these two putative biomarkers were effected significantly by insulin regardless of the intervention. N-4-acetylaminobutanal was affected significantly by the interaction between the GC blockade treatment and the insulin injection (*p* value = 0.006), and GC blockade caused a 6-fold increase in N-4-acetylaminobutanal following insulin injection compared to 13-fold during placebo. Remodelling the plot (Figure 3.7B) without both N-4-acetylaminobutanal and 2,3,4,5-tetrahydropyridine-2-carboxylate rendered the model insignificant at multivariate level with *P* CV-ANOVA = 0.77, but the explained variation in the putative metabolites increased to 67%.

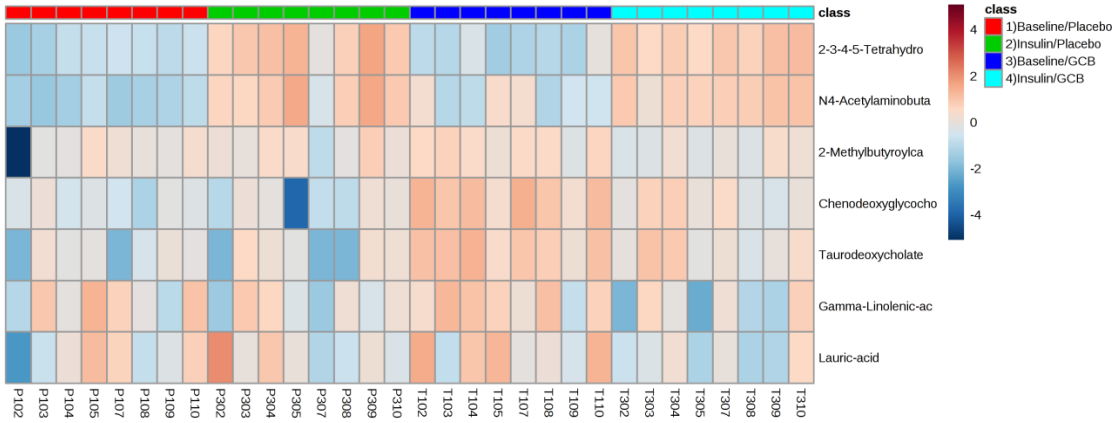

Figure 3.8 Heat map showing the putative metabolites that are significantly affected by insulin following GC blockade treatment.
The top row of the plot represents the phases of sample collection; 1) baseline following placebo (red), 2) insulin follwoing placebo (green), 3) baseline following GC blockade (dark blue) and 4) insulin following GC blockade (light blue). The different colour shades represent intensities of each metabolite (rows) in each observation (column). Stearic acid was not given in the heat map from Metaboanalyst.

The clearest effect in the heat map was that the putative biomarkers N-4-acetylaminobutanal and 2,3,4,5-tetrahydropyridine-2-carboxylate increased in observations following insulin injection regardless the treatment. N-4-acetylaminobutanal showed less certain elevation following insulin administration in GC blockade compared to placebo. Chenodeoxyglycocholate and taurodeoxycholate showed a clear elevation in observations with GC blockade compared to placebo regardless of insulin. Lauric acid showed statistically significant reduction, but was less certain (99% CI, -0.63 to 0.17) following insulin injection in the presence of GC blockade.

3.5 Discussion

Supraphysiological levels of GC have strong association with the development of metabolic syndrome which is composed of T2D and is commonly associated with dyslipidemia, obesity and often hypertension. These complications contribute to the development of cardiovascular disease which is most commonly linked to mortality in T2D (Segal and Kim, 1963, Prawitt *et al.*, 2011). Reducing levels of circulating cortisol might improve insulin resistance. An increasing number of studies have used the mass spectrometer as a powerful tool for biomarker discovery (Huffman *et al.*, 2009), but none of these studies examined the metabolomic changes caused by GC blockade and whether or not it improves insulin sensitivity compared to placebo. In this crossover double blind study, plasma samples of 8 patients with metabolic syndrome were analysed using an LC-MS platform. GC blockade treatment led to a significant elevation of conjugated and unconjugated bile acids in comparison to placebo. Some unconjugated bile acids and free fatty acids were reduced significantly in response to insulin injection following GC blockade, compared to placebo.

In our study, bile acids and their conjugates were elevated significantly following GC blockade compared to placebo. The treatment would disturb the physiological activity of the HPA axis. This was found to affect bile acids levels in patients with Addison's disease who have higher serum levels of bile acids compared to healthy controls (Rose *et al.*, 2011). Bile acids are known as metabolic regulators and

mediate their action via receptor-dependent and independent pathways. The most prominent receptor for these signalling molecules are Farnesoid X receptor (FXR) (Pircher *et al.*, 2003, Goodwin *et al.*, 2000) and TGR5 (Thomas *et al.*, 2009). It was found that FXR expression is reduced in a rat model of T2D, and that insulin administration reverses this effect (Duran-Sandoval *et al.*, 2004). TGR5 which is expressed in muscle and brown adipose tissue is activated by bile acids and this promotes an increase in energy metabolism and attenuates diet-induced obesity (Thomas *et al*., 2009). Both receptors contribute to the regulation of lipid, glucose and energy metabolism (Cariou *et al.*, 2006, Abdelkarim *et al.*, 2010, Maruyama *et al.*, 2006). Metabolic disturbances of these pathways might lead to a predisposition of T2D and associated complications (Prawitt *et al*., 2011).

Previous observations in patients with T2D reported that bile acids (BAs) decreased following insulin injection (Bennion and Grundy, 1977). Consistently, in our study, circulating bile acids reduced significantly upon insulin injection following GC blockade, but were not statistically affected upon insulin injection following placebo. Physiologically, insulin inhibits the expression of the two key enzymes in bile acid biosynthesis, CYP7A1 and CYP27A1, which has been previously reported in rat hepatocytes (Lefebvre *et al.*, 2009).

(Lambert *et al.* (2003) noticed that bile acids regulate cholesterol and triglycerides through hepatic FXR. In this study GC blockade significantly increased the levels of conjugated and unconjugated bile acids. In 1978, before FXR was identified,

chenodeoxycholic acid was administered to decrease plasma lipids in patients with hypertriglyceridemia (Bateson *et al.*, 1978, Duran-Sandoval *et al*., 2004).

On the other hand, 11b-HSD1 influences the expression of the fatty acid transport protein 5 (Fatp5), which not only mediates the hepatic uptake of fatty acids, but also exhibits bile acid-CoA ligase activity, hence activating bile acids to coenzyme A thioesters, which is essential for proper BA conjugation (Doege *et al.*, 2006, Doege *et al.*, 2008, Mihalik *et al.*, 2002, Steinberg *et al.*, 2000).

Fatp5 has been proposed as a potential target for treatment of NAFLD (Doege *et al*., 2008, Anderson and Stahl, 2013). It is appealing to infer that down regulation of Fatp5 upon therapeutic intervention with selective 11b-HSD1 inhibitors may contribute to the observed beneficial effects on lipid profiles in humans (Rosenstock et al., 2010, Shah *et al.*, 2011). In addition, the elevated circulating BAs upon abolishing 11b-HSD1 activity may stimulate energy expenditure in brown adipose tissue (Watanabe *et al.*, 2006), ameliorate atherosclerosis (Pols *et al.*, 2011) and enhance glucose tolerance through the activation of TGR5 (Thomas *et al*., 2009).

GC induce phosphatidylcholine synthesis via enhancing choline uptake through stimulating choline transporter like protein CTL1 and CTL2 (Nakamura *et al.*, 2010). Consistently, in this study, GC blockade significantly reduced plasma levels of phosphocholines. On the other hand, gut microbiota induces the HPA axis to respond to stress (Dinan and Cryan, 2012, Clarke *et al.*, 2014). Plasma levels of

choline reduced due to the conversion of choline to methylamines by gut microbiota in 129S6 strain mouse (Dumas *et al.*, 2006); this goes in line with a choline deficient diet causing NAFLD, both in mice and humans (Clarke *et al*., 2014, Wang *et al.*, 2011b). (Drogan *et al.*, 2015) reported an inverse relationship between level of phosphatidylcholine and T2D in a study of 300 individuals with T2D compared to 300 matched controls. Low levels of phosphocholines were linked to cardiovascular diseases (Wang *et al*., 2011b) which is unwanted. It is possible that GC blockade directly or indirectly promotes stress which might enhance the conversion of choline to methylamines by gut microbiota.

High glucose levels upregulate arginase enzyme activity, which might contribute to vascular endothelial dysfunction in diabetes and obesity (Duarte *et al*., 2007). In this study, insulin injection led to a significant elevation in N4-Acetylaminobutanal, this might indicate upregulation of arginase activity. GC blockade caused insignificant elevation of the arginase activity; this elevation might be due to significant elevation (p = 0.03) in valine levels following GC blockade. L-valine is one of the gluconeogenic amines which are considered precursors for L-arginine. It is worth noting that elevations of N4-Acetylaminobutanal upon insulin injection following GC blockade were significantly reduced (p = 0.0018) to 4-fold compared to 14-fold in placebo with (p = 0.006). GC blockade might improve NO production following insulin which in turn reduces vascular side effects in diabetic patients.

Insulin significantly elevates levels of 2,3,4,5-tetrahydropyridine-2-carboxylate (p = 7.7E-6) which is an intermediate in lysine degradation pathway via pipecolic acid. Upregulation of this pathway was reported in diabetic monkeys, in which SLC6A20 sodium transporter was attenuated compared to non-diabetic controls (Patterson *et al.*, 2011). This could be an early biomarker of diabetic nephropathy (Dunn, 2013). GC blockade did not alter the levels of 2,3,4,5-tetrahydropyridine-2-carboxylate.

It was previously reported that the acylcarnitines; 2-methylbutyroylcarnitine (2-MBC) was elevated in the plasma of patients with NAFLD (Kalhan *et al.*, 2011) and also those with T2D and insulin resistance (Lynch and Adams, 2014). The 2-MBC was also found elevated in obese children with insulin resistance compared to those who were insulin sensitive (Mastrangelo *et al.*, 2016). 2-MBC is a substrate in the catabolic pathway of isoleucine for energy production through tricarboxylic acid (TCA) cycle, thus accumulation of 2-MBC indicates an inhibition of branched chain acyl CoA dehydrogenase (Milburn *et al.*, 2013). In our study 2-methylbutyroylcarnitine was not affected by GC blockade, but insulin injection following GC blockade significantly reduced the plasma level of 2-MBC by half but remained unchanged when insulin injection was given following placebo. This result suggests that GC blockade improves insulin sensitivity.

Unlike insulin and ACTH hormones which increase the rate of esterification and lipolysis respectively, GC have a controversial effect on fatty acid metabolism, since

they induce the lipolytic effect of lipase enzyme, and at the same promote tissue antilipolytic activity (Peckett *et al.*, 2011), but the net result is an increase in plasma level of FFAs (Chatterjea and Shinde, 2008). In the current study, GC blockade significantly increased (*p* value = 0.02) plasma levels of a medium chain fatty acid (C6:0). This might be in part due to the effect of GC blockade on lowering circulating levels of insulin (Macfarlane *et al*., 2014) and also increased levels of ACTH which accelerates FFA release from adipose tissue to plasma. Insulin injection following placebo non-significantly reduced plasma levels of unsaturated long chain fatty acids (C18:3), and almost had no effect on saturated long chain fatty acid levels (C18:0), but increased levels of the medium chain fatty acids (C12:0). Consistently, the Framingham study reported that the lower double bond and lower carbon number fatty acids were associated with T2D (Rhee *et al*., 2011). GC blockade improves insulin action in lowering plasma levels of triacylglycerols.

Finally, the other major alterations in response to GC blockade are, as might be expected, in steroid metabolism. Androsterone glucuronide level is significantly increased (*p* = 0.01) following GC blockade dose. Androsterone can be metabolised from adrenal androgens such as dehydroepiandrosterone, dihydrotestosterone or androstenedione, and is considered an inactive end product. In contrast, pregnenolone sulphate, is not a waste product of sulphated pregnenolone following phase II reaction as one would expect (Harteneck, 2013). Biologically, pregnenolone is synthesised from cholesterol by the rate limiting enzyme CYP11A1, and then sulfonated via cytosolic sulfotransferase enzyme. Pregnenolone sulphate targets

different ligands and receptors leading to potentiation of memory, learning and anxiolysis; enhances neuronal development and synapse formation; and it also induces melanin synthesis and mediates pain modulation. Clinically, pregnenolone sulphate levels in plasma are increased before and during parturition, decreased in hypothyroidism and also reduced 4-fold in patients suffering from rheumatoid arthritis. In this study, pregnenolone sulphate significantly increased (p = 6.3E-6) more than 100-fold indicating dramatic upregulation of steroidogenesis in response to HPA-axis feedback mechanism following GC blockade (Harteneck, 2013).

Chapter 4:

A metabolomic study of the interaction between HC and insulin

4 A metabolomic study of the interaction between HC and insulin

4.1 Abstract

Background and Aims: To date, no direct study on the effects of insulin and HC on metabolic profiles in individuals has been reported in literature. In relation to our interest in the potential inhibition of HC biosynthesis for the treatment of metabolic syndrome, metabolomic profiling of plasma samples was carried out on healthy subjects.

Methodology: The subjects were administered either a low or high insulin infusion along with HC infusion at three different levels. All subjects were administered metyrapone prior to treatment, which blocks formation of HC by the body. Plasma samples were then analysed using untargeted metabolomics.

Results: The clearest effects of insulin were in lowering the levels of the branched chain amino acids (BCAs) leucine and isoleucine, and their deamidated metabolites, in plasma, while also lowering levels of FFAs and acylcarnitines. The clearest interaction between HC and insulin was that hydrocortisone caused the levels of BCAs and their metabolites to become significantly elevated in plasma. HC did not affect levels of FFAs when low doses of insulin were given but, interestingly, did result in elevated levels in subjects treated with a high insulin infusion. HC did not affect the levels of acyl carnitines.

Conclusion: These observations tie in with recent observations on the importance of BCAs in insulin resistance and diabetes, but the direct modulation of these metabolites by insulin and HC is reported here for the first time.

4.2 Introduction

GC such as cortisol have diverse physiological actions. Intracellular GC receptors are widely expressed and affect energy metabolism (e.g. interacting with insulin and inducing gluconeogenesis, stimulating lipolysis and fatty acid turnover, inducing proteolysis) (Andrews and Walker, 1999a, Macfarlane *et al*., 2008b), cardiovascular control (Walker, 2007b) (inducing sodium and water retention, potentiating vasoconstriction, increasing blood pressure), cellular proliferation, central nervous system function (impairing short-term memory, altering mood) (Seckl and Olsson, 1995), and innate immunity (enhancing macrophage apoptosis, inhibiting pro-inflammatory cytokine signalling) (Sapolsky et al., 2000). Most actions of GC are mediated slowly by altered gene transcription in response to altered intracellular cortisol concentrations, whereas plasma level of cortisol exhibit marked circadian and ultradian variation, and so there is a poor correlation between plasma cortisol levels and the clinical and biochemical actions of cortisol.

Acute elevation in cortisol is a crucial component of the stress response, but chronic excess of GC results in Cushing's syndrome, characterised by non-specific features including obesity, T2D, hypertension, impaired immunity, depression, and cognitive dysfunction. Subtle GC excess may be important in diverse conditions, ranging from metabolic syndrome (Walker, 2007b) to neuropsychiatric disease (Segal and Kim, 1963). This may involve increased circulating levels of cortisol or increased local regeneration of cortisol within target tissues by the enzyme 11β-HSD1. GC

deficiency is potentially life-threatening during stress, but is characterised by non-specific clinical features such as lethargy, hypotension, and weight loss. It is especially difficult to diagnose during critical illness when conventional tests of cortisol production, such as ACTH stimulation tests, may be unreliable (Boonen et al., 2013).

A lack of specific biomarkers makes clinical management of patients requiring GC replacement therapy particularly challenging, and may contribute to well-documented excess morbidity and mortality in patients with hypopituitarism or adrenocortical failure (Arlt *et al*., 2010, Filipsson *et al*., 2006, Bergthorsdottir *et al*., 2006). Moreover, several therapeutic strategies have been proposed to reduce cortisol secretion or action in metabolic and psychiatric disease. These include inhibitors of cortisol biosynthesis in the adrenal cortex (such as metyrapone), GR antagonists (such as RU38486) (Jacobson *et al*., 2005), and inhibitors of 11β-HSD1 (Hughes *et al*., 2008). The complexity of GC action imposes a major limitation in the development of such compounds, because of the lack of simple indicators of successful reduction in cortisol effects. Thus, for example, efficacy of early 11β-HSD1 inhibitors was not apparent until completion of a Phase IIa study (Hughes *et al*., 2008).

Novel biomarkers for GC action are urgently needed. Although mass spectrometry has become increasingly applied to this area, this topic has not been widely studied. A previous study using GC-MS reported limited metabolomic profiling in urine and

plasma of subjects treated with anti-inflammatory synthetic GC (Ellero-Simatos *et al.*, 2012). A recent more comprehensive study was carried out using GC-MS and LC-MS methods to both profile and quantify the metabolome of 20 healthy male volunteers following dexamethasone administration (Bordag *et al.*, 2015). They observed many changes in lipid, amino acid and steroid hormone metabolism. The most marked effects were lowering of alanine, methionine, asparagine, phenylalanine, proline and serine in plasma which were consistently affected over the four days of the study. A number of other amino acids were altered but less consistently.

Given the extensive interactions between GC and insulin, any biomarkers of GC action may overlap with those responsive to insulin. A number of recent studies have deployed metabolomics in obesity and insulin resistance. Insulin resistance induced by feeding a high fat diet to mice was associated with an elevation in citrate and a significant fall in the levels of leucine, valine, glycine, suberate, acetate, hippurate and arginine (Shearer *et al.*, 2008). A comparison of people with varying degrees of insulin sensitivity using Fourier Transform mass spectrometry (FT-MS) found a number of markers to be altered in insulin resistant individuals, particularly unsaturated fatty acids (Lucio *et al.*, 2010). Batch *et al* observed a distinct metabolic signature linked to obesity, where plasma levels of the BCAs leucine, isoleucine and valine were elevated in obese subjects. In addition, methionine, glutamine, phenylalanine, tyrosine, asparagine, and arginine were also elevated, with concomitant depression of glycine levels (Batch *et al.*, 2013).

Furthermore, a number of free fatty acids and acyl carnitines exhibited elevated levels. The latest work by the Newgard group, which was carried out on a cohort of 1872 individuals who were subdivided into lean, overweight and obese groups, proposed that BCAA levels can provide a better signature of metabolic wellness than body mass index (Huffman *et al*., 2009). Another group found that elevated levels of BCAA in plasma could be linked to obesity and potentially to development of insulin resistance in children and adolescents (McCormack *et al.*, 2013), although feeding mice a high fat diet (HFD) supplemented with leucine reduced insulin resistance in comparison with mice maintained on a HFD alone (van Raalte *et al.*, 2009).

To date, no direct study on the effects on insulin and HC on metabolic profiles in individuals has been reported. To identify biomarkers which reflect GC and insulin action, metabolomic analysis was performed on plasma samples obtained from healthy men treated with metyrapone followed by HC infusion to induce low, medium and high (supra-physiological) circulating cortisol levels. Moreover, specificity of the response to GC was tested by making measurements before and after insulin infusion, and examining the interaction between insulin and HC.

4.3 Methodology

4.3.1 Sample collection

Twenty (20) healthy men, aged (33.4 ± 15.2 years), with BMI (23.8 ± 1.4 kg/m^2), normal screening blood tests (full blood count, renal and thyroid function) and alcohol intake <28 units/week, who had not received GC therapy by any route in the previous 6 months, were recruited. They each attended for three study days in the morning after taking metyrapone 1 g orally at 2300 h the previous evening and fasting overnight. They were randomly assigned to one of two groups of 10 participants, to be infused with either low dose (0.06 mU/kg/min) or medium dose (0.2 mU/kg/min) insulin on all three occasions, together with dextrose, 6,6-$^2H_2$-glucose, 1,1,2,3,3-$^2H_5$-glycerol, somatostatin, glucagon and growth hormone for 4 hours, with a second dose of metyrapone 1 g orally after 150 min. The three study days were separated by at least 3 weeks and comprised, in random order, 'low', 'medium' and 'high' GC phases. For the low GC phase, subjects took placebo tablets at 2300 h and 0700 h and were infused with saline to achieve peak plasma cortisol after 4 hours for the medium GC phase, subjects took HC 10 mg orally at 2300 h and 5 mg at 0700 h and were infused with HC 0.04 mg/kg bolus followed by 0.025 mg/kg/h to achieve peak plasma cortisol after 4 hours, and for the high GC phase subjects took HC 20 mg orally at 2300 h and 10 mg at 0700 h and were infused with HC 0.18 mg/kg/h bolus and 0.12 mg/kg/h to achieve peak plasma cortisol after 4 hours. Samples for metabolomics analysis were obtained at the end of each 4 hour infusion.

4.3.1.1 Patients numbering

Each subject had a number of 4 characters; the first character was either (1) low insulin or (2) high insulin dose, the seconed character was either (L) low HC, (M) medium HC or (H) high HC doses. The last two characters represented the patients' number. For instance 1M02= first character (1) low insulin dose, second character (M) medium HC dose. The last two characters (02) the subject's number.

4.3.2 LC-MS analysis

- LC-MS conditions and samples preparation are reported in details in section 2.1-2.3 (pages: 47-51).
- Column used in this project are ZICpHILIC and C18-AR.

4.3.3 Data extraction and processing

Details of data extraction and processing are reported in section 2.4 (pages: 51-54).

4.3.4 Data analysis

Most of the details on data analysis have been described in section 2.5 (pages: 54-58). Additionally, split-plot ANOVA were employed on putative metabolites that showed significant changes following administration of insulin, HC, or both. The tests were conducted to examine the differences between low, medium, and high HC doses at repeated measurements in each intervention (low or high insulin dose) separately. In addition, the interaction between HC and insulin dose were also assessed.

4.4 Results

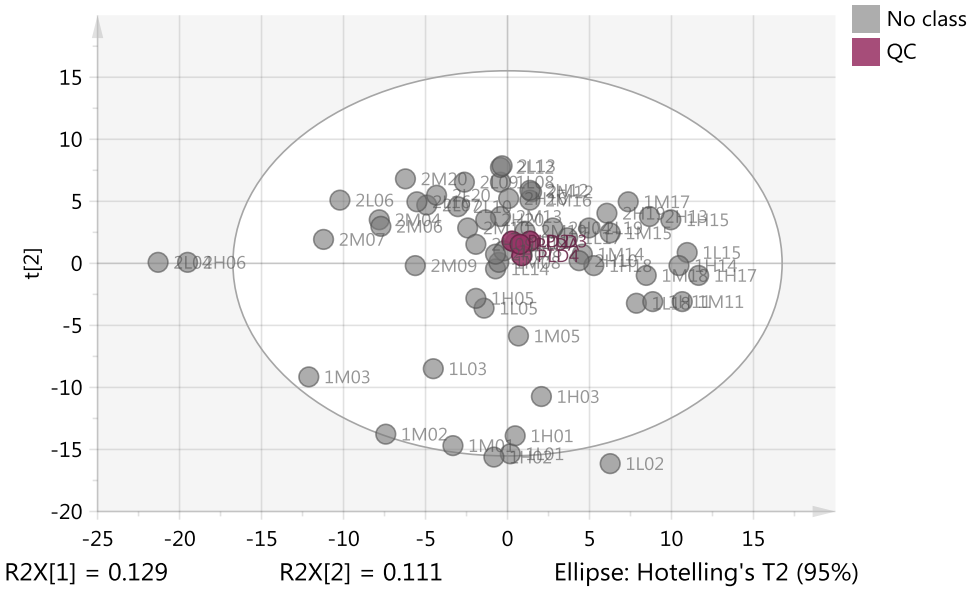

Figure 4.1 2D PCA score plot for QC (pooled) samples in healthy individuals.
The plot shows the clustering of pooled samples (plum-QC) compared to the rest of plasma samples (grey-No class) in healthy individuals.

The instrument was set to inject a pooled sample after every 15 plasma samples, thus the pooled sample had 4 readings (Figure 4.1). To quantify the precision of the measurements, the relative standard deviation (RSD) was calculated between the 4 pooled samples based on sum of the intensities in each sample and an RSD of 0.5% was obtained. RSD was also calculated for each of the putative biomarkers among the pooled samples and the highest RSD was for 1-hexadecanoyl-2-(4Z,7Z,10Z,13Z,16Z,19Z-docosahexaenoyl)-sn-glycero-3-phosphoethanolamine (9.7%) while the lowest RSD was for alanine (0.23%). The precision of these values clearly indicates that any metabolomic differences between groups cannot be due to instrumental factors alone. No any one of the metabolites were removed based on the RSD.

4.4.1 Data visualisation

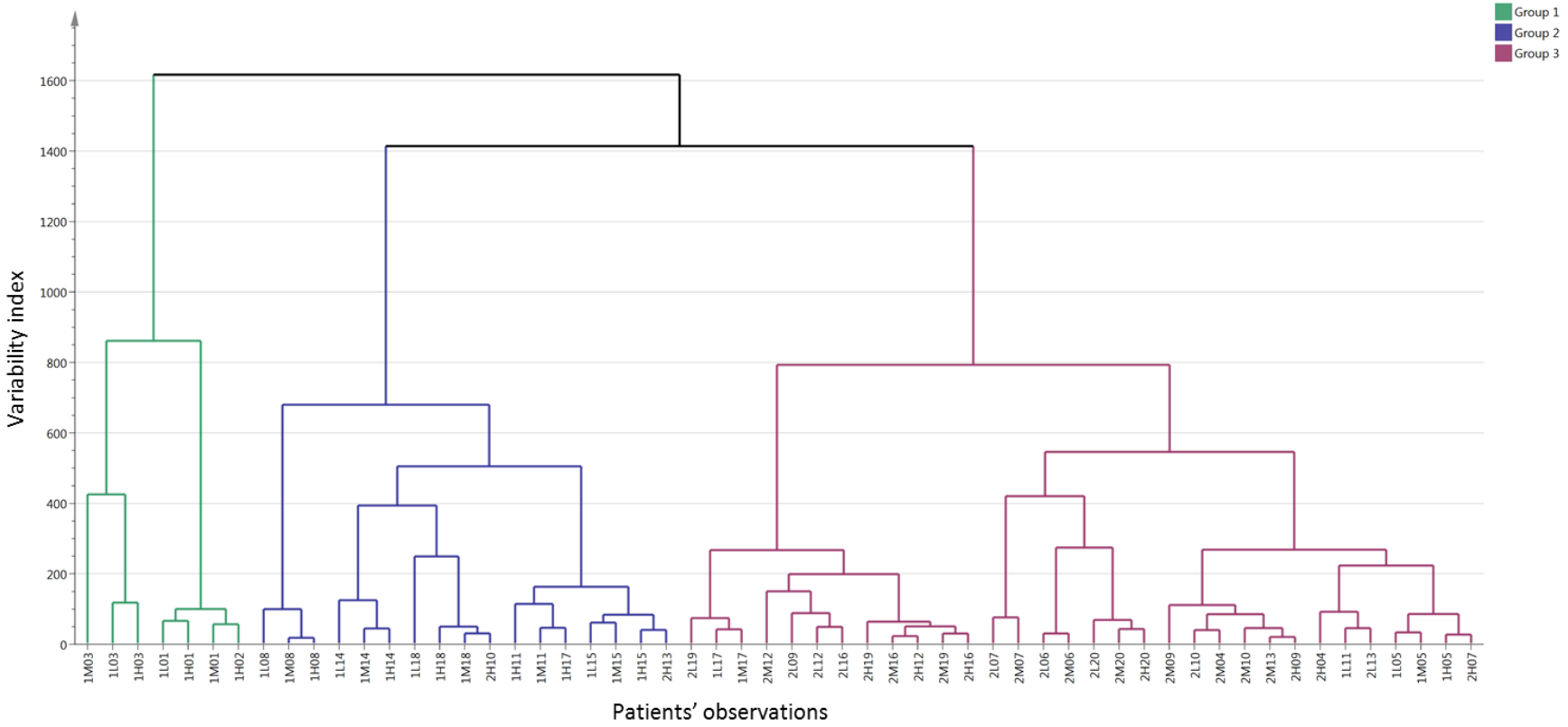

Figure 4.2 Hierarchical Clustering Analysis (HCA) for healthy subjects having different doses of HC and insulin.
The dendrogram shows observations clustered into three groups. X-axis represents the samples and y-axis shows the variability index. The higher the variability index the larger the between group variability and the lower the variability index, the smaller the between group variability. The plot divides samples into three groups; group 1 (green), group 2 (blue) and group 3 (plum).

HCA (Figure 4.2, above) shows that samples almost clustered according to the insulin dose. For instance, group 3 consisted of 32 samples and about 80 % of the samples are for individuals receiving a high insulin dose. 100% of the observations in group 1, and also about 89% of the observations in group 2 are for individuals receiving a low insulin dose (Table 4.1). According to Figure 4.2 and Table 4.1, HC doses did not show as much contribution to the clustering pattern as did insulin dose.

Table 4.1 Shows proportions (%) of samples with different HC and insulin doses based on the HCA grouping.

HCA grouping	Samples (n)	Low insulin dose			High insulin dose		
		L	M	H	L	M	H
1 (Green)	7	28.6	28.6	42.9	0.0	0.0	0.0
2 (Blue)	17	23.5	29.4	35.3	0.0	0.0	11.8
3 (Plum)	32	9.4	6.3	3.1	28.1	31.3	21.9

L= low GC, M= medium GC and H= high GC.

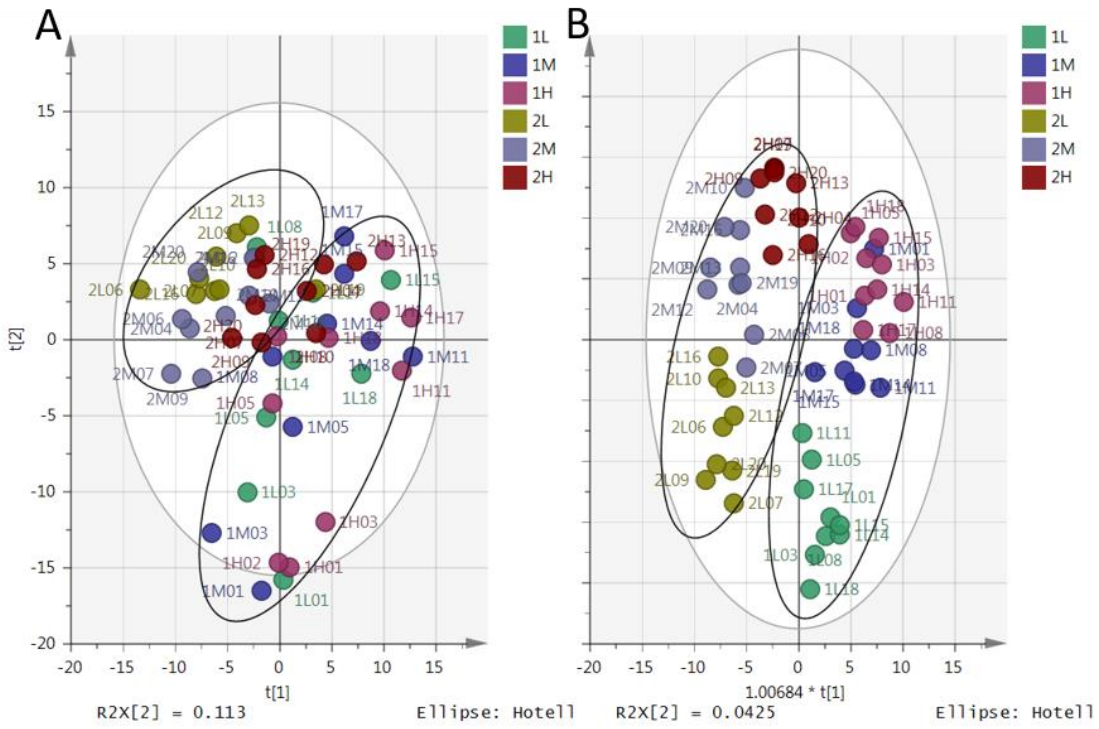

Figure 4.3 (A) PCA vs (B) OPLS-DA score plots for healthy individuals recieving different doses of HC and insulin.

PCA score plot (A) includes 2 groups of subjects (n=30 samples/10 subjects/group). Group 1 denotes samples with low insulin dose (n=30), group 2 denots samples with high insulin dose(n=30). Subjects in each group have 3 different levels of HC treatment; L = low HC, M = medium HC and H = high HC dose, R^2=0.638, Q^2=0.105. OPLS-DA score plot (B) includes the same group of subjects. Subjects in the same oval shapes were given the same insulin dose. In the OPLS-DA, model separation is between low and high GC doses in each insulin group but the domain of the medium GC dose overlaps with that of high GC dose in both insulin groups, while in the high insulin group also overlaps with the low GC dose, R^2=0.313, Q^2=0.243.

PCA score plot (Figure 4.3A) shows that there is separation between subjects having high insulin dose from those receiving a low insulin dose. Although subjects with a high insulin dose tend to show separation based on the HC dose, it is noticeable that subjects receiving a high HC dose overlap with the low insulin group, but this can't be confirmed as the plot is 2 dimensional.

Separation between groups based on both insulin and HC dose can be seen clearly in the OPLS-DA score plot although subjects with medium and high HC dose showed some overlap when low insulin dose had been given.

4.4.2 Biomarker identification

4.4.2.1 Effect of insulin dose on plasma metabolome of healthy individuals.

An OPLS-DA model was built on 606 putative metabolites, which were detected in 60 observations having either low or high insulin dose. Two observations (1M02 and 2H10) were excluded as they were considered to be outliers based on Hotellings' T^2 vs DModX plot, leaving 58 observations (29 observations per group) from high and low insulin groups. The resulting model identified 29 putative metabolites (Table 4.2) which were selected based on their 95% CI, corrected p-values (< 0.05), and AUC of the ROC curves (> 0.7). The identified metabolites were then used to rebuild the OPLS-DA model (Figure 4.4) in order to examine its ability to separate the subjects based on the insulin dose.

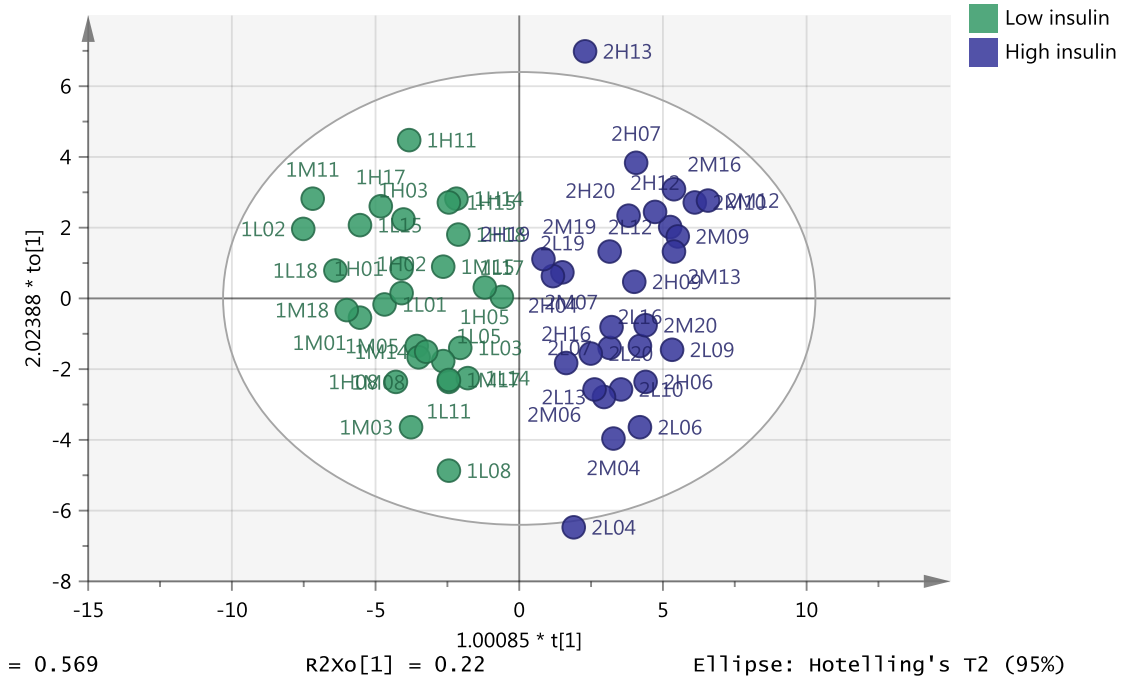

Figure 4.4 OPLS-DA score plot for for healthy individuals having either high or low insulin dose.
The OPLS-DA plot shows two groups of samples(n = 29 samples per group) based on readings of 29 significant putative metabolites in plasma of healthy individuals. Subjects with low insulin dose (green) and subjects with high insulin dose (blue). The model consists of one predictive x-score component; component t[1] and one orthogonal x-score components to[1]. t[1] explains 56.9% of the predictive variation in x, to[1] explains 22% of the orthogonal variation in x, R^2X (cum) = 0.789, R^2Y (cum) = 1, R^2 (cum) = 0.841, Accuracy of prediction Q^2 (cum) = 0.796.

The plot clearly shows separation between the two groups; around 79% of the variability in metabolites was explained by the model, of which 57% was due to insulin dose alone with the rest being linked to orthogonal variations. 84% of the variability between the samples was explained by the variability in the metabolites, of which 80% was predicted by the model following cross-validation. The validity of the number of orthogonal components in the model was examined using observed versus predicted plot (R^2 = 0.84) (Figure S4.1, appendix). Based on the permutation test (Figure S4.1B, appendix) this model has valid predictive ability compared to the newly permuted Q^2. Using 29 putative metabolites (Table 4.2) that were significantly changed by the insulin dose it was possible to classify samples based on the metabolomic change with 100% accuracy.

Table 4.2 Metabolites that change significantly following insulin dose.

Putative metabolite	AUC	High/Low insulin	FDR
Polyunsaturated fatty acids			
C22:4	0.87	0.48	0.0001
C22:6	0.86	0.46	0.0001
C20:2	0.92	0.37	0.000005
C20:4	0.81	0.59	0.002
C18:2	0.94	0.29	6.38E-07
C18:3	0.94	0.27	0.000002
Monounsaturated fatty acid			
C20:1	0.97	0.26	4.40E-07
C18:1	0.94	0.30	0.000003
C16:1	0.95	0.23	6.68E-07
C14:1	0.90	0.32	0.00001
Straight chain fatty acids			
C20:0	0.86	0.53	0.0001
C17:0	0.88	0.44	0.00001
C16:0 *	0.92	0.36	0.000007
C15:0	0.88	0.45	0.0001
C14:0 *	0.89	0.35	0.00002
C10:0 *	0.84	0.60	0.001
Acyl carnitine			
O-Acetylcarnitine *	0.92	0.57	4.60E-07
Decanoylcarnitine	0.91	0.47	0.000002
Oleoylcarnitine	0.96	0.58	0.000007
Branched chain amino acids			
L-Leucine *	0.79	0.74	0.003
3-Methyl-2-oxopentanoic acid ^{C18}	0.77	0.71	0.001
4-Methyl-2-oxopentanoate *	0.75	0.67	0.003
L-Isoleucine *	0.82	0.76	0.00008
L-Valine *	0.77	0.85	0.021
Miscellaneous			
4-Hydroxybutanoic acid	0.93	0.28	0.00006
2-Hydroxybutanoic acid *	0.73	0.64	0.013
Indolepyruvate	0.79	1.34	0.008
Gamma-Glutamylglutamine	0.73	0.81	0.017
Glycerol	0.90	0.74	0.0001

***** Retention time matches standard. ^{C18} metabolites identified using C18-AR column, the rest identified using ZICpHILIC column. (L=low insulin dose, H=high insulin dose).

Table 4.2 shows that all the metabolites were significantly decreased ($p < 0.05$) at high compared to low insulin doses except indolepyruvate which was significantly increased ($p = 0.008$). The majority of these putative metabolites demonstrated excellent classifying ability based on their AUC values (AUC > 0.9). Of the metabolites separated by the C18-AR column, only (S)-3-Methyl-2-oxopentanoic acid was significantly affected (H/L ratio = 0.71; $p = 0.001$) although it had a moderate classifying ability (AUC = 0.77).

Generally, in order to avoid the possibility of over-fitting in an OPLS-DA model, the number of the variables should be less than the total number of observations. (Xia *et al*., 2013) suggested that using 1-10 biomarkers for classification is more statistically robust and clinically more practical. For this reason, a new OPLS-DA model was created based on 10 most significant metabolites (Table 4.3), according to their AUC. The resulting model, shown in Figure 4.5, was able to separate the two insulin groups. This implies that these ten metabolites might be used as potential biomarkers for insulin dose.

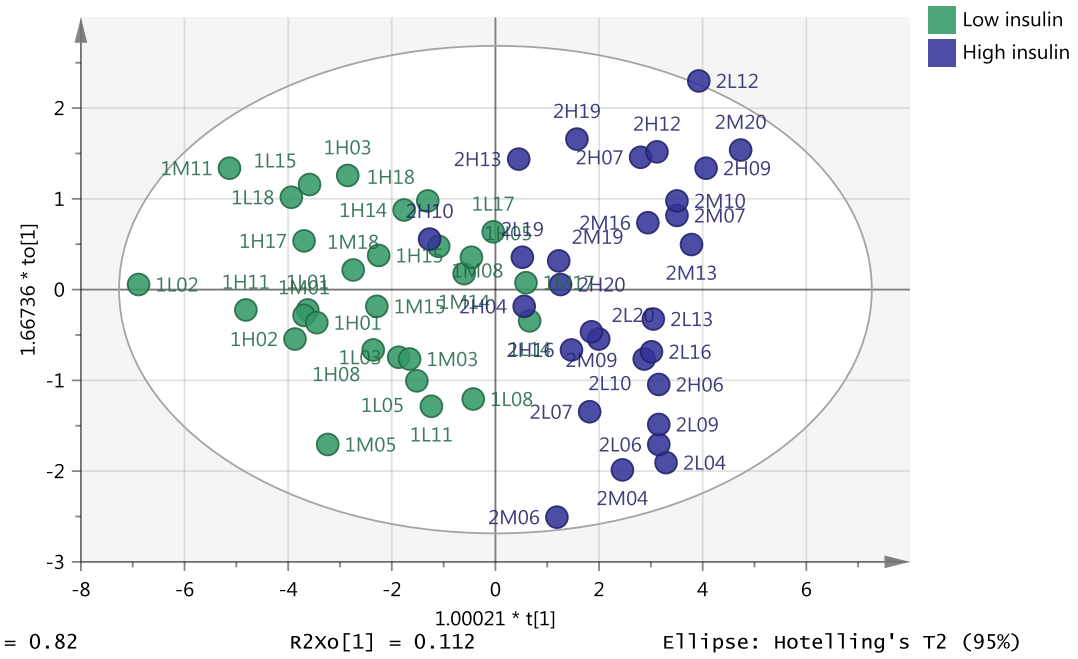

Figure 4.5 OPLS-DA score plot for the effect of insulin on 10 selected metabolites.
The OPLS-DA score plot based on 10 most significant putative biomarkers showing two groups: samples with low insulin dose (green) and sampless with high insulin dose (blue). The model consists of one predictive x-score component; component t[1] and one orthogonal x-score components to[1]. t[1] explains 82% of the predictive variation in x, to[1] explains 11.2% of the orthogonal variation in x, R^2X (cum) = 1, R^2Y (cum) = 1, R^2 (cum) = 0.706. Accuracy of prediction Q^2 (cum) = 0.665.

The OPLS-DA model (Figure 4.5) was based on the readings of 10 variables (Table 4.3) with the highest AUC values among the putative metabolites that were significantly affected by the insulin dose (Table 4.2) in plasma samples of 58 subjects (low insulin = 29, high insulin = 29). All these metabolites were strongly negatively correlated to insulin dose (|r| > 0.88). Two observations (1M02 and 2M12) were excluded as they were strong outliers based on Hotelling's T^2 vs DModX plot. The model shows that approximately 93% of the variations in these putative biomarkers were explained by the model; 82% of this variation was due to the insulin dose with *P* CV-ANOVA = 4.91E-12, while approximately 12% was due to orthogonal

variability. AUC shows an excellent classifying ability of these 10 putative metabolites with 98% accuracy based on the insulin dose.

Table 4.3 The 10 putative metabolites with highest AUC values and their correlations (r) to insulin dose.

Putative biomarkers	r	99% CI of difference
C20:2	-0.88	(-0.301 , -0.227)
C20:1	-0.94	(-0.318 , -0.25)
C18:3	-0.92	(-0.297 , -0.254)
C18:2	-0.92	(-0.3 , -0.254)
C18:1	-0.94	(-0.304 , -0.259)
C16:1	-0.92	(-0.285 , -0.267)
C16:0 *	-0.89	(-0.3 , -0.234)
4-Hydroxybutanoic acid	-0.83	(-0.316 , -0.181)
O-Acetylcarnitine *	-0.88	(-0.33 , -0.194)
Oleoylcarnitine	-0.94	(-0.367 , -0.198)

4.4.2.2 Effect of HC on the plasma metabolome

A total of 606 metabolites were measured in 60 subjects receiving 3 different HC doses: low HC dose = 20 subjects, medium dose = 20 subjects and high dose = 20 subjects. 4 observations (1L02, 1M02, 2L04 and 2H06) were excluded as they were considered to be outliers based on Hotellings' T^2 vs DModX plot. The medium HC dose was found to be a poor classifier (Xia et al., 2013) based on its AUC of 0.67 compared to low and high HC does (AUC = 1.0 each), and had a high proportion of misclassified observations (47.4%) compared to the other two doses (0% each) (Table 4.4). In addition, this dose was found to overlap with both low and high doses (Figure 4.3). For these reasons, the medium HC dose was not considered for further

comparisons in subsequent analysis. Thus only comparisons between low HC vs high HC were expected to give a better indication of how HC dose affects the human plasma metabolome.

Table 4.4 Misclassification table showing the proportions of correctly classified observations using on Fisher's probability.

Class	Smples (n)	Correct	LC	MC	HC
Low HC	14	100%	14	0	0
Medium HC	19	52.63%	1	10	8
High HC	12	100%	0	0	12
No class	9		3	1	5
Total	54	80%	18	11	25
Fisher's prob.	9.6e-009				

In a comparison of low HC vs high HC, 23 putative biomarkers (Table 4.5) which passed the 95% CI filter, showed significant change based on FDR corrected p values, and each had an AUC above 0.7. These 23 putative biomarkers were used to rebuild an OPLS-DA model (Figure 4.7) in order to examine its ability to separate observations based on HC dose.

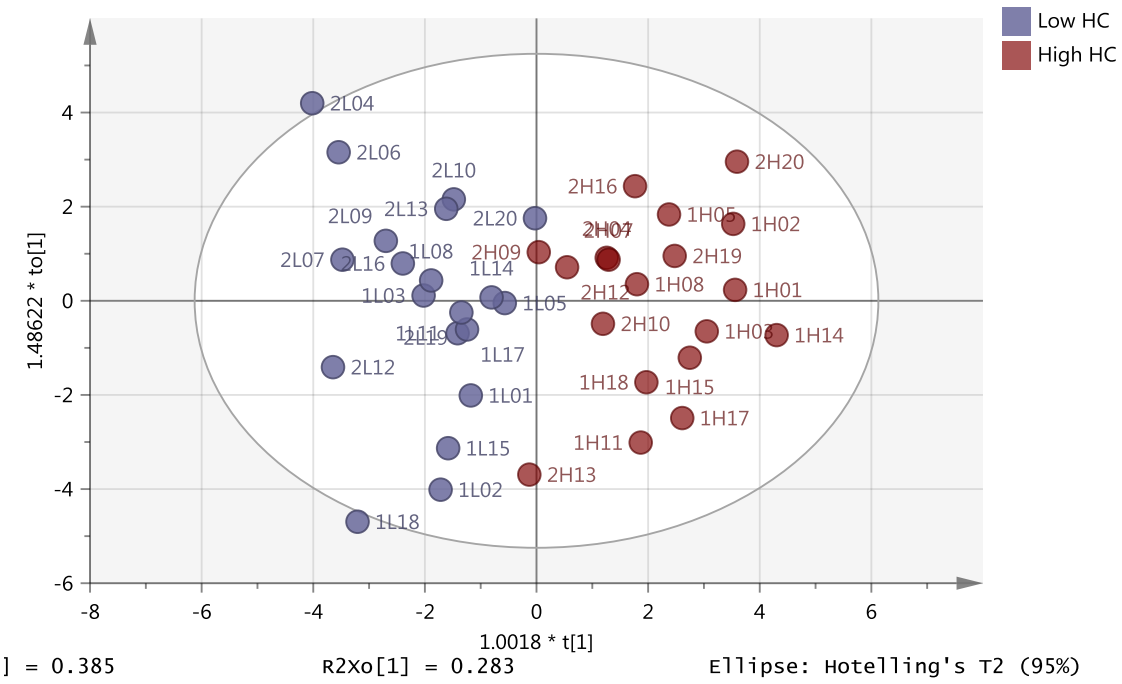

Figure 4.6 OPLS-DA score plot for the effect of HC dose on 23 significant puatative metabolites in plasma of healthy individuals.

The plot shows two groups: low HC dose (grey-blue) and high HC dose (red) observations. The model consists of one predictive x-score component; component t[1] and one orthogonal x-score components to[1]. t[1] explains 38.5% of the predictive variation in x, to[1] explains 28.3% of the orthogonal variation in x, R^2X (cum) = 0.66, R^2Y (cum) = 1, R^2 (cum) = 0.76. Accuracy of prediction Q^2 (cum) = 0.699.

The OPLS-DA score plot (Figure 4.6) was built on 23 putative biomarkers that significantly changed with HC dose. An outlier (2H06) was removed based on Hotelling's T^2 vs DModX plot. The plot clearly shows separation between observations having either low or high HC doses. Approximately 66% of the variability in metabolites was explained by the model, of which 38.5% was due to HC dose alone with the rest being linked to orthogonal variability. According to this model, 76% of the variability between the observations was explained by the variability in the metabolites, and also was able to predict around 70% of this

variability based on cross validated R^2. The validity of the number of orthogonal components in the model was examined using observed versus predicted plot, with a good fit of the regression line (R^2= 0.82) (Figure S4.2A, appendix). Based on the permutation test (Figure S4.2B, appendix), this model has valid predictive ability compared to the newly permuted Q^2. According to the area under the ROC curve, 23 putative biomarkers that were significantly changed by the HC dose have excellent classifying ability with 100% accuracy.

Table 4.5 Putative metabolites that were significantly affected in plasma of healthy individuals following HC dose.

Putative metabolite	AUC	High HC/Low HC	FDR
Lipids			
Fatty acids			
C22:6	0.72	1.58	0.00028
C20:4	0.74	1.41	0.002
C18:0	0.71	1.45	0.005
C17:0	0.72	1.49	0.005
C20:0	0.73	1.45	0.001
Miscellaneous			
2-Hydroxybutanoic acid *	0.83	1.66	0.00001
2-Oxopentanoic acid	0.72	1.23	0.00004
2-Ketobutyric acid *	0.81	2.02	0.00002
Methylacetoacetic acid	0.80	1.27	0.0002
Androsterone glucuronide	0.84	0.48	3.30E-08
Pregnenolone sulphate	0.95	0.30	1.70E-09
Branched chain amino acids			
(S)-3-Hydroxyisobutyrate [C18]	0.77	1.52	0.0004
(S)-3-Methyl-2-oxopentanoic acid [C18]	0.89	1.56	6.10E-08
4-Methyl-2-oxopentanoate *	0.93	1.69	0.001
L-Leucine *	0.76	1.30	0.002
L-Isoleucine *	0.81	1.24	0.00005
3-Methyl-2-oxobutanoic acid *	0.77	1.25	0.0003
L-Valine *	0.75	1.16	0.001
Miscellaneous			
Hypoxanthine *	0.74	1.28	0.004
Xanthine *	0.83	1.30	0.00001
Gamma-Glutamylglutamine	0.75	1.21	0.004
6-methyltetrahydropterin	0.76	1.44	0.008
2-Methylbutyroylcarnitine	0.82	1.58	0.000008

* Confirmed by standard. [C18] metabolites identified using C18 column, the rest identified using ZICpHILIC column. (L= low HC, H=high HC), p-value obtained from split plot ANOVA.

Table 4.5 above shows significant elevation of branched chain amino acids and their deaminated metabolites following high HC dosage. Purine metabolites, represented by xanthine and hypoxanthine, and C20:4, C22:6 and C18:3 fatty acids, were significantly elevated by high HC dose. On the other hand, steroids, that is pregnenolone sulfate and androsterone glucuronide, were the only metabolites that showed significant reduction after higher HC dosage.

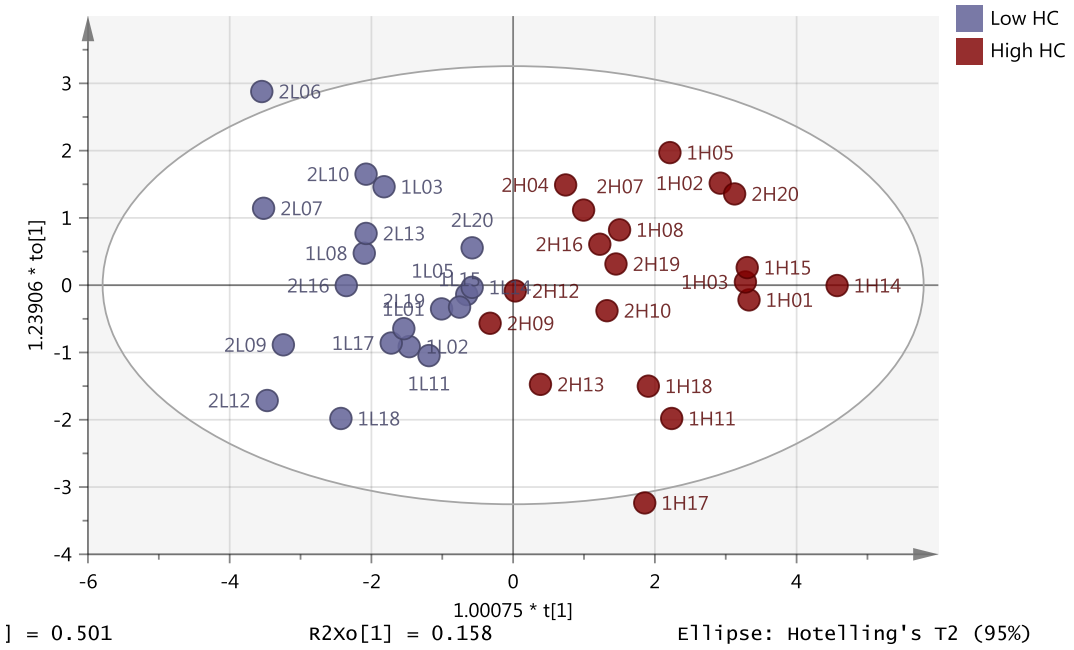

Figure 4.7 OPLS-DA score plot for the effect of HC dose on selected 10 significant putative metabolites with highest AUC valuse in plasma of healthy individuals.
The plot shows two groups: subjects with low HC dose (grey-blue) and subjects with high HC dose (red). The model consists of one predictive x-score component; component t[1] and one orthogonal x-score components to[1]. t[1] explains 50% of the predictive variation in x, to[1] explains 15.8% of the orthogonal variation in x, R^2X (cum) = 0.65.9, R^2Y (cum) = 1, R^2 (cum) = 0.74 and accuracy of prediction Q^2 (cum) = 0.693.

The OPLS-DA model (Figure 4.7) was built on readings of 10 variables having the highest AUC values among the putative metabolites significantly affected by the HC dose (Table 4.6, below) in plasma samples of 38 observations (low= 19, high= 19). All these metabolites showed varying degrees of positive correlation ($0.54 \leq r \leq 0.85$) except the steroid conjugates androsterone glucuronide ($|r| = 0.7$) and pregnenolone sulfate ($|r| = 0.85$) which were negatively correlated with HC dose. Two observations (2L04 and 2H06) were excluded as they were outliers based on Hotellings' T^2 vs DModX plot. The model shows that about 66% of the variations in these putative biomarkers were explained by the model, 50% of this variation was due to the HC dose with *P* CV-ANOVA = 4.32E-08, while about 16% was due to orthogonal variation. The area under the ROC curve shows an excellent ability of these metabolites to classify the samples with 100% accuracy based on the HC dose. When observations of medium HC dose were added to the model, the ability of the 10 putative biomarkers to classify observations based on their HC dose was reduced as follows: low HC = 0.94, medium HC = 0.69 and high HC = 90.

Table 4.6 The 10 metabolites with highest AUC values and their correlations (r) to HC dose.

Putative biomarkers	r	99% CI of difference[b]
(S)-3-Methyl-2-oxopentanoic acid [C18]	0.78	(0.159 , 0.403)
4-Methyl-2-oxopentanoate *	0.85	(0.193 , 0.418)
L-Isoleucine *	0.69	(0.118 , 0.381)
Methylacetoacetic acid	0.56	(0.021 , 0.381)
2-Hydroxybutanoic acid *	0.68	(0.082 , 0.408)
2-Ketobutyric acid *	0.54	(0.045 , 0.344)
2-Methylbutyroylcarnitine	0.66	(0.04 , 0.436)
Xanthine *	0.68	(0.0025 , 0.488)
Androsterone glucuronide	-0.7	(-0.418 , -0.088)
Pregnenolone sulphate	-0.85	(-0.422 , -0.192)

[b] 99% certain that the difference would fall within the defined interval based on cross validation.

4.4.2.3 Metabolites affected by both HC and insulin

Twelve putative metabolites were found to be significant in both insulin and HC treatments ($p < 0.05$) as shown in Table 4.7.

Table 4.7 Putative biomarkers significantly affected by both interventions (Split plot ANOVA).

Putative metabolite	1L : 1H : 2L : 2H	p-value (HC)	p-value (insulin)
Fatty acids			
C22:6	1 : 1.44 : 0.38 : 0.75	0.0003	0.000126
C20:4	1 : 1.34 : 0.54 : 0.84	0.002	0.002
C20:0	1 : 1.26 : 0.41 : 0.79	0.001	0.000106
C18:0	1 : 1.36 : 0.42 : 0.71	0.005	0.00002
C17:0	1 : 1.37 : 0.37 : 0.67	0.005	0.000015
2-Hydroxybutanoic acid *	1 : 1.63 : 0.62 : 1.07	0.000013	0.013
Branched chain amino acids			
L-Isoleucine *	1 : 1.23 : 0.69 : 0.98	0.00006	0.00009
L-Leucine *	1 : 1.25 : 0.77 : 0.95	0.002	0.003
L-Valine *	1 : 1.18 : 0.86 : 0.99	0.001	0.021
4-Methyl-2-oxopentanoate*	1 : 1.62 : 0.62 : 1.13	0.0018	0.003
3-Methyl-2-oxopentanoic acid^{C18}	1 : 1.57 : 0.71 : 1.11	0.00000061	0.001
Peptide			
Gamma-Glutamylglutamine	1 : 1.19 : 0.79 : 0.98	0.004	0.017

* Retention time confirmed by standard. ^{C18} metabolites identified using C18-AR column, the rest identified using ZICpHILIC column. (in the ratio column, 1=low insulin, 2=high insulin, L= low HC, H=high HC). Fold change been calculated based on the average of absolute intensity of each group, and normalised to the first phase (1L= low insulin, low HC) as a reference for comparison. N.B. SPSS out-put.

All the 12 metabolites were elevated by HC and reduced by insulin doses respectively. A heat map of the 12 metabolites which were significant in both inteventions was plotted using Metaboanalyst based on intensitites of each metabolites in each observation (Table 4.8).

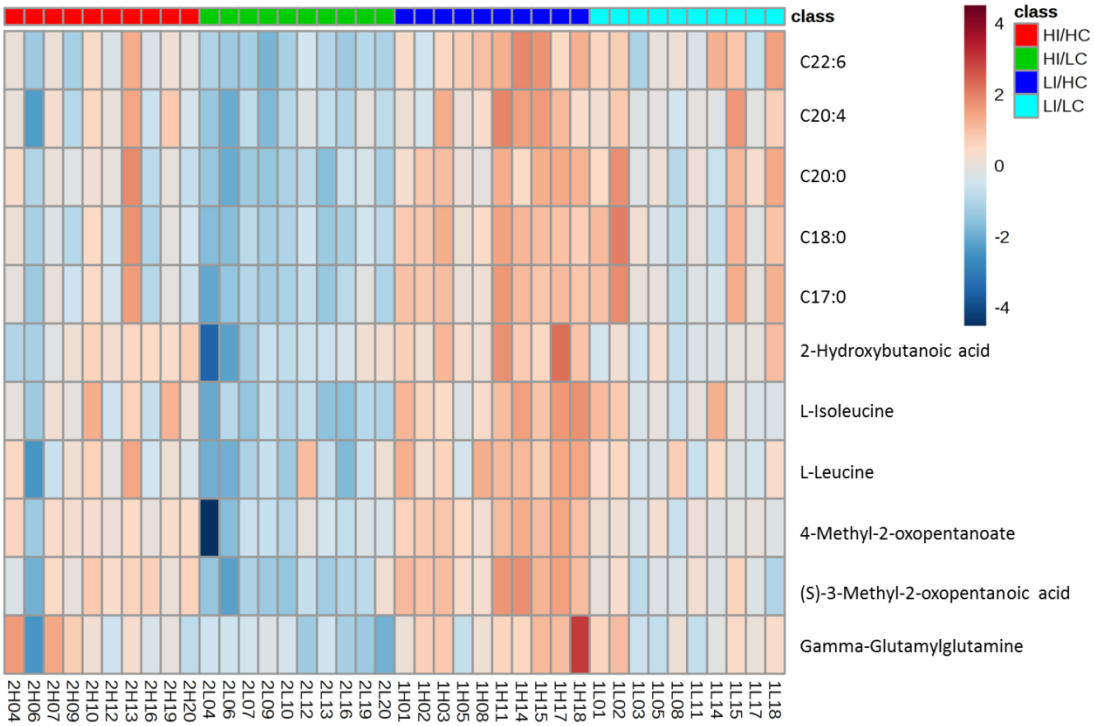

Figure 4.8 Heat map shows putative biomarkers that significantly affected by both interventions insulin and HC.

The plot shows heat map of the putative biomarkers (Table 4.7, above)that significantly changed following insulin and HC doses in individual samples after excluding medium HC dose (n = 40). The different colour shades represent intensities of each metabolite (rows) in each observation (column). The metabolites were generally increased in observations with low insulin/high HC class (LI/HC - dark blue), decreased in high insulin/low HC class (HI/LC - green), and unevenly disturbed in both low and both high insulin and HC respectively. Valine wasn't given in the heat map from Metaboanalyst.

The clearest effect in the heat map was that the putative biomarkers were reduced in observations with a high dose of insulin plus low dose of HC. In contrast, the putative biomarkers were elevated in the samples with low insulin plus high HC doses. In addition, individuals responded differently with regard to these metabolites when high insulin and high HC or low insulin and low HC were given.

Based on a split-plot ANOVA, only three metabolites (Table 4.8) showed significant interaction between insulin and HC doses. All the three metabolites were significantly increased ($p < 0.05$) following high HC dose, while 3-methyl-2-oxobutanoic acid was significantly decreased ($p = 0.036$) following high insulin dose. High insulin dose renders the elevation of methylacetoacetic acid and 3-Methyl-2-oxobutanoic acid following high HC dose insignificant and also reduces the significant elevation of 2-methylbutyroylcarnitine from 1.9 to 1.31.

Table 4.8 Putative metabolites that show significant interaction in both interventions.

Putative metabolite	Ratio	P-value		
	1L : 1H : 2L : 2H	Interaction	HC	Insulin
2-Methylbutyroylcarnitine	1 : 1.9 : 1.1 : 1.38	0.015	0.000008	0.37
Methylacetoacetic acid	1 : 1.4 : 0.9 : 1.04	0.023	0.000272	0.08
3-Methyl-2-oxobutanoic acid	1 : 1.3 : 0.9 : 1.02	0.014	0.000364	0.03

In the ratio column, 1=low insulin, 2=high insulin, L= low HC, H=high HC. Output of split-plot ANOVA (SPSS). Fold change been calculated based on the average of absolute intensity of each group, and normalised to the first phase (1L= low insulin, low HC) as a reference for comparison.

4.5 Discussion

All subjects in the study were given metyrapone which blocks the conversion of inactive cortisone to the active cortisol via 11β-hydroxysteroid dehydrogenase 1 enzyme. With the production of cortisol being inhibited, it was then replaced by infusing HC at three different levels, in the presence of either low or high insulin. The data set presents a clear set of metabolites which impact on a number of pathways that have been linked to the actions of HC and insulin. There are three clear effects which can be observed within this data which are due to insulin alone, HC alone, and where insulin and HC interact with each other.

In Tables 4.2, 4.5 and 4.7 metabolites which were significantly changed by insulin, HC, and their interaction, respectively, are shown. Comparisons between low and high insulin, and between different levels of HC infusion, are presented on the basis of a simple T-test of the log 2 transformed data and the FDR corrected p-value. Metabolites affected by both treatments where tested again using split plot ANOVA in order to examine the significance of the interaction between insulin and HC for each metabolite.

The clearest effect where insulin and HC oppose each other is with regard to an effect on the metabolism of BCAA and their metabolites. High insulin significantly (*p* value < 0.05)reduces the levels of leucine/isoleucine, valine and their metabolites compared with low insulin. Increasing the dose of HC infused increases the levels of

leucine/isoleucine and their metabolites irrespective of insulin dose. HC in the presence of low insulin dose also produces an increase in BCAs as the concentration of HC is increased and this is the strongest metabolic signature of HC action amongst all the significantly altered metabolites. This observation links to the role of BCAs in obesity and insulin resistance observed in the literature (Batch *et al*., 2013, Huffman *et al*., 2009, McCormack *et al*., 2013). Thus, in the current case, a similar effect is observed from a different perspective, where insulin directly lowers BCAA levels significantly (p value < 0.05) and HC opposes this effect. HC is known to promote breakdown of muscle proteins (van Raalte *et al*., 2009), while BCAs are known to promote production of muscle protein (Krebs, 2005, Krebs and Roden, 2004, Rennie *et al.*, 2006). In contrast, insulin is known to promote production of muscle tissue and this would be consistent with an increased requirement for BCAs and hence a reduction of their circulating levels. BCAs are not just a building block of the muscles, but may also have some pharmacological activity. BCAs may exert some beneficial effect in the treatment of insulin resistance associated with chronic liver disease: in a rat model with liver cirrhosis, BCAA improved glucose uptake (Nishitani *et al.*, 2005); in rodents, BCAA improve glucose metabolism in hepatocytes, skeletal muscle, and adipocytes (Nishitani *et al.*, 2002, Hinault *et al.*, 2004, Broca *et al.*, 2004).

Another clear effect where insulin and HC act in opposition is with regard to poly unsaturated fatty acid (PUFA) metabolism. Previously, it was observed that omega-3/omega-6 PUFA levels increased in response to BCAA in two cases (Kawaguchi *et*

al., 2007). In the current case, high insulin lowers the levels of PUFA and, irrespective of insulin, high HC dose increases levels of PUFA.

The most comprehensive list of metabolites within a class that were affected by insulin were the FFAs. Many FFAs are lowered by > x2 by insulin infusion and effects are seen of fatty acids with chain lengths between C10 and C22. HC appears to act in an opposite manner to insulin by promoting higher levels of some FFAs in plasma. Presumably a relatively low level of HC is required to increase levels of FFAs and thus increasing the level of the HC infusion does not promote this process any further—a reason why there was no significant difference between medium and high HC doses. Nevertheless, irrespective of insulin, which lowers the levels of FFAs, the effect of increasing the dose of HC infusion on some fatty acids can be observed. (Bordag *et al*., 2015) observed a decrease in the levels of poly unsaturated fatty acids in plasma following dexamethasone treatment. The difference in the current study may be that the subjects underwent GC block prior to HC replacement.

(Batch *et al*., 2013) also described the elevation of C3 and C5 acylcarnitines in obese compared with lean subjects and the elevation of these metabolites in rats fed a diet enriched with BCAA. Insulin has a marked effect in lowering acyl carnitines. The most marked effect is in lowering decanoylcarnitine. HC generally does not have a marked effect on the levels of these metabolites, but has a significant effect on 2-methylbutyroylcarnitine in particular. However, when HC acts against the insulin

infusion it promotes a marked elevation of oleoylcarnitine. There is no effect on carnitines above chain length C16:0. There is evidence that high levels of long chain fatty acids such as C16:0 are toxic, promoting apoptosis via a mechanism involving caspase 2 (Johnson *et al.*, 2013). Thus, carnitine conjugation provides a means of removing C16:0 and other shorter chain acids. The role of carnitine in tissues is as a buffer for acylCoA/CoA levels. CoA is compartmentalised within the cell and cannot cross membranes (Zammit *et al.*, 2009). Within mitochondria, the transfer of an acyl group from acylCoA to carnitine maintains the level of free CoA and allows the acyl group to enter or leave the organelle in the form of its carnitine ester. Carnitine palmitoyl transferase is present on the outer membrane of mitochondria and only selects long chain fatty acids for entry into mitochondria. However, the availability of a range of carnitine transferases within mitochondria and peroxisomes permits the export of fatty acids with different chain lengths out of these organelles (Zammit *et al*., 2009).

Tryptophan metabolism is regulated by GC and insulin which regulate the enzyme tryptophan dioxygenase (TDO) (Nakamura *et al.*, 1980, Fernstrom and Wurtmen, 1972, Sono, 1989, Ochs *et al.*, 2015). Insulin was found to inhibit the induction of TDO by dexamethasone (Nakamura *et al*., 1980). Indolepyruvate as a metabolite in the tryptophan pathway shows significant elevation following high insulin dose and non-significant reduction following HC dose. (Bordag *et al*., 2015) observed elevation of a number of tryptophan metabolites in plasma following dexamethasone treatment. There is a link between tryptophan metabolism and

purine metabolism. TDO has haem at its active centre and enzyme activity is regenerated by coupling with the superoxide anion. One of the major sources of superoxide in the body is from the action of xanthine oxidase which converts hypoxanthine via xanthine to uric acid (Sono, 1989). Elevated xanthine and hypoxanthine is associated with the high GC group and this could indicate an increase in xanthine oxidase leading to increased availability of the superoxide required to support TDO activity.

Finally, the other major alterations in response to HC are, as might be expected, in steroid metabolism. HC suppresses ACTH resulting in reduced adrenocortical secretion of precursor steroids which, in the presence of metyrapone, are diverted to adrenal androgens. This most likely explains the reduction, with increasing HC, of androsterone glucuronide, a metabolite of adrenal androgens such as dehydroepiandrosterone, dihydrotestosterone or androstenedione; and of pregnenolone sulphate, a metabolic precursor of HC. Bordag *et al* observed that dexamethasone decreased the levels of a number of steroid hormones, particularly androstenedione (Bordag *et al*., 2015).

Of course, metabolite changes detected in plasma are only an indirect indicator of the biochemical changes in target tissues for cortisol and insulin. Moreover, there may be a bias in metabolomic studies in favour of detecting changes in the most abundant, rather than the most biologically important metabolites. Of equal interest, however, is the pragmatic application of changes in metabolites as

biomarkers to measure GC or insulin action. For insulin, fasting plasma insulin/glucose ratios are the only non-invasive approach to determine insulin sensitivity, and classification of risk of T2D could be enhanced by additional biomarkers. By combining 4 markers, we demonstrate high sensitivity to discriminate between high dose and low dose insulin infusion, but further tests in large numbers will be required to test associations with physiological insulin action. For GCs, there are no reliable specific or sensitive biomarkers, since even measurement of plasma cortisol is subject to many caveats. We show that a combination of 10 markers has reasonably high sensitivity to discriminate between low and high dose HC infusion, although the discrimination of medium dose infusion remained relatively poor (AUC = 0.69). It remains to be tested whether these markers, in combination or alone, will be sensitive to physiological or pharmacological variation in cortisol action, and crucially whether they have specificity when compared with effects of obesity and other features which accompany GC excess.

Chapter 5:

Metabolomic Profiling of Patients with Congenital Adrenal Hyperplasia Confirms Uncertainty in Finding Reliable Biomarkers Associated with the Disease Progress

5 Metabolomic profiling of patients with congenital adrenal hyperplasia uncovers significant biomarkers associated with the disease progress.

5.1 Abstract

Background and Aim: Patients with CAH are treated with GC in order to replace the low levels of endogenously produced GC. To date, there are no reliable tools to assess health outcomes arising from under or over treatment. Metabolomics signatures based on anthropometrics and clinical measurements can be used to determine patients at heightened risk of developing further complications.

Methodology: MS based metabolomics profiling was carried out on plasma samples from 119 patients with varying anthropometric and clinical measurements. HCA was initially used to assess the clustering pattern of patients based on their anthropometric measurements; then OPLS-DA was employed to examine the metobolomic differences among the clustered groups.

Results: This analysis revealed that the patients in fact fell into three distinct groups, in which GC dose still had only a minor contribution (VIPpred = 0.44), while BMI (VIPpred = 1.38), BP (VIPpred = D 1.27/S 1.32), and weight (1.39) had major contributions to the between-group differences. Patients in the first group had higher BMI, GC dose, systolic and diastolic blood pressure and lower levels of androstenedione and 17-hydroxyprogesterone compared to the other two groups.

The metabolomics analysis revealed that 13 metabolites including branched chain amino acids and the taurine pathway were significantly elevated in G1 compared to G2 and G3.

Conclusion: These 13 metabolites were employed to produce receiver operator characteristics (ROC) curves with fair classification based on AUCs in the range of 0.75. Further assessment is required to determine the relevance of these molecules as potential predictors of health status of patients with CAH.

5.2 Introduction

GC are some of the most widely prescribed class of drugs, both for treating inflammatory conditions and for replacement therapy in conditions where endogenous GC are deficient such as CAH. CAH is an autosomal recessive diseases affecting cortisol biosynthesis (Merke, 2008). 95% of CAH cases account for mutations in the CYP21A2 gene which encodes 21-Hydroxylase enzyme (Krone *et al.*, 2000), and rarely due to mutation in CYP17A1 wich encodes 17α-hydroxylase enzyme (Guenego *et al.*, 2015). Recently, it has been found that cases with deficiency in both enzymes are due to mutation in P450 oxidoreductase (POR) which facilitates electron transfer from NADPH to those enzymes (Dhir *et al.*, 2007, Krone *et al.*, 2007). 17α-hydroxylase enzyme catalyses the conversion of progesterone to 17-hydroxyprogesterone and pregnenolone to androstenedione, while 21-hydroxylase enzyme catalyses the conversion of 17-hydroxyprogesterone into GCs and mineralocorticoids (Dhir *et al*., 2007).

Currently recommended treatment regimens for GC replacement in patients with CAH involve daily doses of HC or cortisone acetate administered twice- or thrice-daily. Whereas prednisolone is recommended as an alternative to HC for once- or twice-daily dosing in patients with reduced compliance, dexamethasone is not recommended at all due to the risk of Cushing-like side effects arising from dose titration difficulties (Bornstein *et al.*, 2016), and both alternatives have been associated with impaired quality of life among CAH patients (Han *et al.*, 2013b). The

drugs act on intracellular GC receptors widely expressed in mammalian cells to mediate a variety of physiological processes including energy metabolism (Andrews and Walker, 1999a, Macfarlane *et al*., 2008b), cardiovascular control (Walker, 2007b), cellular proliferation, central nervous system (CNS) function (Seckl and Olsson, 1995), and innate immunity (Sapolsky *et al*., 2000).

Determining the optimal dose for GC replacement particularly in CAH is incredibly difficult, with over-replacement leading to Cushing adverse metabolic effects while under-replacement increases the risk of adrenocortical crisis or death, especially during infections and other periods of increased stress (Johannsson *et al*., 2015). At present very few patients with adrenal insufficiency on GC treatment achieve good disease control and their treatment outcomes are generally poor (Han *et al.*, 2013a), with high morbidities and low overall life expectancies (Johannsson *et al*., 2015). This has been attributed to the failure of the treatment to replicate the normal circadian rhythm of cortisol release in the body, as well as a lack of individualised treatment protocols for patients in whom specific dosing would be more beneficial.

In addition, treatment of patients with Cushing's syndrome, a disease associated with chronic GC excess, and in whom surgical intervention is unresponsive, is difficult to monitor particularly when using GC receptors antagonists such as mifepristone. This is further complicated by the fact that biochemical (hormonal) monitoring of GC replacement is currently not recommended (Bornstein *et al*.,

2016) as there are no known reliable biomarkers of GC action. Instead, the recommended monitoring for GC replacement relies on clinical markers such as body weight, postural blood pressure, energy levels and signs of clear GC excess (Bornstein *et al*., 2016) which might not accurately reflect the prevailing state of the patient's GC action.

Models that assess the disease status based on number of admissions/visits to the hospital per year plus other clinical parameters were suggested (Hummel *et al.*, 2016). Although these showed good sensitivity to the disease assessment, these models cost a lot in terms of time and money, and would be a burden on health care systems. Thus, in order to determine the categories of patients at a high risk of developing other diseases arising from GC use, untargeted metabolomics profiling was carried out by liquid chromatography-high resolution mass spectrometry (LC-HRMS) on plasma samples from 119 patients with varying anthropometric (BMI, height, weight, age) and clinical (systolic & diastolic BP and levels of androstenedione & 17-OH progesterone) measurements, undergoing treatment for CAH with different doses of GCs (as prednisolone equivalent, PredEqBNF). Multivariate statistical analysis was applied to the complex metabolite datasets generated in order to pinpoint the key metabolites that would eventually lead to the detection of patients in whom further interventions or monitoring would be required to prevent against risk of GC over- or under-dose.

5.3 Methodology

5.3.1 Anthropometric data collection

The procedures for patient recruitment and assessment have already been described in sections 6.3.1 (Patient recruitment) and 6.3.2 (Procedure for collection of anthropometric data).

5.3.1.1 Patient's numbering

119 patients, each one had a number of 6 characters. The first character was represented the centre of the study, the last 5 characters represented the patient's number in that centre. For example, C05005, C = this patient belongs to centre C, 05005= patient's number.

5.3.2 LC-MS analysis

- LC-MS conditions and sample preparation procedures are reported in detail in section 2.1-2.3 (pages: 47-51).
- Column used in this project is ZICpHILIC.

5.3.3 Data extraction and processing

Details of data extraction and processing are reported in section 2.4 (pages: 51-54).

5.3.4 Data analysis

The data was analysed as described already in section 2.5 (pages: 54-58). Additionally, One-Way ANOVA was employed to test the differences in the anthropometrics and clinical measurements between the three groups.

5.4 Results

5.4.1 Anthropometrics and clinical measurements

5.4.1.1 Multivariate analysis

In order to detect patients at risk of further physiological abnormalities from GC use, a PCA model was built based on the readings of the anthropometric and clinical measurements in all the 119 patients, followed by HCA. The anthropometric and clinical measurements divided the patients into 3 groups on the basis of similarity between the observations as shown in the dendrogram plot (Figure 5.1). Since there were three clear groups uncovered by the unsupervised analysis, a supervised OPLS-DA model was then created based on the groups highlighted by HCA (Figure 5.2A). This model clearly showed separation between the three groups, the model explained 46.4% of the variation in the anthropometric and clinical parameters among the groups. The model attributed 57% of the variation between the patients to the variation in the anthropometric and clinical parameters.

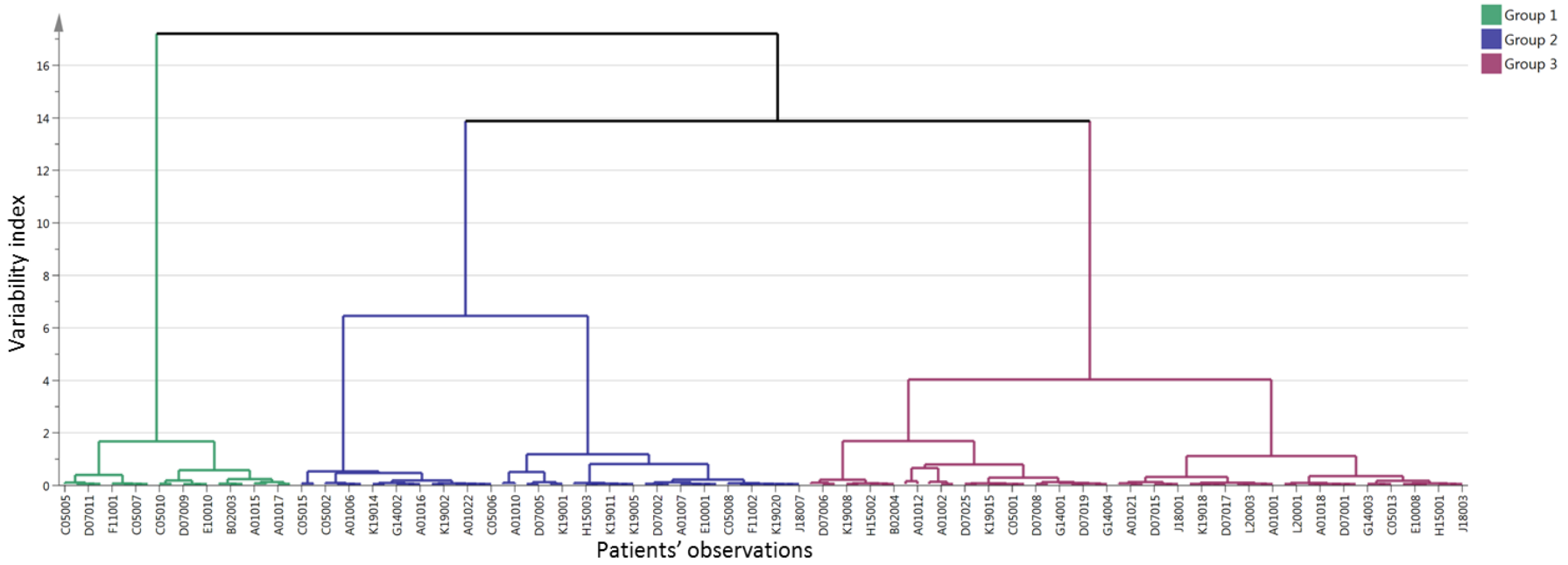

Figure 5.1 Hierarchical Clustering Analysis (HCA) of patients with CAH based on anthropometrics and clinical measurements.
The dendrogram shows clustering of 119 patients into three groups. X-axis represents patient observations (no enough space for all the samples to appear on the figure) and y-axis shows variability index. The higher the variability index, the larger the between group variability; and the smaller the variability index, the smaller the within group variability.

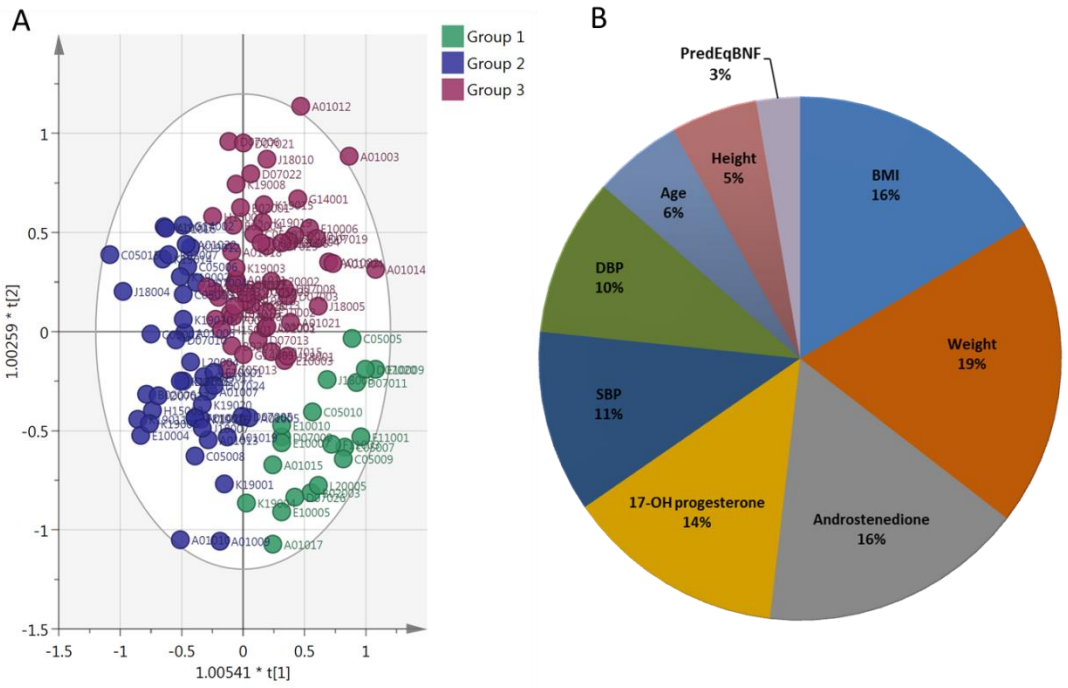

Figure 5.2 (A) OPLS-DA score plot of 119 patients with CAH based on anthropometrics and clinical measurements, and (B) Pie chart showing the contribution of each anthropometric and clinical parameter in the classification.

Plot **A**, shows 119 samples of patients with CAH clustered into three groups based on their anthropometrics and clinical measurements, group 1 (20 samples - green), group 2 (43 samples - blue) and group 3 (56 samples - plum). The model consists of two predictive components t[1-2]. R^2X (cum) = 0.464, R^2Y (cum) = 1, R^2 (cum) = 0.569, Goodness of prediction Q^2 (cum) = 0.547. **(B)** Pie chart showing how each measurement; androstenedione, 17-OH progesterone, weight, height, age, body mass index (BMI), GC treatment (GT), systolic and diastolic blood pressure (SBP & DBP) contributed to the classification of the patients with CAH into 3 groups based on partial eta squared for each parameter.

The current gold standard in testing metabolomics models is the use of a ROC (Xia *et al*., 2013). The AUC for a ROC classification is regarded as excellent when AUC > 0.9. The supervised model classified the patients into 3 groups, and in order to test the ability of the model to produce such a classification, the areas under the ROC curves were employed (Figure S5.1, appendix). The AUC of the ROC for the groups were: group 1 = 0.99, group 2 = 0.99 and group 3 = 0.91, all indicating excellent to perfect classification.

5.4.1.2 Univariate analysis

The pie chart (Figure 5.2B) showed that weight, androstenedione, BMI and 17-OH progesterone had the most significant contribution to the classification of the patients into 3 groups based on one-way ANOVA with p-values: 9.52E-14, 1.03E-9, 3.12E-12 and 1.70E-8 respectively. On the other hand GC treatment had the lowest contribution to the grouping with only a 3% contribution and a *p* value = 0.034. Systolic and diastolic blood pressure measurements also showed a significant contribution to the group classification with *p* values of 8.73E-8 and 9.86E-7 respectively (Figure 5.3).

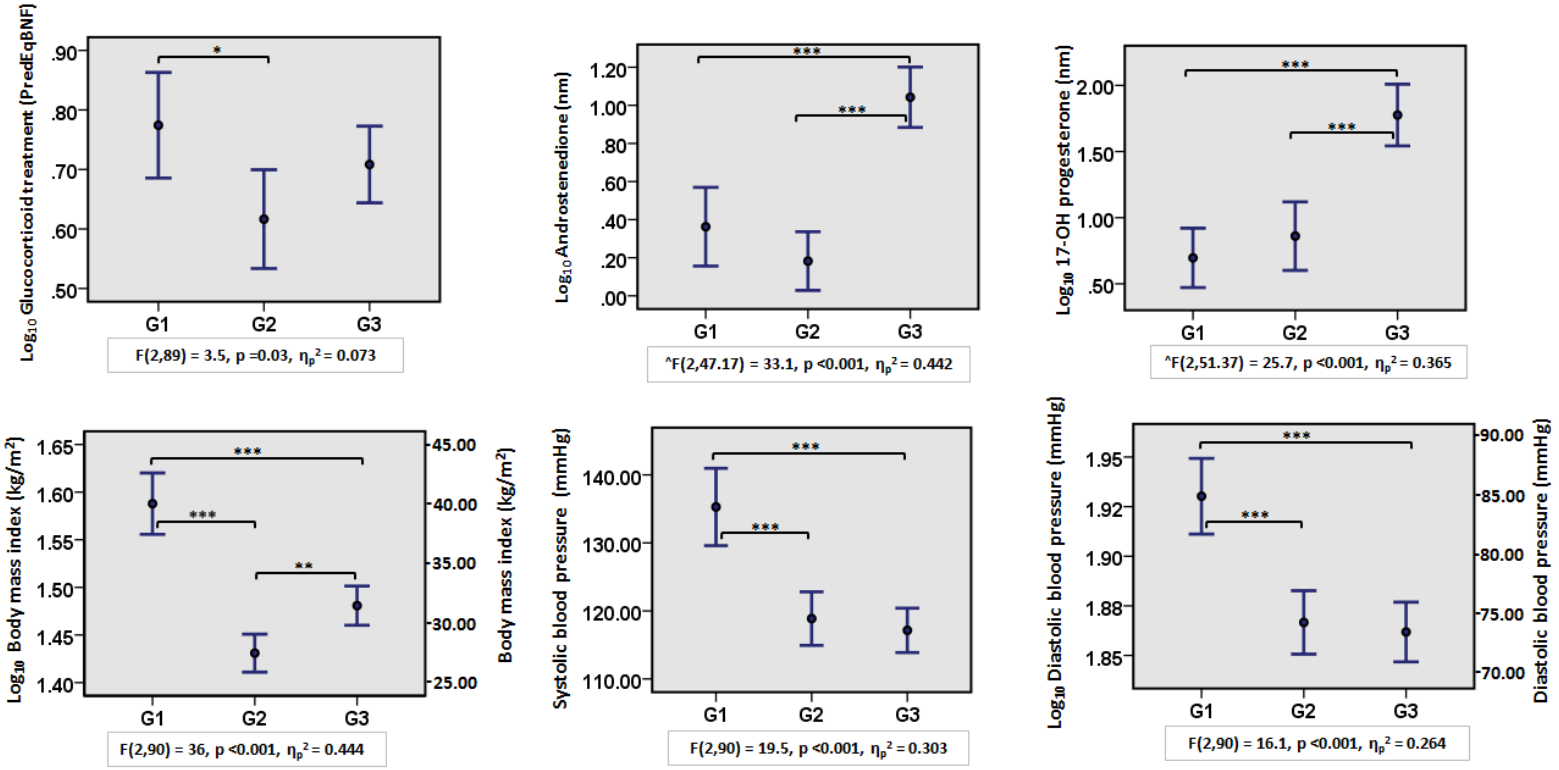

Figure 5.3 Error plots (means and 95% confidence intervals), comparing the anthropometrics and clinical measurements among the three groups using one-way ANOVA.

The plot shows differences of anthropometric and clinical measurements among groups; group 1 (G1), group 2 (G2) and group 3 (G3). The measurements are; GC treatment, androstenedione, 17-OH progesterone, systolic and diastolic blood pressure, body mass index. Each plot presents F statistics, one-way ANOVA based p-value and partial eta squared (η^2_p). ($^{\wedge}F$) = F statistics value based on Welch test, and any significance in these parameters was based on Games-Howell post hoc test, otherwise p-value based on Scheffe post hoc test. (*, p<0.05), (**, p<0.01) and (***, p<0.001).

The error plots (Figure 5.3) show how the anthropometric and clinical measurements varied among the three groups. Based on the similarities in the readings, patients clustered into three groups G1 (n=20), G2 (n=43) and G3 (n=56). Patients in G1 have significantly higher BMI (median=39.1, IQR=37.1-41.6 kg/m^2), SBP (135.55 ± 11.54 mmHg), DBP (median=86.2, IQR=78.4-92.4 mmHg) and GC dose (median=6, IQR=4.75-7.25 predEqBNF) compared to G2 and G3. Similarly, G1 also had significantly lower levels of 17-hydroxyprogesterone (median=4.1, IQR=2.38-6.45 nmol/l) and androstenedione (median=2.25, IQR=1.53-3.9 nmol/l) (Table 5.1, below).

Table 5.1 Shows values of the anthropometrics and clinical measurements among the three groups.

	Median (Q1, Q3) / Mean ± SD		
Parameter	**G1**	**G2**	**G3**
Androstenedione (nmmol/l)[b]	2.25(1.53,3.9)	1.6(1.1, 3)	8(3.7,27.3)
17-OHprogesterone (nmmol/l)[b]	4.1(2.38,6.45)	8.65 (3, 15.48)	64.5(10.08, 185)
GC dose (PredEqBNF)[b]	6(4.75,7.25)	5(2.5,6.13)	5(3.63, 7.5)
BMI (kg/m^2)[b]	39.1 (37.1,41.6)	26.5 (24.65,29.6)	29.6(28.45,33.8)
SPB (mmHg)	135.55±11.54	117.64± 10.31	116.78 ± 9.89
DPB (mmHg)[b]	86.2(78.4,92.4)	73.3 (69, 78)	73.5 (67.3, 78.1)
Age (years)	39.46 ± 11.99	38.8 ± 10.66	32.66 ± 10.08
Weight (Kg)	95.68 ± 11.76	63.71 ± 7.04	79.25 ± 12.59
Height (m)	1.57 ± 0.08	1.54 ± 0.08	1.61 ± 0.07

[b] Not normally distributed, median (Q1, Q3) used instead of Mean ± SD. Q1= first quartiel, Q3= 3rd quartile.

Based on the previous clustering, an OPLS-DA model was built on the readings of 382 putative metabolites in plasma samples of the same patients in order to study the metabolomic differences among the three groups.

5.4.2 Study the metabolomics difference between the groups

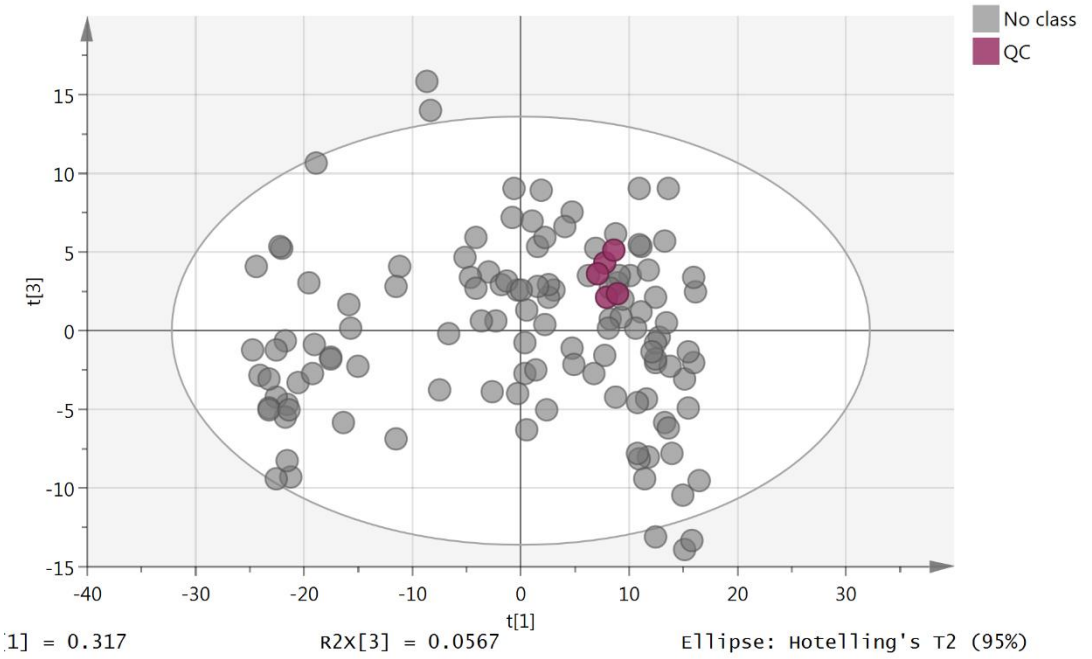

Figure 5.4 2D PCA score plot shows 119 observations for patients with CAH (grey-No class) plus 5 pooled samples (plum-QC).

Starting with the pooled plasma samples (Figure 5.4, above), tight clustering was observed with a calculated RSD of 0.47% based on the sum of the intensities in each sample (n = 5) 0.47%. In addition, the RSD was calculated for each of the putative biomarkers, and the highest RSD was for 4-hydroxy-2-oxopentanoate (9.54%) while the lowest were for L-glutamine and pantothenate with 0.28% and 0.19% respectively. The precision of these values indicated that any metabolomic

differences between groups could not be attributed to instrumental factors. RSD has not been used as primary filter for the metabolites.

5.4.3 Biomarkers identification

Table 5.2 shows the most significant putative biomarkers discriminating between the 3 groups. Group 1 has elevated metabolites which are most typical of metabolic syndrome with highly elevated levels of branched chain amino acids and their acidic metabolites (Newgard *et al*., 2009, Huffman *et al*., 2009, Batch *et al*., 2013, McCormack *et al*., 2013). Since GC dose had only weak significance in separating these three groups, the compounds in the table are not expected to be specific markers of GC activity due to the small contribution of the GC dose in the separation of the three groups.

Table 5.2 List of putative biomarkers that show significant differences among the three groups using one way ANOVA.

			Post-hoc test		
Putative biomarkers	FDR	G1 : G2 : G3	G1*G2	G1*G3	G2*G3
L-Isoleucine *	0.026	1 : 0.32 : 0.41	4.5E-5	0.001	0.05
L-Valine *	0.026	1 : 0.25 : 0.31	8.2E-6	0.001	0.17
3-Methyl-2-oxobutanoic acid *	0.038	1 : 0.18 : 0.25	4.5E-5	0.004	0.10
3-Methyl-2-oxopentanoic acid	0.045	1 : 0.07 : 0.23	0.002	0.094	0.03
2-Methyl-3-oxopropanoate	0.027	1 : 0.24 : 0.32	3.9E-5	0.004	0.06
Gamma-Glutamylglutamine	0.042	1 : 0.58 : 0.67	3.9E-5	0.008	0.10
5-L-Glutamyl-taurine	0.042	1 : 0.45 : 0.54	0.001	0.024	0.15
2-Oxoglutarate *	0.043	1 : 0.46 : 0.58	0.001	0.012	0.01
N-Formimino-L-glutamate	0.043	1 : 0.08 : 0.15	0.002	0.020	0.25
L-Aspartate *	0.038	1 : 0.14 : 0.28	0.005	0.004	0.06
Myristoleic acid(C14:1)	0.023	1 : 0.74 : 0.78	6.7E-5	0.000	0.01
L-Octanoylcarnitine	0.045	1 : 0.78 : 0.8	0.003	0.004	0.07
5-Methylcytosine	0.047	1 : 0.33 : 0.44	0.005	0.030	0.21

*Retention time matches standard. Fold change been calculated based on the average of absolute intensity of each group, and normalised to the first group as a reference for comparison.

FDR corrected p-values following one-way ANOVA revealed 13 putative markers with significant differences. Most of the difference was between patients in G1 compared to G2 and G3. All the presented putative markers were elevated significantly in G1 compared to the other two groups. BCAA; L-isoleucine, L-valine, 3-methyl-2-oxobutanoic acid, 3-methyl-2-oxopentanoic acid, and 2-methyl-3-oxopropanoate represented around 40 % of the metabolomics changes and had a high contribution to the difference between groups and within groups with VIPpred

and VIPorth above 1. 23 % of the metabolomics changes were manifested in the taurine pathway; 5-L-glutamyl-taurine, gamma-glutamylglutamine and 2-oxoglutarate, the putative metabolites in this pathway had a high contribution to the variation between the groups with VIPpred above 1 and had low contribution to the variation within groups with VIPorth below 1. Lipids in this metabolome represented 15 % of the metabolomics changes. However, both myristoleic acid (C14:1) and L-octanoylcarnitine had low contribution to the variation between and within groups with VIPpred and VIPorth below 1.

The metabolomic differences between G2 and G3 are very minimal compared to the difference between G1 vs G2 and G1 vs G3. Patients in group 1 have higher BMI, SBP and DBP compared to G2 and G3, and also have higher GC dose compared to G2; all these measurements might have the implication of higher risk of having chronic diseases among patients in G1 compared to those in G2 or G3. In order to examine the accuracy of predicting those patients susceptible to chronic diseases, ROC curves for both anthropometrics and metabolomics data were modeled as G1 (High risk, 20 patients) vs G2+G3 (Low risk, 99 patients) (Figure 5.5). Anthropometric and clinical measurement based classification were excellent classifiers with 99% accuracy of separating the CAH patients at low risk from those at high risk (Figure 5.5A, below). On the other hand, the plasma metabolome had fair ability (Figure 5.5B) to differenciate patients with low from those with high susceptibility of having chronic diseases, with 75% accuracy (Xia *et al*., 2013).

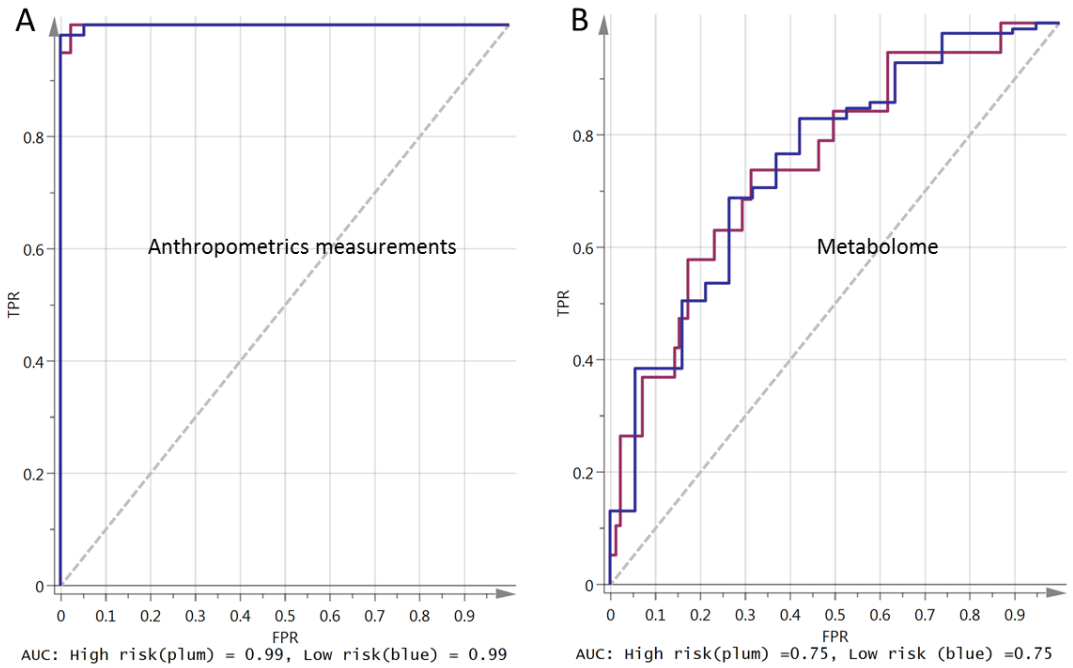

Figure 5.5 The ROC curves of low risk vs high risk groups, (A) for anthropometrics measurements and (B) for corresponding metabolomics difference.
Each plot shows sensitivity (true positive rate (TPR)) on the y-axis versus (false positive rate (FPR = 1 - Specificity)) on the x-axis. **(A)** Shows AUCs based anthropometrics and clinical measurements of high (plum) vs low (blue) risk groups with 0.99 for each group. **(B)** Shows AUCs based metabolome of high (plum) vs low (blue) risk groups with 0.75 for each group.

5.5 Discussion

Patients with CAH have low levels of biosynthesised GC. Different GC replacement therapies are available with different potencies and associated side effects. The challenging point is to what extent we are able to determine patients at risk of further diseases and needing an early intervention. Anthropometric and clinical measurements provide important information about the health status of a patient, but it can not predict it accurately (Wang *et al*., 2011a). We used the provided anthropometrics and clinical measurements as a link to study the metabolome associated with patients at risk according to HCA classification. 13 potential biomarker metabolites were identified and their ability to predict patients at risk was assessed.

Based on the anthropometric and clinical measurements, patients in G1 had a higher BMI, SBP, DBP and GC dose compared to G2 and G3, and also they had lower levels of 17-hydroxyprogesterone and androstenedione. 17-hydroxyprogesterone (median=4.1, IQR=2.38-6.45 nmol/l) level for the patients in G1 was lower than the suggested maintenance level for adult female at fertility of < 24.2 nmol/l and adult male of (< 75.5 nmol/l) (Merke, 2008). This might implicate down regulation of the biosynthesis of GC mediated by high GC dose via the HPA-axis, or inactivity of the 17α-hydroxylase enzyme which converts progesterone to 17-hydroxyprogesterone.

Metabolomics studies have reported an association between high levels of branched chain amino acids with diabetes (Wang *et al*., 2011a), and insulin resistance (Wang *et al*., 2011a, Roberts *et al*., 2014, Newgard *et al*., 2009). Among 2,422 participants followed up for 12 years, 201 individuals developed diabetes and this was associated with high levels of BCAA. A replication study of 163 case-controls was performed and reported the association of BCAA with an incidence of diabetes (Wang *et al*., 2011a).

Gamma-glutamyl-glutamine, 5-L-glutamyl taurine and 2-oxoglutarate are intermediate metabolites in taurine metabolism. These metabolites are elevated significantly in G1, and this elevation indicates enhancement in taurine catabolism, i.e., patients in G1 have low plasma levels of taurine compared to other groups. Association between taurine deficiency and chronic diseases such as T2D, insulin resistance, and cardiovascular diseases were reported previously (Ito *et al.*, 2012). Aspartate is elevated significantly in G1; it is transported from intracellular to extracellular space in an exchange with glutamate, the latter is converted to alpha-ketoglutarate by the aspartate transaminase enzyme (AST). Alpha-ketoglutarate is transported to cytosol in an exchange with malate, the whole process is known as the malate-aspartate shuttle and its aim is to transfer electrons to mitochondria in order to produce ATP. In the Framingham offspring study, aspartate positively correlated with BCAA in control subjects, and had no significant difference compared to diabetic subjects (Wang *et al*., 2011a). The plasma levels of histidine in

9,369 Finnish non diabetics or recently diagnosed men with T2D were reported to be a reliable predictor of incidence of insulin resistance. In the study, low plasma levels of histidine were associated with insulin resistance (Stancakova *et al.*, 2012). In line with this, N-formimino-L-glutamate byproduct of histidine was significantly elevated in G1; this implicates low levels of histidine in this group. Previously, middle aged subjects with arterial stiffness were reported to have high plasma levels of L-octanoylcarnitine (Kim et al., 2015). Compared to non diabetics, patients with T2D have high plasma levels of L-octanoylcarnitine (Adams *et al.*, 2009), as do those with a high risk of prediabetes (Guasch-Ferre et al., 2016). Myristoleic acid (C14:1) was increased significantly in G1 compared to the other groups. Myristoleic acid is formed by desaturation of myristic acid; the latter is positively associated with risk of T2D (Xu *et al.*, 2013). 5-Methylcytosine was also increased significantly in the plasma of patients in G1 compared to those in groups 2 and 3, which is consistent with earlier observations of upregulation of DNA methylation found in patients with atherosclerosis (Zaina *et al.*, 2014).

Patients with CAH clustered into low and high risk groups with 99% accuracy (Figure 6.7A) based on their anthropometric and clinical measurements. The 13 combined biomarkers (Table 6.1) in the plasma of those patients might be used as good prognostic and/or diagnostic biomarkers with 75% accuracy (Figure 6.7B). Although the current study is limited by use of a single analytical platform, the results are statistically strong and clinically consistent with many other studies and could be

used as a reliable basis for further targeted analysis in the way of risk prediction and diagnosis.

Chapter 6:

The exploration of different cut offs of GC dose using metabolomics

6 Exploration of different cut offs of GC dose using metabolomics

6.1 Abstract

Background and Aim: GC replacement therapy is the mainstay of treatment for CAH. However, there are no established biomarkers for GC effect which could indicate the cut-off between physiological replacement, when the metabolic state is normative, and pharmacological therapy, in which GC administration is designed to induce specific responses.

Methods: LC-MS based metabolomic profiling was carried out on plasma samples from 117 patients with CAH being treated with GC replacement therapy. The MS data was processed to produce a metabolite list which was then subjected to analysis by using both multivariate and univariate statistics in which the clinical meta-data was also incorporated**.**

Results: The clearest metabolomic changes were between patients receiving ≤5 mg and > 5 mg prednisolone dose equivalents (PredDEq). The metabolome of patients receiving > 5-15 mg had net result of increased circulating FFA levels, except for palmitoleic acid (16:1) which was decreased in this group. Chenodeoxyglycocholic acid, octanoylcarnitine and tryptophan were elevated significantly in the high dose group as was the metabolite of tyrosine, hydroxy phenyl pyruvic acid.

Conclusion: A combination of seven biomarkers produced excellent discrimination between the patients receiving ≤5 mg and > 5-15 mg of PredDEq based on an AUC of 0.92 for a ROC curve. These biomarkers could be readily incorporated into a rapid targeted screen for GC action.

6.2 Introduction

GC replacement therapy is the mainstay of management interventions for CAH (Han *et al*., 2013a) and both primary and secondary adrenal insufficiency (Johannsson *et al*., 2015). It is also employed in the treatment of a variety of chronic and inflammatory diseases such as rheumatoid arthritis (RA), obstructive lung diseases, asthma, and systemic lupus erythromatosus (Hoes *et al.*, 2008).

Oral HC is one of the most commonly used GC which is administered in divided doses of 2 or 3 times daily (Johannsson *et al*., 2015) and has been associated with better quality of life (QoL) in patients with CAH (Han *et al*., 2013b). Other most commonly used GCs include prednisolone, prednisone, dexamethasone, budesonide, beclometasone, fluticasone and deflazacort (Hoes et al., 2008), but both prednisolone and dexamethasone have been associated with impaired QoL in CAH patients (Han *et al*., 2013b). Treatment with GCs is generally associated with adverse reactions commonest among which are development of osteoporosis (Van Staa *et al.*, 2000), reduced bone density, and risk of bone fractures which occur within 3-6 months of oral therapy at doses >5 mg daily (Van Staa *et al.*, 2002a). Other side effects are cardiovascular diseases including acute myocardial infarction (Wei *et al.*, 2004, Varas-Lorenzo *et al.*, 2007), insulin resistance, obesity, hypertension, and hyperglycaemia (Han *et al*., 2013a, Wei *et al*., 2004).

The frequency and severity of these adverse effects depend largely on the type of drug, duration of treatment, and the dose, calculated as prednisolone dose equivalent (PreDEq), administered (Han *et al*., 2013b). For instance, in a study to determine the effect of drug dose and timing of GC treatment on health outcomes among CAH patients, a once daily dose regimen of dexamethasone was found to produce lower androgens and ACTH levels, suggesting favourable disease control, but it also caused greater insulin resistance than HC or prednisolone (Han *et al*., 2013a).

On the other hand, higher GC dose was associated with increased blood pressure, poor disease control and mutation severity. In children, both prednisolone and dexamethasone are associated with 15- and 70–80-fold higher linear growth suppression effects compared to HC (Rivkees and Crawford, 2000, Punthakee *et al.*, 2003, Bonfig *et al.*, 2007). Thus HC is preferred during childhood over more potent long-acting GCs which are not recommended during this period (Speiser *et al.*, 2010). The choice between GC drugs in CAH thus depends on the age of the patient, gender, evidence of virilisation in women, and desire for fertility (Han *et al*., 2013a). For instance, young women desiring to have children would rather take high dose of synthetic, long-acting GCs while middle-aged men with no requirement for fertility might prefer physiological doses with HC to reduce risk of osteoporosis and cardiometabolic disorders (Walker, 2007a).

The therapeutic dose of GCs is very broad which can vary by more than 200-fold depending on the condition being treated (Buttgereit *et al.*, 2002). Therapeutic effects are mediated by both genomic actions, which occur via binding to cytosolic GC receptors no earlier than 30 minutes of receptor binding, and non-genomic actions which occur immediately (within seconds or minutes) via biological membranes at higher concentrations (Buttgereit *et al*., 2002). To minimise the risk of adverse effects, clinicians should prescribe the least possible doses for the shortest duration possible (Trikudanathan and McMahon, 2008).

The conventional classification for GC dose in rheumatology has been suggested, based on daily PreDEq, as low dose (≤ 7.5 mg), medium dose (> 7.5 mg, but ≤ 30 mg), high dose (> 30 mg, but ≤ 100 mg), very high dose (> 100 mg), and pulse therapy (≥ 250 mg a day for one or a few days) (Buttgereit *et al*., 2002). However, this daily dose can either be given in multiple dosing in reversed circadian rhythm or in single daily doses depending on the type of drug and the condition being treated. Whereas it is clear that higher GC doses lead to cardiometabolic effects, there is currently no reliable information regarding the dose cut-off at which these effects begin to manifest. This has led to a lack of consensus among clinicians and researchers alike on the doses of GC beyond which preventive treatment should be initiated to protect the patient against GC-induced side effects, such as use of bisphosphonate for protection against osteoporosis.

Some researchers have suggested that since the physiological level of GCs in blood is approximately 2.5 mg PreDEq daily, patients receiving daily doses of GCs above 5 mg PreDEq should start taking bisphosphonate for prevention against osteoporosis. Additionally, these studies have suggested that the risk of adverse effects such as hypertension, insulin resistance, etc., becomes more likely when a patient is on a daily dose > 7.5 mg PreDEq, while other adverse effects such as infectious diseases due to deterioration of the immune system might appear when the daily dose exceeds 10 mg PreDEq. However, there is need to collaborate these clinical and pharmacological cut-offs with a more complete analysis of the metabolic profile of patients on different daily doses of GCs to provide precise discrimination at different dose cut-offs to predict the onset of a significantly altered metabolic state that might signify development of adverse effects.

Thus the aim of this study was to employ metabolomics as a tool to explore the changes in metabolites that occur at different GC dose cut-offs in order to rationalise preventive measures against increased likelihood of GC-induced adverse effects. This would also help to establish the cut-off between physiological replacement, when the metabolic state is normative, and pharmacological therapy, in which GC administration is designed to induce specific responses. Ultimately the findings will enable clinicians to make informed decisions about GC therapy including restricting doses to those specifically required to induce the desired

outcomes and early adoption of measures to protect against GC-induced adverse effects.

6.3 Methodology

6.3.1 Patient recruitment

The UK Congenital adrenal Hyperplasia Adult Study Executive (CaHASE) cohort is a cross-sectional study of adult CAH patients recruited from 17 specialised British endocrine centres. The study protocol was approved by West Midlands MREC (MREC/03/7/086) and registered with ClinicalTrials.gov (NCT00749593) and has been previously published in detail (Arlt *et al*., 2010). All centres contacted adult patients (18 years or older) with a confirmed diagnosis of CAH currently under their care. All participants gave written informed consent.

6.3.2 Procedure for collection of anthropometric data

Participants attended the research unit of their respective centre after an overnight fast having taken their regular medication, followed by medical history, physical examination and fasting blood sampling. Physical examination included: blood pressure (three seated, one standing, separated by 5 min), height and weight. Biochemical assessment: steroid hormones including 17-hydroxyprogesterone (17OHP), androstenedione. All laboratories participated in the UK NEQUAS scheme for quality control of steroid immunoassays. Inclusion criteria for the metabolomics

analysis were as follows: known 21-hydroxylase deficiency; additional serum sample collected at time of recruitment; full anthropometric and biochemical data available for each participant. Samples from 117 patients were eligible for metabolomics analysis; subjects were treated with hydrocortisone, prednisolone and dexamethasone or combination therapy. Treatment dose was converted to PreDEq using respective ratios for prednisolone: hydrocortisone: dexamethasone of 1: 4: 0.15 based on British National Formulary (BNF) (Society, 2012).

6.3.2.1 Patient's numbering

117 patients, each one had a number of 6 characters. The first character represented the centre of the study, the last 5 characters represented the patient's number in that centre. For example, C05005, C = this patient belongs to centre C, 05005= patient's number.

6.3.3 LC-MS analysis

- LC-MS conditions and sample preparation are reported in detail in section 2.1-2.3 (pages: 47-51).
- Column used in this project is ZICpHILIC.

6.3.4 Data extraction and processing

Details of data extraction and processing are reported in section 2.4 (pages: 51-54).

6.3.5 Data analysis

Data analysis was carried out as already described in section 2.5 (pages: 54-58).

6.4 Results

6.4.1 Metabolomics profiling of different GC cutoffs

117 patients with CAH receiving four types of GC treatment were employed. In order to examine different GC cut-offs based on metabolomic differences, GC therapies were converted to prednisolone equivalents based on the relative potencies of the steroids reported in the British National Formulary (PredEqBNF) (Society, 2012). Thus, patients were divided into 4 groups based on the GC doses they were receiving, as follows: group 1, 1-2.5 mg; group 2, >2.5-5 mg; group 3, >5-7.5 mg; and group 4, >7.5-15 mg prednisolone dose equivalents on a daily basis (Figure 5.1, Table 5.1). The strongest GC cut-offs were found between patients receiving 1-5 mg daily (low GC, 64 observations) vs patients receiving > 5-15 mg (high GC, 53 observations). The anthropometric and biochemical measurements were examined between these two groups in order to make sure that any metabolomics differences between them were due only to the differences in the GC dose.

The GC dose was found to be significantly different between the two groups (FDR corrected p = 1.4E-19) with median (IQR) of 3.75 (2.5, 5) and 7.5 (6.25, 7.5) for low

and high dose groups respectively, with AUC =1 (Table 5.2) which is obvious based on our classification. In addition, there were no significant differences in the rest of anthropometric and biochemical measurements (*p* value > 0.05) (Table 6.2, below). Since there were no confounding variables, any differences in metabolites between the two groups could be attributed to GC dose alone.

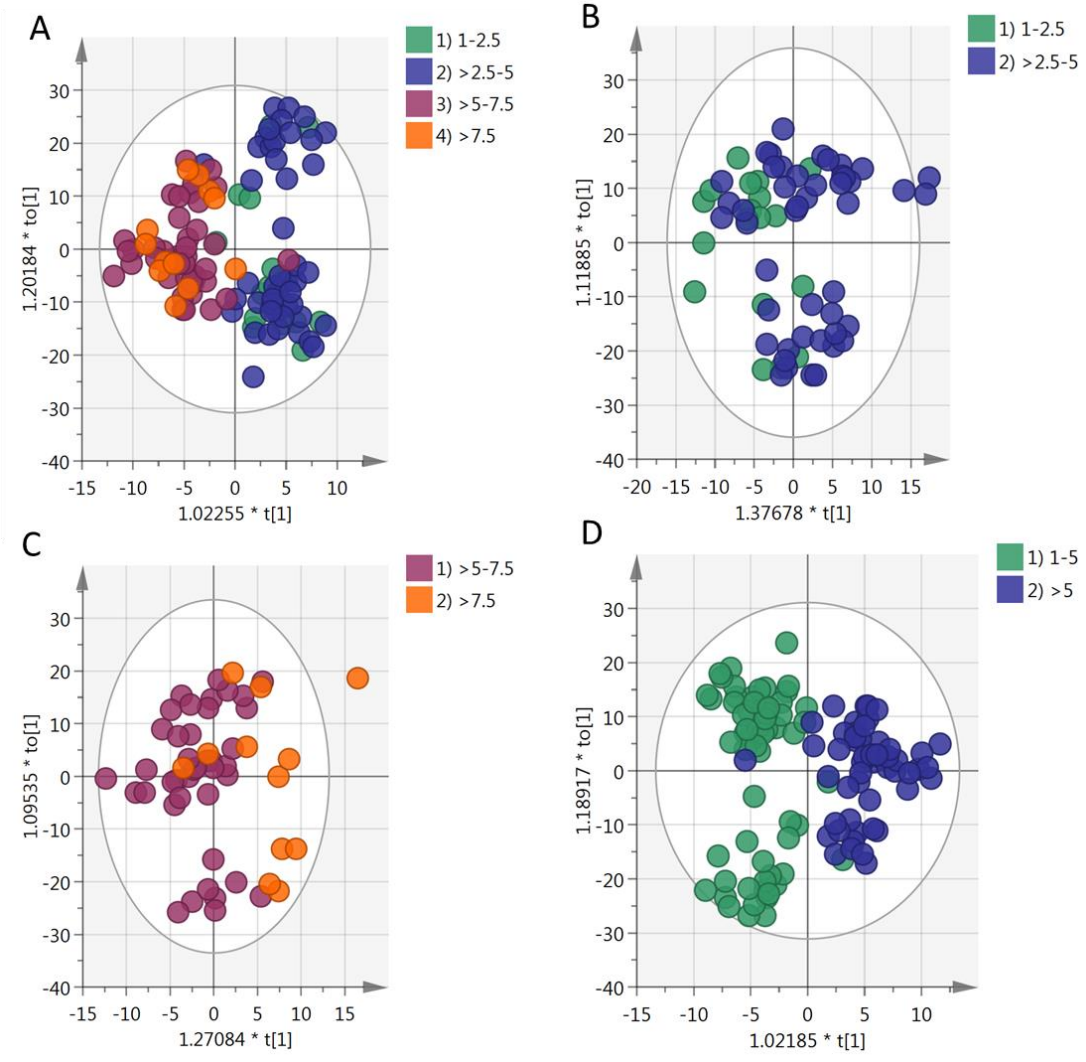

Figure 6.1 OPLS-DA score plots shows 4 comparisons of 117 samples of patients with CAH grouped based on their daily doses of GC.

Comparison [1], plot (A) shows patients divided into 4 groups; (1) patients having 1-2.5 mg (n=18, green), (2) >2.5-5 mg (n=46, blue), (3) >5-7.5 mg (n=41, plum) and (4) >7.5 -15 mg (n=12, orange), R^2= 0.469, Q^2=0.215 . Comparison [2], plot (B) shows patients divided into 2 groups; (1) 1-2.5 mg (n=18, green) and (2) >2.5-5 mg (n=46, blue), R^2= 0.453, Q^2=-0.37. Comparison [3], plot (C) shows patients divided into 2 groups; (1) >5-7.5 mg (n=41, plum) and (2) >7.5-15 mg (n=12, orange), R^2= 0.41, Q^2=-0.36 . Comparison [4], plot (D) shows patients divided into 2 groups; (1) 1-5 mg (n=64, green) and (2) >5-15 mg (n=53, blue), R^2= 0.649, Q^2=-0.612 .

In the first comparison, plot A (Figure 6.1, above) shows that the metabolomics' based groups separation between different dose cutoffs varies (p = 2.5E-06). It clearly shows that groups (1) 1-2.5 and (2) >2.5-5 overlapped and all the samples in group 1 (18 samples) were misclassified as members of group 2 (Table 6.1, below). In the same way, samples in groups (3) >5-7.5 and (4) >7.5-15 mg also overlapped, and all the samples in group 4 (12 samples) were misclassified as members of group 3 (Table 6.1, below). The clearest and most significant separation (*P* CV-ANOVA = 1.5E-20) can be seen when patients are divided into (1) 1-5 mg (64 samples) and (2) >5-15 mg (53 samples) as shown in comparison [4] plot D (Figure 6.1) and we can see that only two samples of group (2) >5-15 mg overlapped with group (1) 1-5 mg according to the misclassification table (Table 6.1).

Table 6.1 Data corresponding to (Figure 6.1) regarding group assignment plus AUC for classification.

Group	Samples(n)	Distribution of samples				(%)[a]	AUC	*P*
[1] Comparison A		**1-2.5**	**>2.5-5**	**>5-7.5**	**>7.5-15**			
1-2.5	**18**	0*	17	1	0	0	0.75	2.5E-6
>2.5- 5	**46**	0	43*	3	0	93.4	0.89	
>5- 7.5	**41**	0	1	40*	0	97.5	0.9	
>7.5-15	**12**	0	1	11	0*	0	0.81	
[2] Comparison B		**1-2.5**		**>2.5 - 5**				
1-2.5	**18**	5*		13		27.7	0.84	1
>2.5-5	**46**	4		42*		91.3	0.84	
[3] Comparison C		**>5 - 7.5**		**>7.5**				
>5-7.5	**41**	40*		1		97.6	0.89	1
>7.5	**12**	4		8*		66.7	0.89	
[4] Comparison D		1-5		>5				
1-5	**64**	64*		0		100	0.98	1.5E-
>5-15	**53**	2		51*		96	0.98	20

*Number of samples that correctly assigned to the correct group. [a] = percentage of correctly classified samples within each group. ***P*** = p value based on CV-ANOVA.

6.4.2 *Metabolomics difference between patients receiving 1-5 mg and those receiving >5-15 mg prednisolone equivalent.*

Table 6.2 Comparison of anthropometric and clinical measurements between the low (L) and high (H) dose GC exposed groups. All measurements were similar between the two groups except for GC dose.

Parameter	Group	Mean±SD/Median(Q1, Q3)	FDR	AUC
Age (year)	**L**	36.5 ± 10.8	0.64	0.52
	H	35.4 ± 11.7		
Weight (kg)	**L**	75.7 ± 13.96	0.76	0.52
	H	77.9 ± 17.4		
Height (m)	**L**	1.56 ± 0.08	0.39	0.57
	H	1.58 ± 0.08		
BMI (kg/m^2)	**L**	30.96 ± 6.04	0.83	0.51
	H	30.84 ± 6.5		
SPB (mmHg)	**L**	118.7 ± 12.1	0.27	0.59
	H	122.7 ± 12.6		
DPB (mmHg)	**L**	73.53 ± 9.01	0.21	0.61
	H	76.9 ± 8.8		
GC dose (PredEqBNF)[b]	**L**	3.75 (2.5, 5)	1.4E-19	1
	H	7.5 (6.25, 7.5)		
Androstenedione (mmol/l)[b]	**L**	3.35 (1.5, 5.9)	0.42	0.54
	H	3.1 (1.7, 15)		
17-OH progesterone(mmol/l)[b]	**L**	11.5 (3, 92.5)	0.81	0.51
	H	12.6 (4.3, 80.9)		

[b] (non-parametric), Mann-Whitney U test used and Median(Q1, Q3) presented instead of Mean±SD, L= 1-5 mg daily prednisolone equivalent, H= >5-15 mg daily prednisolone equivalent according to BNF.

All the anthropometrics and clinical measurementas except GC dose, show insignificant difference between the two groups following FDR correction (Table 6.2, above). So, the change in metabolome between the two groups is mainly driven by the effect of GC dose (Figure 6.2).

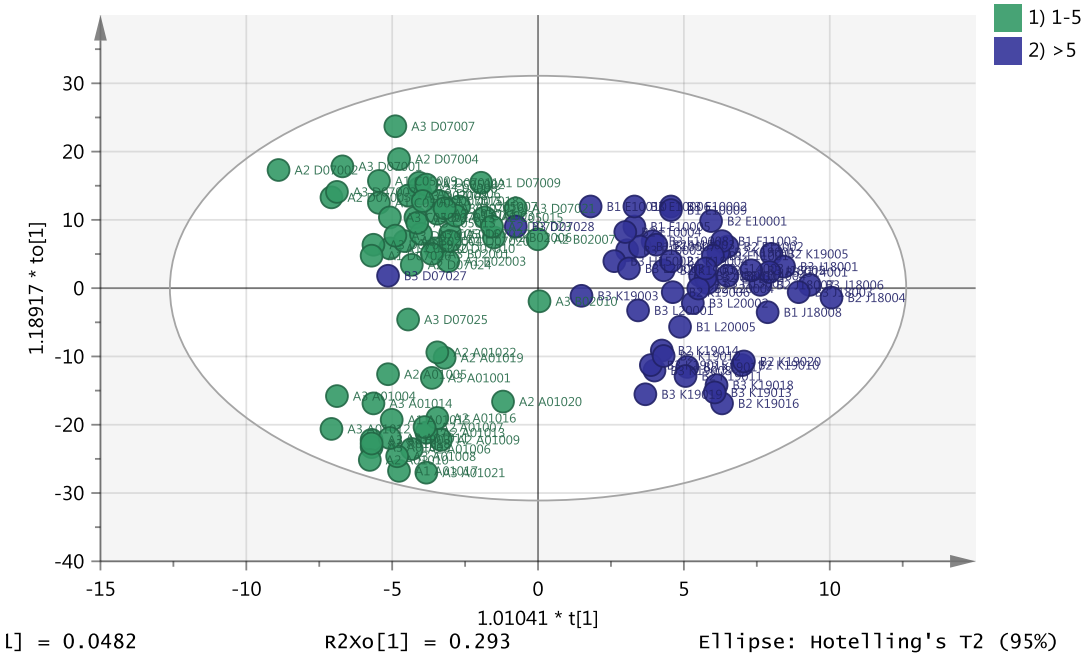

Figure 6.2 OPLS-DA score plot shows samples of patients with CAH receiving either 1-5 mg or >5-15 mg prednisolone equivalent.
The plot built up on readings of 382 putative biomarkers in plasma samples of 117 patients with CAH. Patients divided into two groups, green observations (64 samples) represent patients receiving a GC dose of 1-5 prednisolone equivalent and the blue observations (53 samples) represent patients receiving GC dose > 5 mg prednisolone equivalent. The model consists of one predictive x-score components; component t[1] and three orthogonal x-score components to[1-3]. t[1] explains 4.8% of the predictive variation in x, to[1] explains 45.7% of the orthogonal variation in x, R2X (cum) = 0.506, R2Y (cum) = 1, R2 (cum) = 0.829, Goodness of prediction Q2 (cum) = 0.657.

The OPLS-DA model (Figure 6.2, above) was based on readings of intensities of 382 metabolites in plasma samples of 117 patients; the plot shows a clear and significant separation between the two groups of patients (*P* CV-ANOVA = 7.4E-22).

The plot also shows that within group variability (orthogonal variation) is higher in patients receiving low GC dose (1-5) mg compared to those in the group treated with a higher dose of GC (>5-15) mg. The model exhibits strong predictive power based on the permutations test (Figure S6.1, appendix) which shows that the original Q^2 has higher value compared to the newly permutated (predicted) Q^2 values. The model explained about 83% of the variability among the observations and was able to predict about 66% of this variability based on cross validation. 50.6% of the variation between the metabolites was explained by the model and only 4.8 % of this variation is certainly due to the difference in the GC dose between the two groups. Table 6.3 shows significant metabolites that were affected by the difference in the GC doses between the two groups. Metabolite's selection was based on the following criteria: p value <0.05 following FDR correction, and AUC >0.6.

Table 6.3 Putative biomarkers significantly affected by the difference in GC dose between the low (L) and high (H) GC dose groups.

Putative biomarkers	AUC	FDR	H / L	VIPpred	VIPortho
Saturated fatty acids					
Tridecanoic acid (C13:0)	0.63	0.0162	0.9	0.58	0.54
Pentadecanoic acid (C15:0)	0.64	0.0056	1.3	0.98	0.78
Palmitic acid *(C16:0)	0.66	0.021	1.4	1.06	1.07
Phytanic acid (C20:0)	0.65	0.0117	1.4	1.03	0.92
Unsaturated fatty acids					
Palmitoleic acid (C16:1)	0.77	0.000004	0.7	1.55	0.4
Docosahexaenoic acid (C22:6)	0.65	0.00298	1.2	0.87	0.62
15(S)-Hydroxyeicosatrienoic acid (20:3)	0.65	0.00201	1.3	1.06	0.75
Prostaglandin B1(C20:2)	0.64	0.00596	1.3	1.02	0.8
Nucleotide Metabolism					
Inosine *	0.63	0.0102	0.9	0.69	0.56
Uridine *	0.75	0.00027	0.7	1.21	0.46
Hypoxanthine *	0.73	0.00001	2.4	2.11	1.02
Methionine and taurine metabolism					
L-Methionine *	0.73	0.00041	1.2	0.87	0.4
5-L-Glutamyl-taurine	0.65	0.0114	1.6	1.14	0.85
Aromatic amino acids					
L-Tryptophan *	0.67	0.0003	1.7	1.59	0.97
3-Dehydroquinate	0.67	0.0059	1.3	1.02	0.82
4-Hydroxyphenyl pyruvic acid*	0.75	0.00006	0.5	1.8	0.6
Alpha-N-Phenylacetyl-L-glutamine	0.61	0.0293	0.9	0.55	0.43
4-Hydroxy-2-oxopentanoate	0.65	0.0003	3.5	2.34	1.6
Miscellaneous					
L-Asparagine *	0.72	0.00004	2.6	2.29	1.14
L-Threonine *	0.62	0.0211	0.7	1.14	0.56
2-Keto-glutaramic acid	0.64	0.0103	0.8	0.8	0.65
N-Methylnicotinamide	0.68	0.0003	2.2	1.85	0.85
L-Octanoylcarnitine	0.66	0.00319	1.4	1.16	0.83
Chenodeoxyglycocholic acid	0.82	1.9E-10	4.8	6.73	1.46

*Retention time matches standard

The initial OPLSDA model (Figure 6.2), based on a large set of putative metabolites (382 metabolites), was refined by systematically discarding metabolites which did not contribute strongly to the difference between the two groups (Figure 6.3) until it was possible to produce a robust model based on only seven putative metabolites each with an FDR corrected p-value < 0.001 (Table 6.4). The number of metabolites used as putative biomarkers is thus < 10% of the number of observations which reduces the likelihood of the model being over-fitted.

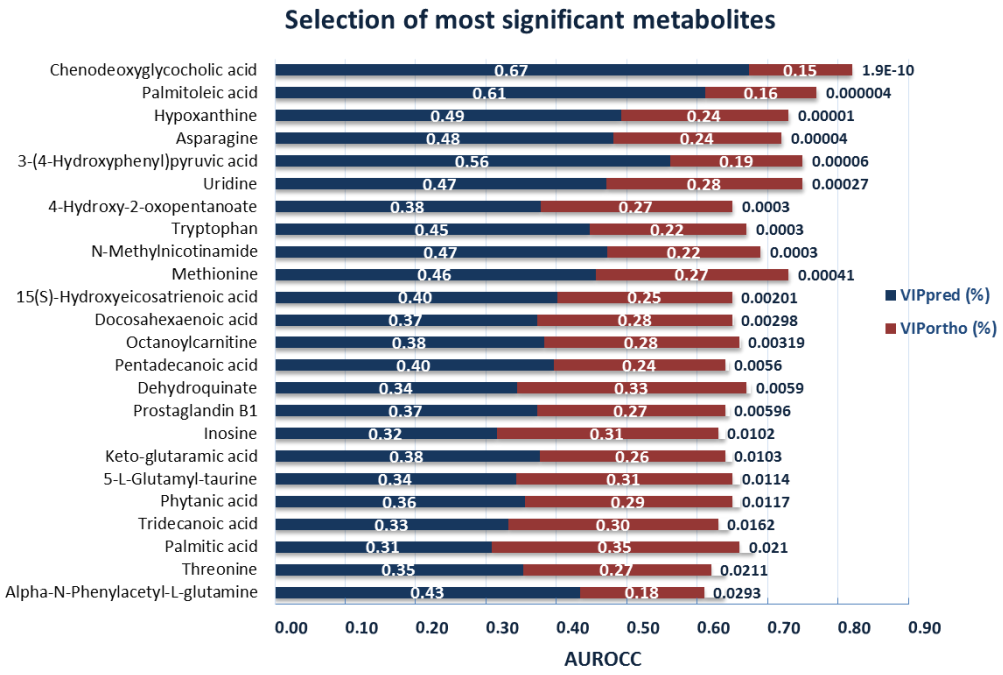

Figure 6.3 Bar chart of the most significant metabolites.
Bars plot shows 24 metabolites (Table 3). Each bar represents a metabolite on y-axis, and its Area Under ROC Curve (AUROCC) value on x-axis. Each metabolite' bar comprises of two segments; VIPpred (blue) and VIPortho (red), their values presented as percentages (white colour), FDR adjusted p-value presented for each metabolite at the right of each bar (dark blue). Metabolites arranged based on their statistical significance from top to down. Metabolites was refined by selecting top 10 statistically significant metabolites, each must have VIPpred ≥ 2*VIPortho to pass the filter.

Based on the 7 biomarkers, a new OPLS-DA model was constructed as shown in (Figure 6.4) These 7 variables in combination produced a ROC curve with an AUC of 0.92 for the classification of the high and low dose corticosteroid response which is regarded as excellent classification (Xia *et al*., 2013).

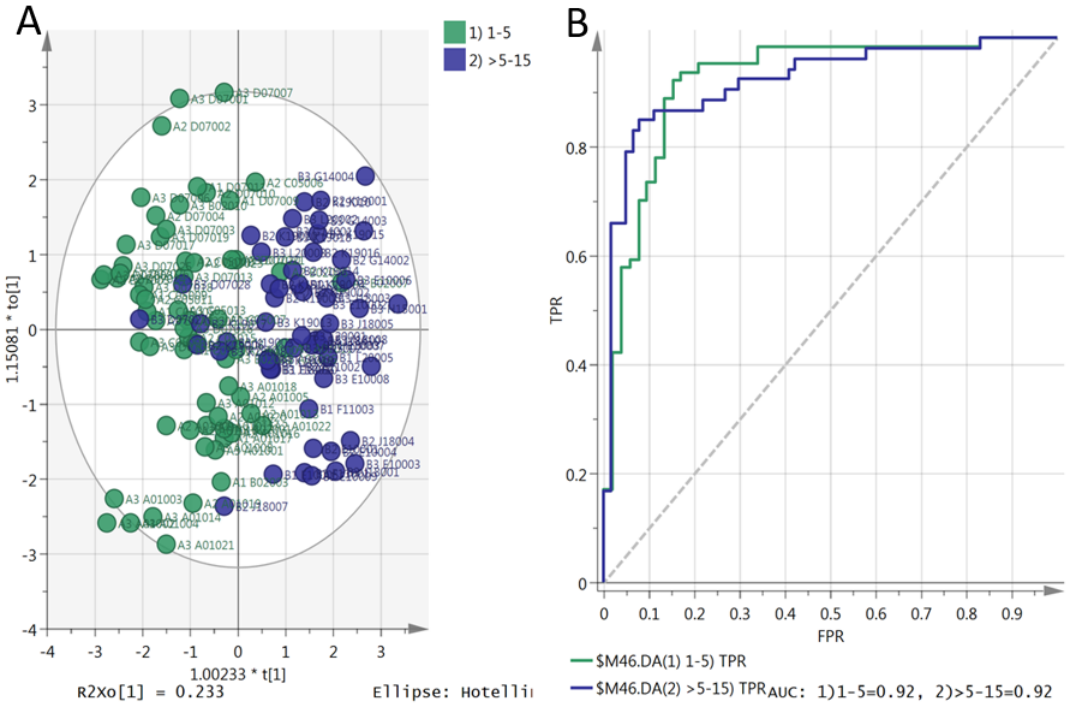

Figure 6.4 (A) OPLS-DA score plot and (B) Area under the ROC, both built up on readings of 7 putative biomarkers (Table 6.4) in 117 patients.

The plot shows two groups of samples, green samples (n=64) represent patients receiving a GC dose of 1-5 prednisolone equivalent and the blue samples (n=53) represent patients receiving GC dose > 5-15 mg prednisolone equivalent. The model consists of one predictive x-score components; component t[1] and one orthogonal x-score components to[1]. t[1] explains 33.7 % of the predictive variation in x, to[1] explains 23% of the orthogonal variation in x, R^2X (cum) = 0.57, R^2Y (cum) = 1, R^2 (cum) = 0.535, Goodness of prediction Q^2 (cum) = 0.497. On the right, plot showing area under the ROC curve (AUC) of the two groups, x-axis showing (FPR) false positive rate (1-specificity), y-axis showing true positive rate (sensitivity). AUC for 1) 1-5 = 0.92 and 2) >5-15 = 0.92.

The new model in plot A (Figure 6.4) explained 33.7% of the variability between the two groups compared to the previous model (Figure 6.2) which explained only 4.3% of the variation between the two groups. The majority of the 7 metabolites were positively correlated to GC dose; chenodeoxyglycocholate had the highest correlation value (r= 0.76) while N-methylnicotinamide has the lowest correlation value (r= 0.46). On the other hand, 4-Hydroxyphenyl pyruvate and palmitoleic acid had negative correlation to GC dose (r = -0.57 and r= -0.66) respectively (Table 6.4).

Table 6.4 List of significant putative biomarkers used to build up the OPLS-DA model in Figure 6.4.

Putative biomarker	FDR	H / L	VIP		r	99% CI
			pred	orth		
L-Asparagine *	4.5E-5	2.6	2.29	1.14	0.52	(0.08 , 0.34)
L-Tryptophan *	3.3E-4	1.6	1.59	0.97	0.53	(0.12 , 0.29)
4-Hydroxyphenyl pyruvate *	6.6E-5	0.5	1.8	0.6	-0.57	(-0.37, -0.08)
Palmitoleic acid	4.1E-6	0.7	1.55	0.4	-0.66	(-0.42 , -0.1)
Chenodeoxyglycocholate	2E-10	4.8	6.73	1.46	0.76	(0.16 , 0.44)
N-Methylnicotinamide	3.0E-4	2.2	1.85	0.85	0.46	(0.02 , 0.34)
Hypoxanthine *	1.8E-5	2.4	2.11	1.02	0.51	(0.05 , 0.34)

*Retention time matches the standard. H= patients receiving high GC dose >5 mg prednisolone equivalent, L= patients receiving low GC dose 1-5 mg prednisolone equivalent.

6.5 Discussion

GC replacement therapy in GC-deficient conditions such as CAH and Addison's disease is challenging because there are no reliable biomarkers for GC action. This often leads to overtreatment causing metabolic side effects or under-replacement leading to increased risk of death from adrenal crisis. In order to discover biomarkers indicating GCs effect mass spectrometry based metabolomic profiling was carried out on plasma samples from 117 patients. The clearest metabolomic separation was found between patients receiving ≤5 and >5-15 mg prednisolone equivalents. A combination of the seven strongest biomarkers produced an AUC of 0.92 for a ROC curve. In addition there were another 17 metabolites with AUC values > 0.6.

Chenodeoxycholic acid levels were nearly five fold in the high compared with the low GC dose groups; increased levels of bile acids have been associated with T2D (Prawitt *et al*., 2011). There is mounting evidence that GC can regulate bile acid biosynthesis and equally that bile acids can regulate GC levels (Baptissart *et al.*, 2013).

Hydroxyphenylpyruvic acid can be converted to tyrosine via transamination. The promotion of tyrosine transaminase by GCs has been known for over 50 years (Segal and Kim, 1963); thus lower levels of hydroxyphenyl pyruvic acid in the high GC dose

samples might reflect its conversion to tyrosine. In a previous study, aromatic amino acid levels were correlated with insulin resistance in 263 lean individuals (Tai *et al.*, 2010). Tyrosine and phenylalanine were significantly increased in patients receiving high GC dose. The bacterial-derived metabolite 4-Hydroxy-2-oxopentanoate also increased significantly, as observed in the current study, implicating gut microbiota in phenylalanine degradation. Many previous studies have focussed on the role of gut microbiota in the incidence of obesity, T2D and insulin resistance (Boulange *et al.*, 2016).

Tryptophan metabolism is regulated by GC activity which regulates the enzyme TDO at the entry to the kynurenine pathway. Corticosteroids have been found to promote TDO (Ochs *et al*., 2015). The observation of elevated tryptophan in the high HC dose samples is the opposite of what would have been expected. However, TDO has haem at its active centre and enzyme activity is regenerated by coupling with the superoxide anion (Sono, 1989). hypoxanthine increased and inosine decreased, the later catabolised to hypoxanthine and xanthine, one of the major sources of superoxide in the body is from the action of xanthine oxidase (XO) which converts hypoxanthine via xanthine to uric acid (Sono, 1989). Dexamethasone reported to induced hypertension in rats via this mechanism (Wallwork *et al.*, 2003).

Palmitoleic acid has been used as a plasma marker for stearoyl CoA desaturase (SCD) activity which is required for the secretion of triglycerides by the liver (Paillard *et al.*, 2008). High SCD activity has been found in diabetic and obese subjects (Warensjo *et al.*, 2009). Significant negative correlation between SCD activity and a homeostasis model for insulin resistance (HOMA-IR) was found in 299 healthy men. Palmitoleic acid was found to correlate closely with plasma triglyceride content; a chronically elevated level of GC is associated with the development of fatty liver disease (Gambino *et al.*, 2016). In this study C15:0, C16:0, C20:3 and C22:6 fatty acids were all elevated significantly in patients receiving GC dose >5-15 mg prednisolone equivalent while C13:0 and C16:1 fatty acids were reduced significantly. Elevated plasma levels of C16:0, C20:3 and C22:6 were reported in patients with NAFLD compared to controls. Palmitic acid (C16:0) has a strong positive association with the incidence of T2D compared to control, while the odd chain pentadecanoic acid (C15:0) has inverse association with T2D (Forouhi *et al.*, 2014). Plasma levels of C15:0 to C13:0 fatty acids indicate downregulation of odd chain FA oxidation. Desaturation of C16:0 to C16:1 was reduced in patients receiving a high GC dose, this might implicate reduced activity of stearoyl CoA desaturase enzyme (SCD).

N-methylnicotinamide (NMN) is a metabolite of tryptophan and urinary levels of NMN have been found to be elevated in diabetes along with its metabolites, the N-

methyl pyridine carboxamides, and knock down of nicotinamide N-methyl transferase has been found to protect against obesity (Kraus *et al.*, 2014).

In a study which closely correlates with our results, (Zhao *et al.*, 2010) studied diabetic and non-diabetic individuals aiming to uncover the metabolomic differences between individuals with impaired glucose tolerance (IGT) compared to controls. They found that individuals with IGT have reduced levels of phenylacetyl-glutamine and increased levels of acylcarnitines, α-ketoglutarate, tryptophan, xanthine, methionine and nucleotides. They also found that phenylacetyl-glutamine and increased levels of acylcarnitines and α-ketoglutarate were markers of TCA intermediate depletion leading to mitochondrial stress which interfered with physiological insulin functions. In line with the observation in this study patients with diabetes have higher plasma levels of octanoylcarnitine compared to nondiabetic individuals (Kim *et al*., 2015).

All the 7 candidate biomarkers had AUC values above 0.7 and a high contribution to the separation between the high GC and low GC groups and gave low within group variability. Although the current study is limited by use of a single analytical platform, the results are consistent with previous studies and the markers discovered could be used as reliable indicators of supraphysiological GC action. The seven biomarkers could readily be incorporated into a rapid targeted screen.

Chapter 7:

General Discussion, Conclusion, Strengths, Limitations and Future Work

7 General discussion

GC play a key role in the development of metabolic disease. As a result, several therapeutic strategies have been proposed to reduce cortisol secretion or action in such disease states. These strategies include use of GR antagonists such as RU38486 (Jacobson *et al*., 2005), and inhibitors of 11β-HSD1 such as metyrapone (Hughes *et al.*, 2008). One of the major limitations in the development of these therapies is the lack of simple indicators of successful reduction in cortisol effects. This lack of specific biomarkers makes clinical management of patients requiring GC replacement therapy particularly challenging (Hummel *et al*., 2016), and may contribute to well-documented excess morbidity and mortality in patients with hypopituitarism or adrenocortical failure (Arlt *et al*., 2010, Filipsson *et al*., 2006, Bergthorsdottir *et al.*, 2006).

In the current work, the aim was to identify biomarkers which reflect GC action. To investigate GC deficiency, metabolomics analysis was performed on plasma samples obtained from healthy men and patients with T2D following administration of the GR antagonist RU38486 together with the inhibitor of cortisol biosynthesis, metyrapone, a combination which has been termed 'GC blockade' (Wake *et al*., 2007a, Macfarlane *et al*., 2014). To investigate GC dose effects, plasma samples were obtained from healthy men treated with metyrapone followed by varying doses of HC to induce low, medium and high (supra-physiological) circulating

cortisol levels. In each study, the specificity of the response to GC was tested by making measurements before and after insulin infusion. The metabolomic features of GC excess were also investigated in plasma samples of patients with CAH who had been receiving GC replacement therapy from the UK Congenital Adrenal Hyperplasia Adult Study (CAHase) (Arlt et al., 2010).

In order to obtain broader coverage for polar and non-polar metabolites, ZICpHILIC and C18-AR columns were employed. Metabolites from the two columns were integrated into SIMCA software for multivariate analysis. R^2 and Q^2 produced by SIMCA for such integration were valid, and the effect of interventions / phenotypic differences was clear. Pooled samples were employed to examine the instrument's precision and to exclude any instrumental factor that would impact on the results. The practice in relation to pooled samples is to make a pooled sample of all the samples in the run or to buy a QC sample. However, buying a QC sample seems impractical, because it contains compounds which are likely to be different than those in the examined samples, based on that, the judgment of stability of the detected metabolites is not achievable. On the other hand, making a pooled sample from all the examined samples, is financially better than buying a QC sample, but, practically time consuming. In this thesis, a pooled sample was made from 10 semi-randomly selected samples i.e when control vs treatment was available, 5 control and 5 treatment sample were randomly selected.

Eight metabolites (chenodeoxyglycocholate, 5-L-glutamyl-taurine, gamma-glutamylglutamine, hypoxanthine, valine, 2-methylbutyroylcarnitine, androsterone glucuronide and pregnenolone sulfate) were significantly affected by GC interventions in more than one study. The bile acid conjugate, chenodeoxy glycocholate, was significantly elevated following GC blockade in patients with T2D, and was also elevated significantly in patients with CAH receiving high GC dose. The increase in the levels of bile acids following GC blockade is probably an indication of increased HPA-axis activity in order to meet the body's demand for GC. Disturbances in HPA-axis have previously been found to raise serum bile acid levels in patients with Addison's disease relative to healthy controls (Rose *et al*., 2011). On the other hand, the increase in bile acids observed at high GC doses in CAH patients agrees with a previous report of acute treatment of mice with prednisolone which was found to elevate plasma levels of bile acids by promoting the apical sodium-dependent bile acid transporter (Asbt) expression thus enhancing BA absorption from the intestine (Out *et al.*, 2014).

HC increased plasma levels of gamma-glutamylglutamine in healthy individuals, and this metabolite was also found to be elevated in plasma samples from a group of patients with CAH who received high GC dose, and had high BMI, high SPB, and high DBP (G1). In the same group of CAH patients, 5- L-glutamyl-taurine was also elevated. Both gamma-glutamyl-glutamine and 5-L-glutamyl taurine are intermediate metabolites in taurine metabolism and their elevated levels indicate

enhancement of taurine catabolism. Thus it is expected that patients in G1 had low plasma levels of taurine compared to other groups. Associations between taurine deficiency and chronic diseases such as T2D, insulin resistance, and cardiovascular diseases have been reported previously (Ito *et al*., 2012).

Xanthine and hypoxanthine were elevated significantly in healthy individuals infused with high HC dose, but in CAH patients who received a high GC dose, hypoxanthine was increased while inosine was decreased. Inosine is catabolised to hypoxanthine and xanthine, one of the major sources of superoxide in the body, is from the action of xanthine oxidase (XO) which converts hypoxanthine via xanthine to uric acid (Sono, 1989). Dexamethasone was reported to induce hypertension in rats via this mechanism (Wallwork *et al*., 2003).

L-valine is a BCAA and it was found to be significantly elevated in plasma samples of patients with T2D following GC blockade. Additionally, it was also elevated in healthy individuals following a high dose of HC. In patients with CAH, L-valine was elevated in those who had high GC dose, BMI, SBP and DBP (G1 group). Elevation of L-valine might be due to protein wasting caused by excess plasma levels of GC (Schakman *et al.*, 2013). Moreover, hyperactivity of HPA-axis is associated with enhanced protein breakdown (Tataranni *et al.*, 1996). On the other hand, insulin, an anabolic hormone, significantly reduces levels of L-valine in healthy individuals. This

means that deviations in the levels of L-valine in blood from the physiological norm can be indicative of the imbalance between insulin and cortisol levels.

2-MBC was significantly elevated in patients with T2D following GC blockade. It was also elevated following high HC dose in healthy individuals. 2-MBC is a catabolic product of isoleucine used for energy production through TCA, thus its accumulation indicates an inhibition of branched chain acyl CoA dehydrogenase (Milburn *et al*., 2013). It was previously reported that patients with NAFLD had high plasma levels of this metabolite (Kalhan *et al*., 2011), as did those with T2D and insulin resistance (Lynch and Adams, 2014). The 2-MBC was also found elevated in obese children with insulin resistance compared to those who were insulin sensitive (Mastrangelo *et al*., 2016). Insulin injection following GC blockade significantly reduced the plasma levels of 2-methylbutyroylcarnitine by half but remained unchanged when insulin injection was given following placebo. These observations suggest that GC blockade improves insulin sensitivity. 2-MBC was affected significantly by the interaction between insulin dose and HC infusion (p = 0.015). High HC infusion significantly increased plasma levels of 2-MBC (p = 0.000008), but high insulin dose insignificantly elevates the plasma baseline of the metabolite (p = 0.37) and renders high HC dose less effective.

Androsterone glucuronide and pregnenolone sulfate are intermediate conjugates in the steroidogenesis pathway. Both were elevated significantly following GC

blockade in patients with T2D but as expected, they were decreased significantly following high HC dose in healthy individuals probably in response to HPA-axis inhibitory feedback mechanism (Harteneck, 2013). Androsterone glucuronide is considered an inactive end product. In contrast, pregnenolone sulphate, is not a waste product of sulphated pregnenolone following phase II reaction as one would expect (Harteneck, 2013).

The studies were limited to a single analytical platform using LC-MS, this increases the chance of missing some biomarkers, but the metabolomics changes in our studies were consistant with other studies. Moreover, application of stringent criteria in statistical analysis reduces number of significant biomarkers, but this in turn reduces the chance of type I error (false positive) and gives reliability to the clinical results. Although GC blockade and insulin vs HC interaction studies had small sample sizes the design of these studies and multiple sampling give high significance values for these studies.

Metabolomic response to GC action shows sensitivity but not specificity. For instance, chenodeoxyglycocholate is elevated in response to high GC dose in patients with CAH, but not affected in healthy subjects following high HC dose. Moreover, in TMRI-6 study, GC blockade treatment of 5 lean and 7 obese subjects did not detect alterations in bile acid levels (Alzweiri, 2008). On the other hand, in TMRI-4 study, 6 diabetic and 6 healthy subjects treated with carbenoxolone, which

blocks the interconversion between cortisone and cortisol, had significantly high levels of chenodeoxyglycocholic acid glucuronide compared to placebo (Alzweiri, 2008). These discrepancies in results might be due to differences in the health status of subjects recruited in each study, in which baseline levels of metabolites might vary, and this in turn might affect, to some extent, the metabolomic responses obtained with similar interventions.

7.1 Conclusion

Hypothesis-free metabolomics screening has identified putative metabolites in plasma which are differentially sensitive to GC deficiency or excess and may be useful in clinical assessment of GC therapy.

7.2 Strengths and limitations

Metabolomic profiling was employed to address clinical implications of the effect of GC abnormalities in humans using plasma samples. GC blockade and insulin HC interaction studies benefited from robust statistical designs, but on the other hand were limited by small sample sizes. GC dose cutoffs linked the biological perturbations to GC action in patients with CAH for the first time and produced reliable predictive biomarkers. In the same patients, HCA was able to detect patients at a high risk of cardiovascular complications based on their anthropometric and clinical measurements, but it would not be able to detect those

with heightened risk of adrenal crisis due to lack of sufficient clinical information about this complication in this study.

Generally, these studies were limited by using a single analytical technique, and also by a lack of replication studies, but benefited from the statistical approach used at multi- and uni-variate levels which guarantee proper and reliable biomarker selection. In particular the CAH study used a large co-hort of subjects making the application of supervised multivariate methods very robust.

7.3 Future work

Practically, an important area to address will be to tidy up the identification of some of the putative biomarkers using available standards and in the absence of suitable standards, MS2 fragmentation. This can be made more difficult by the very small sample volumes provided by clinical collaborators following their use in other aspects of a study.

Over and under replacement therapy of GC dose in patients with CAH is a point of concern, due to lack of reliable biomarkers that predict further complications. Addisonian crisis is a lethal complication as a result of under GC treatment. Until now, clinicians rely on questionnaires and annual assessments to address those at risk of Addisonian crisis (Hummel *et al*., 2016), which is time consuming and might lead to late medical interventions. Metabolomics profiling of plasma samples of

those with CAH at different stages would be a great area of research and it would provide potential biomarkers that predict those at risk of an Addisonian crisis.

Gut microbiota plays an important role in the development of some chronic diseases such as NAFLD (Dumas *et al*., 2006). This effect is either mediated directly through output of this flora and/or indirectly by manipulating GC biosynthesis (Hussain, 2013). Many metabolomic pathways are affected, such as aromatic amino acids, choline biosynthesis and bile acids. Thus targeting these pathways by integrating faeces and plasma metabolomes of patients with NAFLD compared to those without NAFLD would be of great benefit in the understanding of the pathophysiological perturbations and therapeutic targets.

References

Abdelkarim, M., Caron, S., Duhem, C., Prawitt, J., Dumont, J., Lucas, A., Bouchaert, E., Briand, O., Brozek, J., Kuipers, F., Fievet, C., Cariou, B. & Staels, B. 2010. The farnesoid X receptor regulates adipocyte differentiation and function by promoting peroxisome proliferator-activated receptor-gamma and interfering with the Wnt/beta-catenin pathways. *J Biol Chem,* 285**,** 36759-67.

Adams, S. H., Hoppel, C. L., Lok, K. H., Zhao, L., Wong, S. W., Minkler, P. E., Hwang, D. H., Newman, J. W. & Garvey, W. T. 2009. Plasma acylcarnitine profiles suggest incomplete long-chain fatty acid beta-oxidation and altered tricarboxylic acid cycle activity in type 2 diabetic African-American women. *J Nutr,* 139**,** 1073-81.

Ahmed, A., Rabbitt, E., Brady, T., Brown, C., Guest, P., Bujalska, I. J., Doig, C., Newsome, P. N., Hubscher, S. & Elias, E. 2012. A switch in hepatic cortisol metabolism across the spectrum of non alcoholic fatty liver disease. *PloS one,* 7**,** e29531.

Al Zweiri, M., Sills, G. J., Leach, J. P., Brodie, M. J., Robertson, C., Watson, D. G. & Parkinson, J. A. 2010. Response to drug treatment in newly diagnosed epilepsy: A pilot study of 1 H NMR-and MS-based metabonomic analysis. *Epilepsy research,* 88**,** 189-195.

Alberts, P., Rönquist-Nii, Y., Larsson, C., Klingström, G., Engblom, L., Edling, N., Lidell, V., Berg, I., Edlund, P.-O. & Ashkzari, M. 2005. Effect of high-fat diet on KKAy and ob/ob mouse liver and adipose tissue corticosterone and 11-dehydrocorticosterone concentrations. *Hormone and metabolic research,* 37**,** 402-407.

Alzweiri, M. 2008. *Investigation and Optimizations of Metabonomics as a Clinical Tool of Analysis.* PhD, Strathclyde University.

Anderson, C. M. & Stahl, A. 2013. SLC27 fatty acid transport proteins. *Mol Aspects Med,* 34**,** 516-28.

Andrews, R. C. & Walker, B. R. 1999a. Glucocorticoids and insulin resistance: old hormones, new targets. *Clin Sci (Lond),* 96**,** 513-23.

Andrews, R. C. & Walker, B. R. 1999b. Glucocorticoids and insulin resistance: old hormones, new targets. *Clinical Science,* 96**,** 513-523.

Angeli, A., Guglielmi, G., Dovio, A., Capelli, G., De Feo, D., Giannini, S., Giorgino, R., Moro, L. & Giustina, A. 2006. High prevalence of asymptomatic vertebral fractures in post-menopausal women receiving chronic glucocorticoid therapy: a cross-sectional outpatient study. *Bone,* 39**,** 253-9.

Anstee, Q. M. & Goldin, R. D. 2006. Mouse models in non-alcoholic fatty liver disease and steatohepatitis research. *International journal of experimental pathology,* 87**,** 1-16.

Arlt, W., Willis, D. S., Wild, S. H., Krone, N., Doherty, E. J., Hahner, S., Han, T. S., Carroll, P. V., Conway, G. S., Rees, D. A., Stimson, R. H., Walker, B. R., Connell, J. M., Ross, R. J. & United Kingdom Congenital Adrenal Hyperplasia Adult Study, E. 2010. Health status of adults with congenital adrenal hyperplasia: a cohort study of 203 patients. *J Clin Endocrinol Metab,* 95**,** 5110-21.

Baptissart, M., Vega, A., Martinot, E., Baron, S., Lobaccaro, J. M. & Volle, D. H. 2013. Farnesoid X receptor alpha: a molecular link between bile acids and steroid signaling? *Cell Mol Life Sci,* 70**,** 4511-26.

Batch, B. C., Shah, S. H., Newgard, C. B., Turer, C. B., Haynes, C., Bain, J. R., Muehlbauer, M., Patel, M. J., Stevens, R. D., Appel, L. J., Newby, L. K. & Svetkey, L. P. 2013. Branched chain amino acids are novel biomarkers for discrimination of metabolic wellness. *Metabolism,* 62**,** 961-9.

Batchelor, T. T., Taylor, L. P., Thaler, H. T., Posner, J. B. & Deangelis, L. M. 1997. Steroid myopathy in cancer patients. *Neurology,* 48**,** 1234-8.

Bateson, M. C., Maclean, D., Evans, J. R. & Bouchier, I. A. 1978. Chenodeoxycholic acid therapy for hypertriglyceridaemia in men. *Br J Clin Pharmacol,* 5**,** 249-54.

Benjamini, Y. & Hochberg, Y. 1995. Controlling the False Discovery Rate a Practical and powerful Approach to Multiple Testing. *Journal of the Royal Statistical Society,* 57**,** 289-300.

Bennion, L. J. & Grundy, S. M. 1977. Effects of diabetes mellitus on cholesterol metabolism in man. *N Engl J Med,* 296**,** 1365-71.

Bergthorsdottir, R., Leonsson-Zachrisson, M., Oden, A. & Johannsson, G. 2006. Premature mortality in patients with Addison's disease: a population-based study. *J Clin Endocrinol Metab,* 91**,** 4849-53.

Berthiaume, M., Laplante, M., Festuccia, W., Gélinas, Y., Poulin, S., Lalonde, J., Joanisse, D. R., Thieringer, R. & Deshaies, Y. 2007. Depot-specific modulation of rat intraabdominal adipose tissue lipid metabolism by pharmacological inhibition of 11β-hydroxysteroid dehydrogenase type 1. *Endocrinology,* 148**,** 2391-2397.

Bewick, V., Cheek, L. & Ball, J. 2004. Statistics review 13: receiver operating characteristic curves. *Crit Care,* 8**,** 508-12.

Bivalacqua, T. J., Hellstrom, W. J., Kadowitz, P. J. & Champion, H. C. 2001. Increased expression of arginase II in human diabetic corpus cavernosum: in diabetic-associated erectile dysfunction. *Biochem Biophys Res Commun,* 283**,** 923-7.

Bonfig, W., Bechtold, S., Schmidt, H., Knorr, D. & Schwarz, H. P. 2007. Reduced final height outcome in congenital adrenal hyperplasia under prednisone treatment: deceleration of growth velocity during puberty. *The Journal of Clinical Endocrinology & Metabolism,* 92**,** 1635-1639.

Boonen, E., Vervenne, H., Meersseman, P., Andrew, R., Mortier, L., Declercq, P. E., Vanwijngaerden, Y. M., Spriet, I., Wouters, P. J., Vander Perre, S., Langouche,

L., Vanhorebeek, I., Walker, B. R. & Van Den Berghe, G. 2013. Reduced cortisol metabolism during critical illness. *N Engl J Med,* 368**,** 1477-88.

Bordag, N., Klie, S., Jurchott, K., Vierheller, J., Schiewe, H., Albrecht, V., Tonn, J. C., Schwartz, C., Schichor, C. & Selbig, J. 2015. Glucocorticoid (dexamethasone)-induced metabolome changes in healthy males suggest prediction of response and side effects. *Sci Rep,* 5**,** 15954.

Bornstein, S. R., Allolio, B., Arlt, W., Barthel, A., Don-Wauchope, A., Hammer, G. D., Husebye, E. S., Merke, D. P., Murad, M. H., Stratakis, C. A. & Torpy, D. J. 2016. Diagnosis and Treatment of Primary Adrenal Insufficiency: An Endocrine Society Clinical Practice Guideline. *J Clin Endocrinol Metab,* 101**,** 364-89.

Boulange, C. L., Neves, A. L., Chilloux, J., Nicholson, J. K. & Dumas, M. E. 2016. Impact of the gut microbiota on inflammation, obesity, and metabolic disease. *Genome Med,* 8**,** 42.

Broca, C., Breil, V., Cruciani-Guglielmacci, C., Manteghetti, M., Rouault, C., Derouet, M., Rizkalla, S., Pau, B., Petit, P., Ribes, G., Ktorza, A., Gross, R., Reach, G. & Taouis, M. 2004. Insulinotropic agent ID-1101 (4-hydroxyisoleucine) activates insulin signaling in rat. *Am J Physiol Endocrinol Metab,* 287**,** E463-71.

Bugianesi, E., Gastaldelli, A., Vanni, E., Gambino, R., Cassader, M., Baldi, S., Ponti, V., Pagano, G., Ferrannini, E. & Rizzetto, M. 2005. Insulin resistance in non-diabetic patients with non-alcoholic fatty liver disease: sites and mechanisms. *Diabetologia,* 48**,** 634-642.

Bundy, J. G., Willey, T. L., Castell, R. S., Ellar, D. J. & Brindle, K. M. 2005. Discrimination of pathogenic clinical isolates and laboratory strains of Bacillus cereus by NMR-based metabolomic profiling. *FEMS microbiology letters,* 242**,** 127-136.

Buttgereit, F., Da Silva, J., Boers, M., Burmester, G., Cutolo, M., Jacobs, J., Kirwan, J., Köhler, L., Van Riel, P. & Vischer, T. 2002. Standardised nomenclature for glucocorticoid dosages and glucocorticoid treatment regimens: current questions and tentative answers in rheumatology. *Annals of the rheumatic diseases,* 61**,** 718-722.

Caldwell, R. B., Toque, H. A., Narayanan, S. P. & Caldwell, R. W. 2015. Arginase: an old enzyme with new tricks. *Trends Pharmacol Sci,* 36**,** 395-405.

Campino, C., Carvajal, C. A., Cornejo, J., San Martin, B., Olivieri, O., Guidi, G., Faccini, G., Pasini, F., Sateler, J., Baudrand, R., Mosso, L., Owen, G. I., Kalergis, A. M., Padilla, O. & Fardella, C. E. 2010. 11beta-Hydroxysteroid dehydrogenase type-2 and type-1 (11beta-HSD2 and 11beta-HSD1) and 5beta-reductase activities in the pathogenia of essential hypertension. *Endocrine,* 37**,** 106-14.

Canalis, E. 2005. Mechanisms of glucocorticoid action in bone. *Curr Osteoporos Rep,* 3**,** 98-102.

Canalis, E., Mazziotti, G., Giustina, A. & Bilezikian, J. P. 2007. Glucocorticoid-induced osteoporosis: pathophysiology and therapy. *Osteoporos Int,* 18**,** 1319-28.

Cariou, B., Van Harmelen, K., Duran-Sandoval, D., Van Dijk, T. H., Grefhorst, A., Abdelkarim, M., Caron, S., Torpier, G., Fruchart, J. C., Gonzalez, F. J., Kuipers, F. & Staels, B. 2006. The farnesoid X receptor modulates adiposity and peripheral insulin sensitivity in mice. *J Biol Chem,* 281**,** 11039-49.

Chatterjea, M. N. & Shinde, R. 2008. Metabolism of Lipids. *In:* JYPEE (ed.) *Textbook of Medical Biochemistry.* 7th ed. New Delhi: Jaypee Brothers Medical Publishers (P) Ltd, 374-377.

Chen, X., Iqbal, N. & Boden, G. 1999. The effects of free fatty acids on gluconeogenesis and glycogenolysis in normal subjects. *The Journal of clinical investigation,* 103**,** 365-372.

Chong, I.-G. & Jun, C.-H. 2005. Performance of some variable selection methods when multicollinearity is present. *Chemometrics and Intelligent Laboratory Systems,* 78**,** 103-112.

Clarke, G., Stilling, R. M., Kennedy, P. J., Stanton, C., Cryan, J. F. & Dinan, T. G. 2014. Minireview: Gut microbiota: the neglected endocrine organ. *Mol Endocrinol,* 28**,** 1221-38.

Cole, T., Wilcox, H. & Heimberg, M. 1982. Effects of adrenalectomy and dexamethasone on hepatic lipid metabolism. *Journal of lipid research,* 23**,** 81-91.

Creek, D. J., Jankevics, A., Breitling, R., Watson, D. G., Barrett, M. P. & Burgess, K. E. 2011. Toward global metabolomics analysis with hydrophilic interaction liquid chromatography-mass spectrometry: improved metabolite identification by retention time prediction. *Anal Chem,* 83**,** 8703-10.

Creek, D. J., Jankevics, A., Burgess, K. E., Breitling, R. & Barrett, M. P. 2012. IDEOM: an Excel interface for analysis of LC-MS-based metabolomics data. *Bioinformatics,* 28**,** 1048-9.

Dallman, M. F., Akana, S. F., Bhatnagar, S., Bell, M. E. & Strack, A. M. 2000. Bottomed out: metabolic significance of the circadian trough in glucocorticoid concentrations. *Int J Obes Relat Metab Disord,* 24 Suppl 2**,** S40-6.

De Nijs, R. N., Jacobs, J. W., Lems, W. F., Laan, R. F., Algra, A., Huisman, A. M., Buskens, E., De Laet, C. E., Oostveen, A. C., Geusens, P. P., Bruyn, G. A., Dijkmans, B. A., Bijlsma, J. W. & Investigators, S. 2006. Alendronate or alfacalcidol in glucocorticoid-induced osteoporosis. *N Engl J Med,* 355**,** 675-84.

Dhir, V., Ivison, H. E., Krone, N., Shackleton, C. H., Doherty, A. J., Stewart, P. M. & Arlt, W. 2007. Differential inhibition of CYP17A1 and CYP21A2 activities by the P450 oxidoreductase mutant A287P. *Mol Endocrinol,* 21**,** 1958-68.

Dinan, T. G. & Cryan, J. F. 2012. Regulation of the stress response by the gut microbiota: implications for psychoneuroendocrinology. *Psychoneuroendocrinology,* 37**,** 1369-78.

Doege, H., Baillie, R. A., Ortegon, A. M., Tsang, B., Wu, Q., Punreddy, S., Hirsch, D., Watson, N., Gimeno, R. E. & Stahl, A. 2006. Targeted deletion of FATP5

reveals multiple functions in liver metabolism: alterations in hepatic lipid homeostasis. *Gastroenterology,* 130**,** 1245-58.

Doege, H., Grimm, D., Falcon, A., Tsang, B., Storm, T. A., Xu, H., Ortegon, A. M., Kazantzis, M., Kay, M. A. & Stahl, A. 2008. Silencing of hepatic fatty acid transporter protein 5 in vivo reverses diet-induced non-alcoholic fatty liver disease and improves hyperglycemia. *J Biol Chem,* 283**,** 22186-92.

Donnelly, K. L., Smith, C. I., Schwarzenberg, S. J., Jessurun, J., Boldt, M. D. & Parks, E. J. 2005. Sources of fatty acids stored in liver and secreted via lipoproteins in patients with nonalcoholic fatty liver disease. *The Journal of clinical investigation,* 115**,** 1343-1351.

Drogan, D., Dunn, W. B., Lin, W., Buijsse, B., Schulze, M. B., Langenberg, C., Brown, M., Floegel, A., Dietrich, S., Rolandsson, O., Wedge, D. C., Goodacre, R., Forouhi, N. G., Sharp, S. J., Spranger, J., Wareham, N. J. & Boeing, H. 2015. Untargeted metabolic profiling identifies altered serum metabolites of type 2 diabetes mellitus in a prospective, nested case control study. *Clin Chem,* 61**,** 487-97.

Duarte, N. C., Becker, S. A., Jamshidi, N., Thiele, I., Mo, M. L., Vo, T. D., Srivas, R. & Palsson, B. Ø. 2007. Global reconstruction of the human metabolic network based on genomic and bibliomic data. *Proceedings of the National Academy of Sciences,* 104**,** 1777-1782.

Dumas, M. E., Barton, R. H., Toye, A., Cloarec, O., Blancher, C., Rothwell, A., Fearnside, J., Tatoud, R., Blanc, V., Lindon, J. C., Mitchell, S. C., Holmes, E., Mccarthy, M. I., Scott, J., Gauguier, D. & Nicholson, J. K. 2006. Metabolic profiling reveals a contribution of gut microbiota to fatty liver phenotype in insulin-resistant mice. *Proc Natl Acad Sci U S A,* 103**,** 12511-6.

Dunn, W. B. 2013. Diabetes-the Role of Metabolomics in the Discovery of New Mechanisms and Novel Biomarkers. *Current Cardiovascular Risk Reports,* 7**,** 25-32.

Dunn, W. B., Bailey, N. J. & Johnson, H. E. 2005. Measuring the metabolome: current analytical technologies. *Analyst,* 130**,** 606-625.

Dunn, W. B., Broadhurst, D. I., Atherton, H. J., Goodacre, R. & Griffin, J. L. 2011. Systems level studies of mammalian metabolomes: the roles of mass spectrometry and nuclear magnetic resonance spectroscopy. *Chem Soc Rev,* 40**,** 387-426.

Duran-Sandoval, D., Mautino, G., Martin, G., Percevault, F., Barbier, O., Fruchart, J. C., Kuipers, F. & Staels, B. 2004. Glucose regulates the expression of the farnesoid X receptor in liver. *Diabetes,* 53**,** 890-8.

Eastell, R., Reid, D. M., Compston, J., Cooper, C., Fogelman, I., Francis, R. M., Hosking, D. J., Purdie, D. W., Ralston, S. H., Reeve, J., Russell, R. G., Stevenson, J. C. & Torgerson, D. J. 1998. A UK Consensus Group on management of glucocorticoid-induced osteoporosis: an update. *J Intern Med,* 244**,** 271-92.

Efron, B. & Gong, G. 1983. A Leisurely Look at the Bootstrap, the Jackknife, and Cross-validation. *The American Statistician,* 37**,** 36-48.

Ellero-Simatos, S., Szymanska, E., Rullmann, T., Dokter, W. H. A., Ramaker, R., Berger, R., Van Iersel, T. M. P., Smilde, A. K., Hankemeier, T. & Alkema, W. 2012. Assessing the metabolic effects of prednisolone in healthy volunteers using urine metabolic profiling. *Genome Medicine,* 4.

Ellero-Simatos. S, Szymanska. E, Rullmann. T, Dokter. Wh, Ramaker. R, Berger. R, Van Iersel. Tm, Smilde. Ak, Hankemeier. T & Alkema. W 2012. Assessing the metabolic effects of prednisolone in healthy volunteers using urine metabolic profiling. *Genome Medicine,* 4**,** 84-94.

Eriksson, L., Byrne, T., Johansson, E., Trygg, J. & Vikstrom, C. 2013a. Centering and Scaling. *Multi- and Megavariate Data Analysis: Basic Principles and Application.* 3 ed. Sweden: MKS Umetrics AB, 247-248.

Eriksson, L., Byrne, T., Johansson, E., Trygg, J. & Vikstrom, C. 2013b. Cross validation. *Multi- and Megavariate Data Analysis: Basic Principles and Application.* 3 ed. Sweden: MKS Umetrics AB, 461.

Eriksson, L., Byrne, T., Johansson, E., Trygg, J. & Vikstrom, C. 2013c. How do we analyze our data today? *Multi- and Megavariate Data Analysis: Basic Principles and Application.* 3 ed. Sweden: MKS Umetrics AB, 21-22.

Eriksson, L., Byrne, T., Johansson, E., Trygg, J. & Vikstrom, C. 2013d. *Multi- and Megavariate Data Analysis: Basic Principles and Application,* Sweden, MKS Umetrics AB.

Eriksson, L., Byrne, T., Johansson, E., Trygg, J. & Vikstrom, C. 2013e. Observation diagnostics - Are there outliers in the data? *Multi- and Megavariate Data Analysis: Basic Principles and Application.* 3 ed. Sweden: MKS Umetrics AB, 46-50.

Eriksson, L., Byrne, T., Johansson, E., Trygg, J. & Vikstrom, C. 2013f. Response permutation and cross-validation. *Multi- and Megavariate Data Analysis: Basic Principles and Application.* 3 ed. Sweden: MKS Umetrics AB, 421-424.

Eriksson, L., Byrne, T., Johansson, E., Trygg, J. & Vikstrom, C. 2013g. Transformation and expansion. *In:* UMETRICS, M. (ed.) *Multi- and Megavariate Data Analysis.* Sweden: MKS, 233-238.

Eriksson, L., Byrne, T., Johansson, E., Trygg, J. & Vikstrom, C. 2013h. Variable importance, VIP. *Multi- and Megavariate Data Analysis: Basic Principles and Application.* 3 ed. Sweden: MKS Umetrics AB, 455-456.

Eriksson, L., Trygg, J. & Wold, S. 2008a. CV-ANOVA for significance testing of PLS and OPLS (R) models. *Journal of Chemometrics,* 22**,** 594-600.

Eriksson, L., Trygg, J. & Wold, S. 2008b. CV-ANOVA for significance testing of PLS and OPLS® models. *Journal of Chemometrics,* 22**,** 594-600.

Fabbrini, E., Mohammed, B. S., Magkos, F., Korenblat, K. M., Patterson, B. W. & Klein, S. 2008. Alterations in adipose tissue and hepatic lipid kinetics in obese men and women with nonalcoholic fatty liver disease. *Gastroenterology,* 134**,** 424-431.

Fardet, A., Llorach, R., Martin, J. F., Besson, C., Lyan, B., Pujos-Guillot, E. & Scalbert, A. 2008. A liquid chromatography-quadrupole time-of-flight (LC-QTOF)-based metabolomic approach reveals new metabolic effects of catechin in rats fed high-fat diets. *J Proteome Res,* 7**,** 2388-98.

Feig, P., Shah, S., Hermanowski-Vosatka, A., Plotkin, D., Springer, M., Donahue, S., Thach, C., Klein, E., Lai, E. & Kaufman, K. 2011. Effects of an 11β-hydroxysteroid dehydrogenase type 1 inhibitor, MK-0916, in patients with type 2 diabetes mellitus and metabolic syndrome. *Diabetes, Obesity and Metabolism,* 13**,** 498-504.

Fernstrom, J. D. & Wurtmen, R. J. 1972. Elevation of plasma tryptophan by insulin in rat. *Metabolism,* 21**,** 337-42.

Ferrari, P. 2010. The role of 11beta-hydroxysteroid dehydrogenase type 2 in human hypertension. *Biochim Biophys Acta,* 1802**,** 1178-87.

Fiehn, O. 2002. Metabolomics–the link between genotypes and phenotypes. *Plant molecular biology,* 48**,** 155-171.

Filipsson, H., Monson, J. P., Koltowska-Haggstrom, M., Mattsson, A. & Johannsson, G. 2006. The impact of glucocorticoid replacement regimens on metabolic outcome and comorbidity in hypopituitary patients. *J Clin Endocrinol Metab,* 91**,** 3954-61.

Forouhi, N. G., Koulman, A., Sharp, S. J., Imamura, F., Kröger, J., Schulze, M. B., Crowe, F. L., Huerta, J. M., Guevara, M., Beulens, J. W. J., Van Woudenbergh, G. J., Wang, L., Summerhill, K., Griffin, J. L., Feskens, E. J. M., Amiano, P., Boeing, H., Clavel-Chapelon, F., Dartois, L., Fagherazzi, G., Franks, P. W., Gonzalez, C., Jakobsen, M. U., Kaaks, R., Key, T. J., Khaw, K.-T., Kühn, T., Mattiello, A., Nilsson, P. M., Overvad, K., Pala, V., Palli, D., Quirós, J. R., Rolandsson, O., Roswall, N., Sacerdote, C., Sánchez, M.-J., Slimani, N., Spijkerman, A. M. W., Tjonneland, A., Tormo, M.-J., Tumino, R., Van Der A, D. L., Van Der Schouw, Y. T., Langenberg, C., Riboli, E. & Wareham, N. J. 2014. Differences in the prospective association between individual plasma phospholipid saturated fatty acids and incident type 2 diabetes: the EPIC-InterAct case-cohort study. *The Lancet Diabetes & Endocrinology,* 2**,** 810-818.

Fukusaki, E. & Kobayashi, A. 2005. Plant metabolomics: potential for practical operation. *Journal of Bioscience and Bioengineering,* 100**,** 347-354.

Gambino, R., Bugianesi, E., Rosso, C., Mezzabotta, L., Pinach, S., Alemanno, N., Saba, F. & Cassader, M. 2016. Different Serum Free Fatty Acid Profiles in NAFLD Subjects and Healthy Controls after Oral Fat Load. *Int J Mol Sci,* 17.

Gastaldelli, A., Cusi, K., Pettiti, M., Hardies, J., Miyazaki, Y., Berria, R., Buzzigoli, E., Sironi, A. M., Cersosimo, E. & Ferrannini, E. 2007. Relationship between hepatic/visceral fat and hepatic insulin resistance in nondiabetic and type 2 diabetic subjects. *Gastroenterology,* 133**,** 496-506.

Goodacre, R. 2007. Metabolomics of a Superorganism[1–3.] *The Journal of Nutrition,* 137**,** 137259S–266S.

Goodwin, B., Jones, S. A., Price, R. R., Watson, M. A., Mckee, D. D., Moore, L. B., Galardi, C., Wilson, J. G., Lewis, M. C., Roth, M. E., Maloney, P. R., Willson, T. M. & Kliewer, S. A. 2000. A regulatory cascade of the nuclear receptors FXR, SHP-1, and LRH-1 represses bile acid biosynthesis. *Mol Cell,* 6**,** 517-26.

Grainger, D. J. 2003. Megavariate Statistics meets High Data-density Analytical Methods: The Future of Medical Diagnostics? *IRTL Reviews,* 1**,** 6.

Gromski, P. S., Xu, Y., Kotze, H. L., Correa, E., Ellis, D. I., Armitage, E. G., Turner, M. L. & Goodacre, R. 2014. Influence of missing values substitutes on multivariate analysis of metabolomics data. *Metabolites,* 4**,** 433-52.

Guasch-Ferre, M., Hruby, A., Toledo, E., Clish, C. B., Martinez-Gonzalez, M. A., Salas-Salvado, J. & Hu, F. B. 2016. Metabolomics in Prediabetes and Diabetes: A Systematic Review and Meta-analysis. *Diabetes Care,* 39**,** 833-46.

Guenego, A., Morel, Y., Ionesco, O., Mallet, D. & Priou-Guesdon, M. 2015. A late 17 alpha-hydroxylase deficiency diagnosis that leads to the discovery of a new CYP17 gene mutation. *Annales D Endocrinologie,* 76**,** 71-74.

Han, T., Stimson, R., Rees, D., Krone, N., Willis, D., Conway, G., Arlt, W., Walker, B. & Ross, R. 2013a. Glucocorticoid treatment regimen and health outcomes in adults with congenital adrenal hyperplasia. *Clinical endocrinology,* 78**,** 197-203.

Han, T. S., Krone, N., Willis, D. S., Conway, G. S., Hahner, S., Rees, D. A., Stimson, R. H., Walker, B. R., Arlt, W. & Ross, R. J. 2013b. Quality of life in adults with congenital adrenal hyperplasia relates to glucocorticoid treatment, adiposity and insulin resistance: United Kingdom Congenital adrenal Hyperplasia Adult Study Executive (CaHASE). *European Journal of Endocrinology,* 168**,** 887-893.

Harrigan, G. G. & Goodacre, R. 2012. *Metabolic profiling: its role in biomarker discovery and gene function analysis*, Springer Science & Business Media.

Harteneck, C. 2013. Pregnenolone sulfate: from steroid metabolite to TRP channel ligand. *Molecules,* 18**,** 12012-28.

Heszele, M. F. C. & Price, S. R. 2004. Insulin-like growth factor I: the yin and yang of muscle atrophy. *Endocrinology,* 145**,** 4803-4805.

Hinault, C., Mothe-Satney, I., Gautier, N., Lawrence, J. C., Jr. & Van Obberghen, E. 2004. Amino acids and leucine allow insulin activation of the PKB/mTOR pathway in normal adipocytes treated with wortmannin and in adipocytes from db/db mice. *FASEB J,* 18**,** 1894-6.

Hirai, M. Y., Yano, M., Goodenowe, D. B., Kanaya, S., Kimura, T., Awazuhara, M., Arita, M., Fujiwara, T. & Saito, K. 2004. Integration of transcriptomics and metabolomics for understanding of global responses to nutritional stresses in Arabidopsis thaliana. *Proceedings of the National Academy of Sciences of the United States of America,* 101**,** 10205-10210.

Hoes, J., Jacobs, J. W., Verstappen, S. M., Bijlsma, J. W. & Van Der Heijden, G. J. 2008. Adverse events of low-to-medium-dose oral glucocorticoids in inflammatory diseases: a meta-analysis. *Annals of the rheumatic diseases*.

Huffman, K. M., Shah, S. H., Stevens, R. D., Bain, J. R., Muehlbauer, M., Slentz, C. A., Tanner, C. J., Kuchibhatla, M., Houmard, J. A., Newgard, C. B. & Kraus, W. E. 2009. Relationships between circulating metabolic intermediates and insulin action in overweight to obese, inactive men and women. *Diabetes Care,* 32**,** 1678-83.

Hughes, K. A., Webster, S. P. & Walker, B. R. 2008. 11-Beta-hydroxysteroid dehydrogenase type 1 (11beta-HSD1) inhibitors in type 2 diabetes mellitus and obesity. *Expert Opin Investig Drugs,* 17**,** 481-96.

Hummel, S. R., Sadler, S., Whitaker, M. J., Ara, R. M., Dixon, S. & Ross, R. J. 2016. A Model for Measuring the Health Burden of Classic Congenital Adrenal Hyperplasia in Adults. *Clin Endocrinol (Oxf)*.

Ito, T., Schaffer, S. W. & Azuma, J. 2012. The potential usefulness of taurine on diabetes mellitus and its complications. *Amino Acids,* 42**,** 1529-39.

Ivosev, G., Burton, L. & Bonner, R. 2008. Dimensionality reduction and visualization in principal component analysis. *Anal Chem,* 80**,** 4933-44.

Jacobson, P. B., Von Geldern, T. W., Ohman, L., Osterland, M., Wang, J., Zinker, B., Wilcox, D., Nguyen, P. T., Mika, A., Fung, S., Fey, T., Goos-Nilsson, A., Grynfarb, M., Barkhem, T., Marsh, K., Beno, D. W., Nga-Nguyen, B., Kym, P. R., Link, J. T., Tu, N., Edgerton, D. S., Cherrington, A., Efendic, S., Lane, B. C. & Opgenorth, T. J. 2005. Hepatic glucocorticoid receptor antagonism is sufficient to reduce elevated hepatic glucose output and improve glucose control in animal models of type 2 diabetes. *J Pharmacol Exp Ther,* 314**,** 191-200.

Joels, M., Fernandez, G. & Roozendaal, B. 2011. Stress and emotional memory: a matter of timing. *Trends Cogn Sci,* 15**,** 280-8.

Johannsson, G., Falorni, A., Skrtic, S., Lennernäs, H., Quinkler, M., Monson, J. P. & Stewart, P. M. 2015. Adrenal insufficiency: review of clinical outcomes with current glucocorticoid replacement therapy. *Clinical endocrinology,* 82**,** 2-11.

John, S. & Schmieder, R. E. 2003. Potential mechanisms of impaired endothelial function in arterial hypertension and hypercholesterolemia. *Current Hypertension Reports,* 5**,** 199-207.

Johnson, E. S., Lindblom, K. R., Robeson, A., Stevens, R. D., Ilkayeva, O. R., Newgard, C. B., Kornbluth, S. & Andersen, J. L. 2013. Metabolomic profiling reveals a role for caspase-2 in lipoapoptosis. *J Biol Chem,* 288**,** 14463-75.

Kalhan, S. C., Guo, L., Edmison, J., Dasarathy, S., Mccullough, A. J., Hanson, R. W. & Milburn, M. 2011. Plasma metabolomic profile in nonalcoholic fatty liver disease. *Metabolism,* 60**,** 404-13.

Kamleh, A., Barrett, M. P., Wildridge, D., Burchmore, R. J., Scheltema, R. A. & Watson, D. G. 2008. Metabolomic profiling using Orbitrap Fourier transform mass spectrometry with hydrophilic interaction chromatography: a method with wide applicability to analysis of biomolecules. *Rapid Commun Mass Spectrom,* 22**,** 1912-8.

Kampfer, H., Pfeilschifter, J. & Frank, S. 2003. Expression and activity of arginase isoenzymes during normal and diabetes-impaired skin repair. *J Invest Dermatol,* 121**,** 1544-51.

Kanda, F., Okuda, S., Matsushita, T., Takatani, K., Kimura, K. I. & Chihara, K. 2001. Steroid myopathy: pathogenesis and effects of growth hormone and insulin-like growth factor-I administration. *Horm Res,* 56 Suppl 1**,** 24-8.

Kanda, F., Takatani, K., Okuda, S., Matsushita, T. & Chihara, K. 1999. Preventive effects of insulinlike growth factor-I on steroid-induced muscle atrophy. *Muscle Nerve,* 22**,** 213-7.

Kawaguchi, T., Taniguchi, E., Itou, M., Sumie, S., Oriishi, T., Matsuoka, H., Nagao, Y. & Sata, M. 2007. Branched-chain amino acids improve insulin resistance in patients with hepatitis C virus-related liver disease: report of two cases. *Liver Int,* 27**,** 1287-92.

Kim, J., Jung, Y., Song, B., Bong, Y.-S., Lee, K.-S. & Hwang, G.-S. 2013. Discrimination of cabbage (Brassica rapa ssp. pekinensis) cultivars grown in different geographical areas using 1 H NMR-based metabolomics. *Food chemistry,* 137**,** 68-75.

Kim, M., Jung, S., Lee, S. H. & Lee, J. H. 2015. Association between arterial stiffness and serum L-octanoylcarnitine and lactosylceramide in overweight middle-aged subjects: 3-year follow-up study. *PLoS One,* 10**,** e0119519.

Kimura, K., Kanda, F., Okuda, S. & Chihara, K. 2001. Insulin-like growth factor 1 inhibits glucocorticoid-induced glutamine synthetase activity in cultured L6 rat skeletal muscle cells. *Neurosci Lett,* 302**,** 154-6.

Kirk, L. F., Jr., Hash, R. B., Katner, H. P. & Jones, T. 2000. Cushing's disease: clinical manifestations and diagnostic evaluation. *Am Fam Physician,* 62**,** 1119-27, 1133-4.

Kirwan, G. M., Johansson, E., Kleemann, R., Verheij, E. R., Wheelock, A. M., Goto, S., Trygg, J. & Wheelock, C. E. 2012. Building multivariate systems biology models. *Anal Chem,* 84**,** 7064-71.

Kishimoto, M., Oishi, A. & Motojima, S. 2006. Alendronate or alfacalcidol in glucocorticoid-induced osteoporosis. *N Engl J Med,* 355**,** 2156; author reply 2157.

Klein, M. S. & Shearer, J. 2016. Metabolomics and Type 2 Diabetes: Translating Basic Research into Clinical Application. *J Diabetes Res,* 2016**,** 3898502.

Kondo, Y., Nishiumi, S., Shinohara, M., Hatano, N., Ikeda, A., Yoshie, T., Kobayashi, T., Shiomi, Y., Irino, Y. & Takenawa, T. 2011. Serum fatty acid profiling of colorectal cancer by gas chromatography/mass spectrometry. *Biomarkers in medicine,* 5**,** 451-460.

Konopelska, S., Kienitz, T., Hughes, B., Pirlich, M., Bauditz, J., Lochs, H., Strasburger, C. J., Stewart, P. M. & Quinkler, M. 2009. Hepatic 11beta-HSD1 mRNA expression in fatty liver and nonalcoholic steatohepatitis. *Clinical endocrinology,* 70**,** 554-560.

Kovamees, O., Shemyakin, A. & Pernow, J. 2016. Amino acid metabolism reflecting arginase activity is increased in patients with type 2 diabetes and associated with endothelial dysfunction. *Diab Vasc Dis Res*.

Kraus, D., Yang, Q., Kong, D., Banks, A. S., Zhang, L., Rodgers, J. T., Pirinen, E., Pulinilkunnil, T. C., Gong, F., Wang, Y. C., Cen, Y., Sauve, A. A., Asara, J. M., Peroni, O. D., Monia, B. P., Bhanot, S., Alhonen, L., Puigserver, P. & Kahn, B. B. 2014. Nicotinamide N-methyltransferase knockdown protects against diet-induced obesity. *Nature,* 508**,** 258-62.

Krebs, M. 2005. Amino acid-dependent modulation of glucose metabolism in humans. *Eur J Clin Invest,* 35**,** 351-4.

Krebs, M. & Roden, M. 2004. Nutrient-induced insulin resistance in human skeletal muscle. *Curr Med Chem,* 11**,** 901-8.

Krone, N., Braun, A., Roscher, A. A., Knorr, D. & Schwarz, H. P. 2000. Predicting phenotype in steroid 21-hydroxylase deficiency? Comprehensive genotyping in 155 unrelated, well defined patients from southern Germany. *J Clin Endocrinol Metab,* 85**,** 1059-65.

Krone, N., Dhir, V., Ivison, H. E. & Arlt, W. 2007. Congenital adrenal hyperplasia and P450 oxidoreductase deficiency. *Clin Endocrinol (Oxf),* 66**,** 162-72.

Lambert, G., Amar, M. J., Guo, G., Brewer, H. B., Jr., Gonzalez, F. J. & Sinal, C. J. 2003. The farnesoid X-receptor is an essential regulator of cholesterol homeostasis. *J Biol Chem,* 278**,** 2563-70.

Lambillotte, C., Gilon, P. & Henquin, J.-C. 1997. Direct glucocorticoid inhibition of insulin secretion. An in vitro study of dexamethasone effects in mouse islets. *Journal of Clinical Investigation,* 99**,** 414.

Lefebvre, P., Cariou, B., Lien, F., Kuipers, F. & Staels, B. 2009. Role of bile acids and bile acid receptors in metabolic regulation. *Physiol Rev,* 89**,** 147-91.

Lefer, A. M. & Lefer, D. J. 1996. The role of nitric oxide and cell adhesion molecules on the microcirculation in ischaemia-reperfusion. *Cardiovascular Research,* 32**,** 743-751.

Letteron, P., Brahimi-Bourouina, N., Robin, M., Moreau, A., Feldmann, G. & Pessayre, D. 1997. Glucocorticoids inhibit mitochondrial matrix acyl-CoA dehydrogenases and fatty acid beta-oxidation. *American Journal of Physiology-Gastrointestinal and Liver Physiology,* 272**,** G1141-G1150.

Lightman, S. L., Wiles, C. C., Atkinson, H. C., Henley, D. E., Russell, G. M., Leendertz, J. A., Mckenna, M. A., Spiga, F., Wood, S. A. & Conway-Campbell, B. L. 2008. The significance of glucocorticoid pulsatility. *Eur J Pharmacol,* 583**,** 255-62.

Liu, Y., Porta, A., Peng, X., Gengaro, K., Cunningham, E. B., Li, H., Dominguez, L. A., Bellido, T. & Christakos, S. 2004. Prevention of glucocorticoid-induced apoptosis in osteocytes and osteoblasts by calbindin-D28k. *J Bone Miner Res,* 19**,** 479-90.

Livingstone, D. E., Jones, G. C., Smith, K., Jamieson, P. M., Andrew, R., Kenyon, C. J. & Walker, B. R. 2000. Understanding the role of glucocorticoids in obesity:

tissue-specific alterations of corticosterone metabolism in obese Zucker rats. *Endocrinology,* 141**,** 560-3.

Lozano, N. B., Oliveira, R. F., Weber, K. C., Honorio, K. M., Guido, R. V., Andricopulo, A. D., De Sousa, A. G. & Da Silva, A. B. 2014. Pattern recognition techniques applied to the study of leishmanial glyceraldehyde-3-phosphate dehydrogenase inhibition. *Int J Mol Sci,* 15**,** 3186-203.

Lucio, M., Fekete, A., Weigert, C., Wagele, B., Zhao, X., Chen, J., Fritsche, A., Haring, H. U., Schleicher, E. D., Xu, G., Schmitt-Kopplin, P. & Lehmann, R. 2010. Insulin sensitivity is reflected by characteristic metabolic fingerprints--a Fourier transform mass spectrometric non-targeted metabolomics approach. *PLoS One,* 5**,** e13317.

Lynch, C. J. & Adams, S. H. 2014. Branched-chain amino acids in metabolic signalling and insulin resistance. *Nat Rev Endocrinol,* 10**,** 723-36.

Macfarlane, D. P., Forbes, S. & Walker, B. R. 2008a. Glucocorticoids and fatty acid metabolism in humans: fuelling fat redistribution in the metabolic syndrome. *Journal of Endocrinology,* 197**,** 189-204.

Macfarlane, D. P., Forbes, S. & Walker, B. R. 2008b. Glucocorticoids and fatty acid metabolism in humans: fuelling fat redistribution in the metabolic syndrome. *J Endocrinol,* 197**,** 189-204.

Macfarlane, D. P., Raubenheimer, P. J., Preston, T., Gray, C. D., Bastin, M. E., Marshall, I., Iredale, J. P., Andrew, R. & Walker, B. R. 2014. Effects of acute glucocorticoid blockade on metabolic dysfunction in patients with Type 2 diabetes with and without fatty liver. *American Journal of Physiology-Gastrointestinal and Liver Physiology,* 307**,** G760-G768.

Makarov, A., Denisov, E., Kholomeev, A., Balschun, W., Lange, O., Strupat, K. & Horning, S. 2006. Performance evaluation of a hybrid linear ion trap/orbitrap mass spectrometer. *Anal Chem,* 78**,** 2113-20.

Mangiapane, E. H. & Brindley, D. N. 1986. Effects of dexamethasone and insulin on the synthesis of triacylglycerols and phosphatidylcholine and the secretion of very-low-density lipoproteins and lysophosphatidylcholine by monolayer cultures of rat hepatocytes. *Biochemical Journal,* 233**,** 151-160.

Mantha, L., Palacios, E. & Deshaies, Y. 1999. Modulation of triglyceride metabolism by glucocorticoids in diet-induced obesity. *American Journal of Physiology-Regulatory, Integrative and Comparative Physiology,* 277**,** R455-R464.

Marchesini, G., Brizi, M., Bianchi, G., Tomassetti, S., Bugianesi, E., Lenzi, M., Mccullough, A. J., Natale, S., Forlani, G. & Melchionda, N. 2001. Nonalcoholic fatty liver disease a feature of the metabolic syndrome. *Diabetes,* 50**,** 1844-1850.

Maruyama, T., Tanaka, K., Suzuki, J., Miyoshi, H., Harada, N., Nakamura, T., Miyamoto, Y., Kanatani, A. & Tamai, Y. 2006. Targeted disruption of G protein-coupled bile acid receptor 1 (Gpbar1/M-Bar) in mice. *J Endocrinol,* 191**,** 197-205.

Mastrangelo, A., Martos-Moreno, G. A., Garcia, A., Barrios, V., Ruperez, F. J., Chowen, J. A., Barbas, C. & Argente, J. 2016. Insulin resistance in prepubertal obese children correlates with sex-dependent early onset metabolomic alterations. *Int J Obes (Lond)*.

Masuzaki, H., Paterson, J., Shinyama, H., Morton, N. M., Mullins, J. J., Seckl, J. R. & Flier, J. S. 2001. A transgenic model of visceral obesity and the metabolic syndrome. *Science,* 294**,** 2166-2170.

Mccormack, S. E., Shaham, O., Mccarthy, M. A., Deik, A. A., Wang, T. J., Gerszten, R. E., Clish, C. B., Mootha, V. K., Grinspoon, S. K. & Fleischman, A. 2013. Circulating branched-chain amino acid concentrations are associated with obesity and future insulin resistance in children and adolescents. *Pediatr Obes,* 8**,** 52-61.

Mcdougall, R., Sibley, J., Haga, M. & Russell, A. 1994. Outcome in patients with rheumatoid arthritis receiving prednisone compared to matched controls. *J Rheumatol,* 21**,** 1207-13.

Mcewen, B. S. 1998. Stress, Adaptation, and Disease: Allostasis and Allostatic Load. *Annals of the New York Academy of Sciences,* 840**,** 33-44.

Mendoza-Figueroa, T., Hernandez, A., Lopez, M. D. L. & Kuri-Harcuch, W. 1988. Intracytoplasmic triglyceride accumulation produced by dexamethasone in adult rat hepatocytes cultivated on 3T3 cells. *Toxicology,* 52**,** 273-286.

Merke, D. P. 2008. Approach to the adult with congenital adrenal hyperplasia due to 21-hydroxylase deficiency. *J Clin Endocrinol Metab,* 93**,** 653-60.

Mihalik, S. J., Steinberg, S. J., Pei, Z., Park, J., Kim, D. G., Heinzer, A. K., Dacremont, G., Wanders, R. J., Cuebas, D. A., Smith, K. D. & Watkins, P. A. 2002. Participation of two members of the very long-chain acyl-CoA synthetase family in bile acid synthesis and recycling. *J Biol Chem,* 277**,** 24771-9.

Milburn, M. V., Jhon, A. R. & Lining, G. 2013. Toxicometabolomic: Technology and Applications. *In:* FAQI, A. S. (ed.) *A Comprehensive Guide to Toxicology in Preclinical Drug Development.* 1 ed. United States of America: Academic press is an imprint of Elsevier, 815-819.

Miller, W. L. & Auchus, R. J. 2011. The molecular biology, biochemistry, and physiology of human steroidogenesis and its disorders. *Endocr Rev,* 32**,** 81-151.

Minisola, S., Scillitani, A. & Romagnoli, E. 2006. Alendronate or alfacalcidol in glucocorticoid-induced osteoporosis. *N Engl J Med,* 355**,** 2156-7; author reply 2157.

Minokoshi, Y., Kahn, C. R. & Kahn, B. B. 2003. Tissue-specific ablation of the GLUT4 glucose transporter or the insulin receptor challenges assumptions about insulin action and glucose homeostasis. *J Biol Chem,* 278**,** 33609-12.

Morgan, S. A. & Tomlinson, J. W. 2010. 11beta-hydroxysteroid dehydrogenase type 1 inhibitors for the treatment of type 2 diabetes. *Expert Opin Investig Drugs,* 19**,** 1067-76.

Nakamura, T., Fujiwara, R., Ishiguro, N., Oyabu, M., Nakanishi, T., Shirasaka, Y., Maeda, T. & Tamai, I. 2010. Involvement of choline transporter-like proteins, CTL1 and CTL2, in glucocorticoid-induced acceleration of phosphatidylcholine synthesis via increased choline uptake. *Biol Pharm Bull,* 33**,** 691-6.

Nakamura, T., Shinno, H. & Ichihara, A. 1980. Insulin and Glucagon as a New Regulator System for Tryptophan Oxygenase Activity Demonstrated in Primary Cultured Rat Hepatocytes. *Journal of Biological Chemistry,* 255**,** 7533-7535.

Newgard, C. B., An, J., Bain, J. R., Muehlbauer, M. J., Stevens, R. D., Lien, L. F., Haqq, A. M., Shah, S. H., Arlotto, M., Slentz, C. A., Rochon, J., Gallup, D., Ilkayeva, O., Wenner, B. R., Yancy, W. S., Jr., Eisenson, H., Musante, G., Surwit, R. S., Millington, D. S., Butler, M. D. & Svetkey, L. P. 2009. A branched-chain amino acid-related metabolic signature that differentiates obese and lean humans and contributes to insulin resistance. *Cell Metab,* 9**,** 311-26.

Nishitani, S., Matsumura, T., Fujitani, S., Sonaka, I., Miura, Y. & Yagasaki, K. 2002. Leucine promotes glucose uptake in skeletal muscles of rats. *Biochem Biophys Res Commun,* 299**,** 693-6.

Nishitani, S., Takehana, K., Fujitani, S. & Sonaka, I. 2005. Branched-chain amino acids improve glucose metabolism in rats with liver cirrhosis. *Am J Physiol Gastrointest Liver Physiol,* 288**,** G1292-300.

O'brien, C. A., Jia, D., Plotkin, L. I., Bellido, T., Powers, C. C., Stewart, S. A., Manolagas, S. C. & Weinstein, R. S. 2004. Glucocorticoids act directly on osteoblasts and osteocytes to induce their apoptosis and reduce bone formation and strength. *Endocrinology,* 145**,** 1835-41.

Ochs, K., Ott, M., Rauschenbach, K. J., Deumelandt, K., Sahm, F., Opitz, C. A., Von Deimling, A., Wick, W. & Platten, M. 2015. Tryptophan-2,3-dioxygenase is regulated by prostaglandin E2 in malignant glioma via a positive signaling loop involving prostaglandin E receptor-4. *J Neurochem*.

Oliver, S. G., Winson, M. K., Kell, D. B. & Baganz, F. 1998. Systematic functional analysis of the yeast genome. *Trends in biotechnology,* 16**,** 373-378.

Out, C., Dikkers, A., Laskewitz, A., Boverhof, R., Van Der Ley, C., Kema, I. P., Wolters, H., Havinga, R., Verkade, H. J., Kuipers, F., Tietge, U. J. & Groen, A. K. 2014. Prednisolone increases enterohepatic cycling of bile acids by induction of Asbt and promotes reverse cholesterol transport. *J Hepatol,* 61**,** 351-7.

Paillard, F., Catheline, D., Duff, F. L., Bouriel, M., Deugnier, Y., Pouchard, M., Daubert, J. C. & Legrand, P. 2008. Plasma palmitoleic acid, a product of stearoyl-coA desaturase activity, is an independent marker of triglyceridemia and abdominal adiposity. *Nutr Metab Cardiovasc Dis,* 18**,** 436-40.

Paterson, J. M., Morton, N. M., Fievet, C., Kenyon, C. J., Holmes, M. C., Staels, B., Seckl, J. R. & Mullins, J. J. 2004. Metabolic syndrome without obesity: hepatic overexpression of 11β-hydroxysteroid dehydrogenase type 1 in

transgenic mice. *Proceedings of the National Academy of Sciences of the United States of America,* 101**,** 7088-7093.

Patterson, A. D., Bonzo, J. A., Li, F., Krausz, K. W., Eichler, G. S., Aslam, S., Tigno, X., Weinstein, J. N., Hansen, B. C., Idle, J. R. & Gonzalez, F. J. 2011. Metabolomics reveals attenuation of the SLC6A20 kidney transporter in nonhuman primate and mouse models of type 2 diabetes mellitus. *J Biol Chem,* 286**,** 19511-22.

Peckett, A. J., Wright, D. C. & Riddell, M. C. 2011. The effects of glucocorticoids on adipose tissue lipid metabolism. *Metabolism,* 60**,** 1500-10.

Pircher, P. C., Kitto, J. L., Petrowski, M. L., Tangirala, R. K., Bischoff, E. D., Schulman, I. G. & Westin, S. K. 2003. Farnesoid X receptor regulates bile acid-amino acid conjugation. *J Biol Chem,* 278**,** 27703-11.

Plotkin, L. I., Weinstein, R. S., Parfitt, A. M., Roberson, P. K., Manolagas, S. C. & Bellido, T. 1999. Prevention of osteocyte and osteoblast apoptosis by bisphosphonates and calcitonin. *J Clin Invest,* 104**,** 1363-74.

Pols, T. W., Nomura, M., Harach, T., Lo Sasso, G., Oosterveer, M. H., Thomas, C., Rizzo, G., Gioiello, A., Adorini, L., Pellicciari, R., Auwerx, J. & Schoonjans, K. 2011. TGR5 activation inhibits atherosclerosis by reducing macrophage inflammation and lipid loading. *Cell Metab,* 14**,** 747-57.

Prawitt, J., Caron, S. & Staels, B. 2011. Bile acid metabolism and the pathogenesis of type 2 diabetes. *Curr Diab Rep,* 11**,** 160-6.

Prelorendjos, A. 2014. *Multivariate Analysis of Metabonomic Data.* PhD, Strathclyde.

Punthakee, Z., Legault, L. & Polychronakos, C. 2003. Prednisolone in the treatment of adrenal insufficiency: a re-evaluation of relative potency. *The Journal of pediatrics,* 143**,** 402-405.

Rask, E., Olsson, T., Soderberg, S., Andrew, R., Livingstone, D. E., Johnson, O. & Walker, B. R. 2001. Tissue-specific dysregulation of cortisol metabolism in human obesity. *J Clin Endocrinol Metab,* 86**,** 1418-21.

Rask, E., Walker, B. R., SöDerberg, S., Livingstone, D. E., Eliasson, M., Johnson, O., Andrew, R. & Olsson, T. 2002. Tissue-specific changes in peripheral cortisol metabolism in obese women: increased adipose 11β-hydroxysteroid dehydrogenase type 1 activity. *The Journal of Clinical Endocrinology & Metabolism,* 87**,** 3330-3336.

Reid, D. M., Hughes, R. A., Laan, R. F., Sacco-Gibson, N. A., Wenderoth, D. H., Adami, S., Eusebio, R. A. & Devogelaer, J. P. 2000. Efficacy and safety of daily risedronate in the treatment of corticosteroid-induced osteoporosis in men and women: a randomized trial. European Corticosteroid-Induced Osteoporosis Treatment Study. *J Bone Miner Res,* 15**,** 1006-13.

Rennie, M. J., Bohe, J., Smith, K., Wackerhage, H. & Greenhaff, P. 2006. Branched-chain amino acids as fuels and anabolic signals in human muscle[1-3]. *The Journal of Nutrition***,** 5.

Reynolds, R. M., Walker, B. R., Syddall, H. E., Whorwood, C. B., Wood, P. J. & Phillips, D. I. 2001. Elevated plasma cortisol in glucose-intolerant men: differences in responses to glucose and habituation to venepuncture. *J Clin Endocrinol Metab,* 86**,** 1149-53.

Rhee, E. P., Cheng, S., Larson, M. G., Walford, G. A., Lewis, G. D., Mccabe, E., Yang, E., Farrell, L., Fox, C. S., O'donnell, C. J., Carr, S. A., Vasan, R. S., Florez, J. C., Clish, C. B., Wang, T. J. & Gerszten, R. E. 2011. Lipid profiling identifies a triacylglycerol signature of insulin resistance and improves diabetes prediction in humans. *J Clin Invest,* 121**,** 1402-11.

Rivkees, S. A. & Crawford, J. D. 2000. Dexamethasone treatment of virilizing congenital adrenal hyperplasia: the ability to achieve normal growth. *Pediatrics,* 106**,** 767-773.

Roberts, L. D., Koulman, A. & Griffin, J. L. 2014. Towards metabolic biomarkers of insulin resistance and type 2 diabetes: progress from the metabolome. *Lancet Diabetes Endocrinol,* 2**,** 65-75.

Rose, A. J., Berriel Diaz, M., Reimann, A., Klement, J., Walcher, T., Krones-Herzig, A., Strobel, O., Werner, J., Peters, A., Kleyman, A., Tuckermann, J. P., Vegiopoulos, A. & Herzig, S. 2011. Molecular control of systemic bile acid homeostasis by the liver glucocorticoid receptor. *Cell Metab,* 14**,** 123-30.

Rosenstock, J., Banarer, S., Fonseca, V. A., Inzucchi, S. E., Sun, W., Yao, W., Hollis, G., Flores, R., Levy, R. & Williams, W. V. 2010. The 11-β-hydroxysteroid dehydrogenase type 1 inhibitor INCB13739 improves hyperglycemia in patients with type 2 diabetes inadequately controlled by metformin monotherapy. *Diabetes care,* 33**,** 1516-1522.

Ruxton, G. D. & Beauchamp, G. 2008. Time for some a priori thinking about post hoc testing. *Behavioral Ecology,* 19**,** 690-693.

Saag, K. G., Shane, E., Boonen, S., Marin, F., Donley, D. W., Taylor, K. A., Dalsky, G. P. & Marcus, R. 2007. Teriparatide or alendronate in glucocorticoid-induced osteoporosis. *N Engl J Med,* 357**,** 2028-39.

Saltiel, A. R. & Kahn, C. R. 2001. Insulin signalling and the regulation of glucose and lipid metabolism. *Nature,* 414**,** 799-806.

Sapolsky, R. M., Romero, L. M. & Munck, A. U. 2000. How do glucocorticoids influence stress responses? Integrating permissive, suppressive, stimulatory, and preparative actions. *Endocr Rev,* 21**,** 55-89.

Schakman, O., Kalista, S., Barbe, C., Loumaye, A. & Thissen, J. P. 2013. Glucocorticoid-induced skeletal muscle atrophy. *Int J Biochem Cell Biol,* 45**,** 2163-72.

Seckl, J. R. & Olsson, T. 1995. Glucocorticoid hypersecretion and the age-impaired hippocampus: cause or effect? *J Endocrinol,* 145**,** 201-11.

Segal, H. L. & Kim, Y. S. 1963. Glucocorticoid Stimulation of the Biosynthesis of Glutamic-Alanine Transaminase. *Proc Natl Acad Sci U S A,* 50**,** 912-8.

Shah, S., Hermanowski-Vosatka, A., Gibson, K., Ruck, R. A., Jia, G., Zhang, J., Hwang, P. M., Ryan, N. W., Langdon, R. B. & Feig, P. U. 2011. Efficacy and safety of

the selective 11beta-HSD-1 inhibitors MK-0736 and MK-0916 in overweight and obese patients with hypertension. *J Am Soc Hypertens,* 5**,** 166-76.

Shearer, J., Duggan, G., Weljie, A., Hittel, D. S., Wasserman, D. H. & Vogel, H. J. 2008. Metabolomic profiling of dietary-induced insulin resistance in the high fat-fed C57BL/6J mouse. *Diabetes Obes Metab,* 10**,** 950-8.

Shyangdan, D., Clar, C., Ghouri, N., Henderson, R., Gurung, T., Preiss, D., Sattar, N., Fraser, A. & Waugh, N. 2011. Insulin sensitisers in the treatment of non-alcoholic fatty liver disease: a systematic review. *Health Technology Assessment,* 15**,** 1-110.

Slavin, B. G., Ong, J. M. & Kern, P. A. 1994. Hormonal regulation of hormone-sensitive lipase activity and mRNA levels in isolated rat adipocytes. *J Lipid Res,* 35**,** 1535-41.

Smyth, S. & Heron, A. 2006. Diabetes and obesity: the twin epidemics. *Nat Med,* 12**,** 75-80.

Society, B. M. a. a. R. P. 2012. *British National Formulary* London, British Medical Journal Publishing Group and Pharmaceutical Press.

Sono, M. 1989. The roles of superoxide anion and methylene blue in the reductive activation of indoleamine 2,3-dioxygenase by ascorbic acid or by xanthine oxidase-hypoxanthine. *J Biol Chem,* 264**,** 1616-22.

Soriano, F., Virág, L. & Szabó, C. 2014. Diabetic endothelial dysfunction: role of reactive oxygen and nitrogen species production and poly(ADP-ribose) polymerase activation. *Journal of Molecular Medicine,* 79**,** 437-448.

Speiser, P. W., Azziz, R., Baskin, L. S., Ghizzoni, L., Hensle, T. W., Merke, D. P., Meyer-Bahlburg, H. F., Miller, W. L., Montori, V. M. & Oberfield, S. E. 2010. Congenital adrenal hyperplasia due to steroid 21-hydroxylase deficiency: an Endocrine Society clinical practice guideline. *The Journal of Clinical Endocrinology & Metabolism,* 95**,** 4133-4160.

Stancakova, A., Civelek, M., Saleem, N. K., Soininen, P., Kangas, A. J., Cederberg, H., Paananen, J., Pihlajamaki, J., Bonnycastle, L. L., Morken, M. A., Boehnke, M., Pajukanta, P., Lusis, A. J., Collins, F. S., Kuusisto, J., Ala-Korpela, M. & Laakso, M. 2012. Hyperglycemia and a common variant of GCKR are associated with the levels of eight amino acids in 9,369 Finnish men. *Diabetes,* 61**,** 1895-902.

Steinberg, S. J., Mihalik, S. J., Kim, D. G., Cuebas, D. A. & Watkins, P. A. 2000. The human liver-specific homolog of very long-chain acyl-CoA synthetase is cholate:CoA ligase. *J Biol Chem,* 275**,** 15605-8.

Stimson, R. H., Andersson, J., Andrew, R., Redhead, D. N., Karpe, F., Hayes, P. C., Olsson, T. & Walker, B. R. 2009. Cortisol release from adipose tissue by 11β-hydroxysteroid dehydrogenase type 1 in humans. *Diabetes,* 58**,** 46-53.

Stimson, R. H., Andrew, R., Mcavoy, N. C., Tripathi, D., Hayes, P. C. & Walker, B. R. 2011. Increased whole-body and sustained liver cortisol regeneration by 11β-hydroxysteroid dehydrogenase type 1 in obese men with type 2 diabetes provides a target for enzyme inhibition. *Diabetes,* 60**,** 720-725.

Stitt, T. N., Drujan, D., Clarke, B. A., Panaro, F., Timofeyva, Y., Kline, W. O., Gonzalez, M., Yancopoulos, G. D. & Glass, D. J. 2004. The IGF-1/PI3K/Akt pathway prevents expression of muscle atrophy-induced ubiquitin ligases by inhibiting FOXO transcription factors. *Mol Cell,* 14**,** 395-403.

Sumner, L. W., Amberg, A., Barrett, D., Beale, M. H., Beger, R., Daykin, C. A., Fan, T. W., Fiehn, O., Goodacre, R., Griffin, J. L., Hankemeier, T., Hardy, N., Harnly, J., Higashi, R., Kopka, J., Lane, A. N., Lindon, J. C., Marriott, P., Nicholls, A. W., Reily, M. D., Thaden, J. J. & Viant, M. R. 2007. Proposed minimum reporting standards for chemical analysis Chemical Analysis Working Group (CAWG) Metabolomics Standards Initiative (MSI). *Metabolomics,* 3**,** 211-221.

Tai, E. S., Tan, M. L., Stevens, R. D., Low, Y. L., Muehlbauer, M. J., Goh, D. L., Ilkayeva, O. R., Wenner, B. R., Bain, J. R., Lee, J. J., Lim, S. C., Khoo, C. M., Shah, S. H. & Newgard, C. B. 2010. Insulin resistance is associated with a metabolic profile of altered protein metabolism in Chinese and Asian-Indian men. *Diabetologia,* 53**,** 757-67.

Tataranni, P. A., Larson, D. E., Snitker, S., Young, J. B., Flatt, J. P. & Ravussin, E. 1996. Effects of glucocorticoids on energy metabolism and food intake in humans. *Am J Physiol,* 271**,** E317-25.

Thomas, C., Gioiello, A., Noriega, L., Strehle, A., Oury, J., Rizzo, G., Macchiarulo, A., Yamamoto, H., Mataki, C., Pruzanski, M., Pellicciari, R., Auwerx, J. & Schoonjans, K. 2009. TGR5-mediated bile acid sensing controls glucose homeostasis. *Cell Metab,* 10**,** 167-77.

Tisdale, M. J. 2002. Cachexia in cancer patients. *Nature Reviews Cancer,* 2**,** 862-871.

Triba, M. N., Le Moyec, L., Amathieu, R., Goossens, C., Bouchemal, N., Nahon, P., Rutledge, D. N. & Savarin, P. 2015. PLS/OPLS models in metabolomics: the impact of permutation of dataset rows on the K-fold cross-validation quality parameters. *Mol Biosyst,* 11**,** 13-9.

Trikudanathan, S. & Mcmahon, G. T. 2008. Optimum management of glucocorticoid-treated patients. *Nature Reviews Endocrinology,* 4**,** 262-271.

Trygg, J., Holmes, E. & Lundstedt, T. 2007. Chemometrics in metabonomics. *J Proteome Res,* 6**,** 469-79.

Van Ginneken, V., Verhey, E., Poelmann, R., Ramakers, R., Van Dijk, K. W., Ham, L., Voshol, P., Havekes, L., Van Eck, M. & Van Der Greef, J. 2007. Metabolomics (liver and blood profiling) in a mouse model in response to fasting: a study of hepatic steatosis. *Biochim Biophys Acta,* 1771**,** 1263-70.

Van Raalte, D. H., Ouwens, D. M. & Diamant, M. 2009. Novel insights into glucocorticoid-mediated diabetogenic effects: towards expansion of therapeutic options? *Eur J Clin Invest,* 39**,** 81-93.

Van Staa, T., Leufkens, H., Abenhaim, L., Begaud, B., Zhang, B. & Cooper, C. 2000. Use of oral corticosteroids in the United Kingdom. *Qjm,* 93**,** 105-111.

Van Staa, T., Leufkens, H. & Cooper, C. 2002a. The epidemiology of corticosteroid-induced osteoporosis: a meta-analysis. *Osteoporosis International,* 13**,** 777-787.

Van Staa, T. P. 2006. The pathogenesis, epidemiology and management of glucocorticoid-induced osteoporosis. *Calcif Tissue Int,* 79**,** 129-37.

Van Staa, T. P., Leufkens, H. G. & Cooper, C. 2002b. The epidemiology of corticosteroid-induced osteoporosis: a meta-analysis. *Osteoporos Int,* 13**,** 777-87.

Varas-Lorenzo, C., Rodriguez, L. a. G., Maguire, A., Castellsague, J. & Perez-Gutthann, S. 2007. Use of oral corticosteroids and the risk of acute myocardial infarction. *Atherosclerosis,* 192**,** 376-383.

Vegiopoulos, A. & Herzig, S. 2007. Glucocorticoids, metabolism and metabolic diseases. *Molecular and Cellular Endocrinology,* 275**,** 43-61.

Wake, D. J., Stimson, R. H., Tan, G. D., Homer, N. Z., Andrew, R., Karpe, F. & Walker, B. R. 2007a. Effects of peroxisome proliferator-activated receptor-alpha and -gamma agonists on 11beta-hydroxysteroid dehydrogenase type 1 in subcutaneous adipose tissue in men. *J Clin Endocrinol Metab,* 92**,** 1848-56.

Wake, D. J., Stimson, R. H., Tan, G. D., Homer, N. Z., Andrew, R., Karpe, F. & Walker, B. R. 2007b. Effects of peroxisome proliferator-activated receptor-α and-γ agonists on 11β-hydroxysteroid dehydrogenase type 1 in subcutaneous adipose tissue in men. *The Journal of Clinical Endocrinology & Metabolism,* 92**,** 1848-1856.

Walker, B. 2006a. Cortisol—cause and cure for metabolic syndrome? *Diabetic Medicine,* 23**,** 1281-1288.

Walker, B. R. 2006b. Cortisol - cause and cure for metabolic syndrome? *Diabetic Medicine,* 23**,** 1281-1288.

Walker, B. R. 2007a. Glucocorticoids and cardiovascular disease. *European Journal of Endocrinology,* 157**,** 545-559.

Walker, B. R. 2007b. Glucocorticoids and cardiovascular disease. *Eur J Endocrinol,* 157**,** 545-59.

Wallach, S., Cohen, S., Reid, D. M., Hughes, R. A., Hosking, D. J., Laan, R. F., Doherty, S. M., Maricic, M., Rosen, C., Brown, J., Barton, I. & Chines, A. A. 2000. Effects of risedronate treatment on bone density and vertebral fracture in patients on corticosteroid therapy. *Calcif Tissue Int,* 67**,** 277-85.

Wallwork, C. J., Parks, D. A. & Schmid-Schönbein, G. W. 2003. Xanthine oxidase activity in the dexamethasone-induced hypertensive rat. *Microvascular Research,* 66**,** 30-37.

Wang, J.-C. & Harris, C. 2015. *Glucocorticoid Signaling: From Molecules to Mice to Man*, Springer.

Wang, T. J., Larson, M. G., Vasan, R. S., Cheng, S., Rhee, E. P., Mccabe, E., Lewis, G. D., Fox, C. S., Jacques, P. F., Fernandez, C., O'donnell, C. J., Carr, S. A., Mootha, V. K., Florez, J. C., Souza, A., Melander, O., Clish, C. B. & Gerszten, R. E. 2011a. Metabolite profiles and the risk of developing diabetes. *Nat Med,* 17**,** 448-53.

Wang, Z., Klipfell, E., Bennett, B. J., Koeth, R., Levison, B. S., Dugar, B., Feldstein, A. E., Britt, E. B., Fu, X., Chung, Y. M., Wu, Y., Schauer, P., Smith, J. D., Allayee,

H., Tang, W. H., Didonato, J. A., Lusis, A. J. & Hazen, S. L. 2011b. Gut flora metabolism of phosphatidylcholine promotes cardiovascular disease. *Nature,* 472**,** 57-63.

Warensjo, E., Rosell, M., Hellenius, M. L., Vessby, B., De Faire, U. & Riserus, U. 2009. Associations between estimated fatty acid desaturase activities in serum lipids and adipose tissue in humans: links to obesity and insulin resistance. *Lipids Health Dis,* 8**,** 37.

Watanabe, M., Houten, S. M., Mataki, C., Christoffolete, M. A., Kim, B. W., Sato, H., Messaddeq, N., Harney, J. W., Ezaki, O., Kodama, T., Schoonjans, K., Bianco, A. C. & Auwerx, J. 2006. Bile acids induce energy expenditure by promoting intracellular thyroid hormone activation. *Nature,* 439**,** 484-9.

Wei, L., Macdonald, T. M. & Walker, B. R. 2004. Taking glucocorticoids by prescription is associated with subsequent cardiovascular disease. *Annals of internal medicine,* 141**,** 764-770.

Weiner, P., Azgad, Y. & Weiner, M. 1993. The effect of corticosteroids on inspiratory muscle performance in humans. *Chest,* 104**,** 1788-91.

Westerbacka, J., Yki-JäRvinen, H., Vehkavaara, S., HäKkinen, A.-M., Andrew, R., Wake, D. J., Seckl, J. R. & Walker, B. R. 2003. Body fat distribution and cortisol metabolism in healthy men: enhanced 5β-reductase and lower cortisol/cortisone metabolite ratios in men with fatty liver. *The Journal of Clinical Endocrinology & Metabolism,* 88**,** 4924-4931.

Westerhuis, J. A., Hoefsloot, H. C. J., Smit, S., Vis, D. J., Smilde, A. K., Van Velzen, E. J. J., Van Duijnhoven, J. P. M. & Van Dorsten, F. A. 2008. Assessment of PLSDA cross validation. *Metabolomics,* 4**,** 81-89.

Wheelock, A. M. & Wheelock, C. E. 2013. Trials and tribulations of 'omics data analysis: assessing quality of SIMCA-based multivariate models using examples from pulmonary medicine. *Mol Biosyst,* 9**,** 2589-96.

Wiklund, S., Johansson, E., Sjostrom, L., Mellerowicz, E. J., Edlund, U., Shockcor, J. P., Gottfries, J., Moritz, T. & Trygg, J. 2008. Visualization of GC/TOF-MS-based metabolomics data for identification of biochemically interesting compounds using OPLS class models. *Analytical Chemistry,* 80**,** 115-122.

Xi, B., Gu, H., Baniasadi, H. & Raftery, D. 2014. Statistical analysis and modeling of mass spectrometry-based metabolomics data. *Methods Mol Biol,* 1198**,** 333-53.

Xia, J., Broadhurst, D. I., Wilson, M. & Wishart, D. S. 2013. Translational biomarker discovery in clinical metabolomics: an introductory tutorial. *Metabolomics,* 9**,** 280-299.

Xia, J., Sinelnikov, I. V., Han, B. & Wishart, D. S. 2015. MetaboAnalyst 3.0--making metabolomics more meaningful. *Nucleic Acids Res,* 43**,** W251-7.

Xu, F., Tavintharan, S., Sum, C. F., Woon, K., Lim, S. C. & Ong, C. N. 2013. Metabolic signature shift in type 2 diabetes mellitus revealed by mass spectrometry-based metabolomics. *J Clin Endocrinol Metab,* 98**,** E1060-5.

Yamamoto, H., Yamaji, H., Abe, Y., Harada, K., Waluyo, D., Fukusaki, E., Kondo, A., Ohno, H. & Fukuda, H. 2009. Dimensionality reduction for metabolome data using PCA, PLS, OPLS, and RFDA with differential penalties to latent variables. *Chemometrics and Intelligent Laboratory Systems,* 98**,** 136-142.

Zaina, S., Heyn, H., Carmona, F. J., Varol, N., Sayols, S., Condom, E., Ramirez-Ruz, J., Gomez, A., Goncalves, I., Moran, S. & Esteller, M. 2014. DNA methylation map of human atherosclerosis. *Circ Cardiovasc Genet,* 7**,** 692-700.

Zammit, V. A., Ramsay, R. R., Bonomini, M. & Arduini, A. 2009. Carnitine, mitochondrial function and therapy. *Adv Drug Deliv Rev,* 61**,** 1353-62.

Zhang, R., Zhang, T., Ali, A. M., Al Washih, M., Pickard, B. & Watson, D. G. 2016. Metabolomic Profiling of Post-Mortem Brain Reveals Changes in Amino Acid and Glucose Metabolism in Mental Illness Compared with Controls. *Comput Struct Biotechnol J,* 14**,** 106-16.

Zhang, T., Watson, D. G., Wang, L., Abbas, M., Murdoch, L., Bashford, L., Ahmad, I., Lam, N. Y., Ng, A. C. & Leung, H. Y. 2013. Application of Holistic Liquid Chromatography-High Resolution Mass Spectrometry Based Urinary Metabolomics for Prostate Cancer Detection and Biomarker Discovery. *PLoS One,* 8**,** e65880.

Zhao, X., Fritsche, J., Wang, J., Chen, J., Rittig, K., Schmitt-Kopplin, P., Fritsche, A., Haring, H. U., Schleicher, E. D., Xu, G. & Lehmann, R. 2010. Metabonomic fingerprints of fasting plasma and spot urine reveal human pre-diabetic metabolic traits. *Metabolomics,* 6**,** 362-374.

Zhen, Y., Krausz, K. W., Chen, C., Idle, J. R. & Gonzalez, F. J. 2007. Metabolomic and genetic analysis of biomarkers for peroxisome proliferator-activated receptor alpha expression and activation. *Mol Endocrinol,* 21**,** 2136-51.

Zoppini, G., Targher, G., Venturi, C., Zamboni, C. & Muggeo, M. 2004. Relationship of nonalcoholic hepatic steatosis to overnight low-dose dexamethasone suppression test in obese individuals. *Clinical endocrinology,* 61**,** 711-715.

Appendices

Appendices for Chapter 3

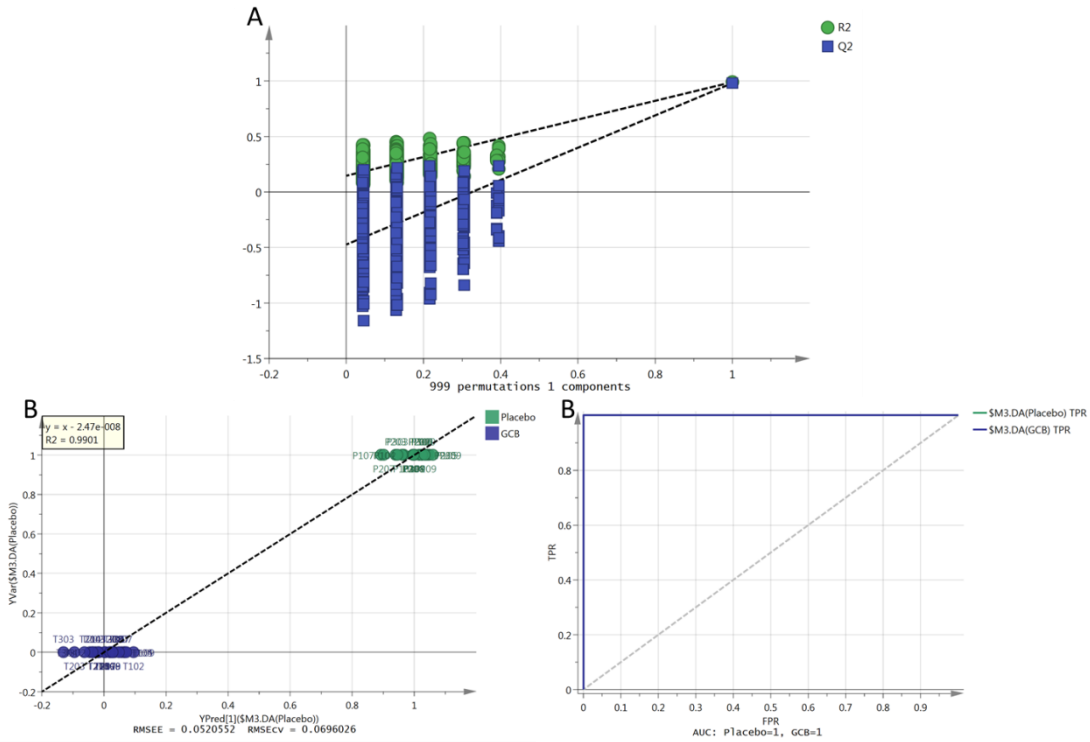

Figure S3.1 (A) Permutations test. The plot shows, for a selected Y-variables, on the vertical axis the values of R^2 and Q^2 for the original model (far to the right) and of the Y-permuted models further to the left. The horizontal axis shows the correlation between the permuted Y-vectors and the original Y-vector for the selected Y. The original Y has the correlation 1.0. (B) The plot displays the observed (y-axis) versus predicted (x-axis) values of the selected Y-variable of the model. The R^2 of the regression line indicates the goodness of Fit = 0.99, with a good model all the observations will fall close to this 45 degree of the line, and with less good models the observations are scattered around the regression line. (C) Receiver Operating Characteristics (ROC) curve shows sensitivity (true positive rate (TPR)) on the y-axis versus (false positive rate (FPR = 1 - Specificity)) on the x-axis. The area under ROC curve (AUROCC) =1 for each group.

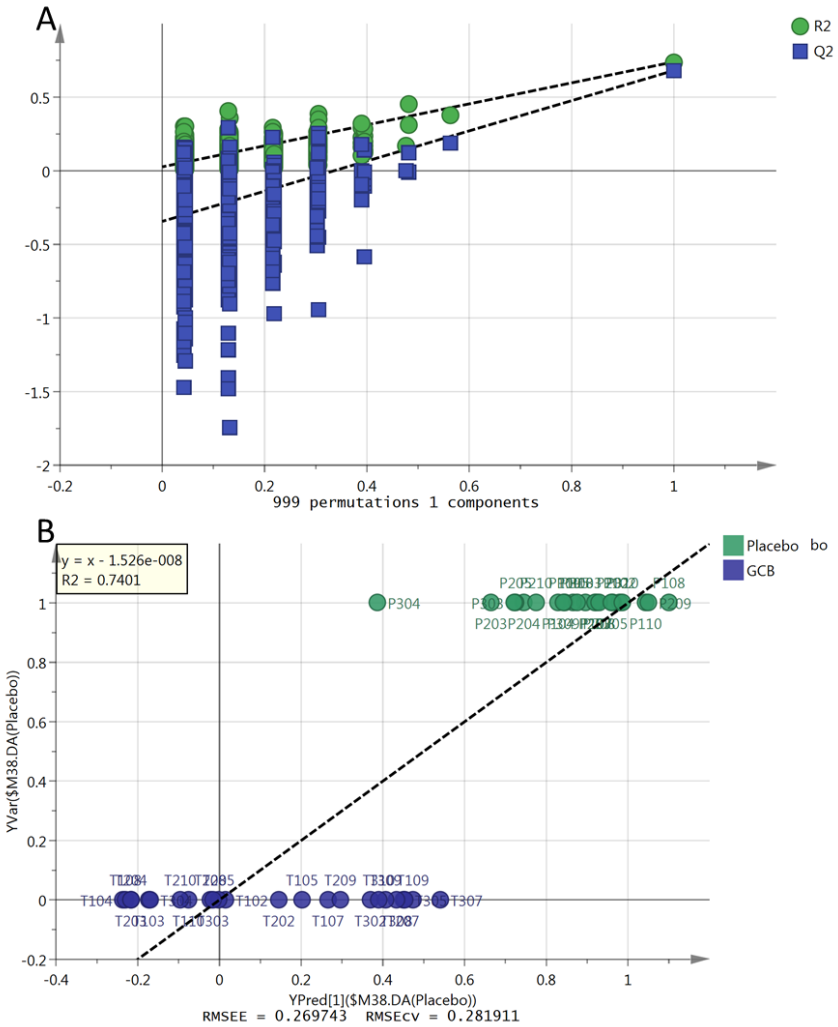

Figure S3.2 (A) Permutations test. The plot shows, for a selected Y-variables, on the vertical axis the values of R^2 and Q^2 for the original model (far to the right) and of the Y-permuted models further to the left. The horizontal axis shows the correlation between the permuted Y-vectors and the original Y-vector for the selected Y. The original Y has the correlation 1.0. (B) The plot displays the observed (y-axis) versus predicted (x-axis) values of the selected Y-variable of the model. The R^2 of the regression line indicates the goodness of Fit = 0.74.

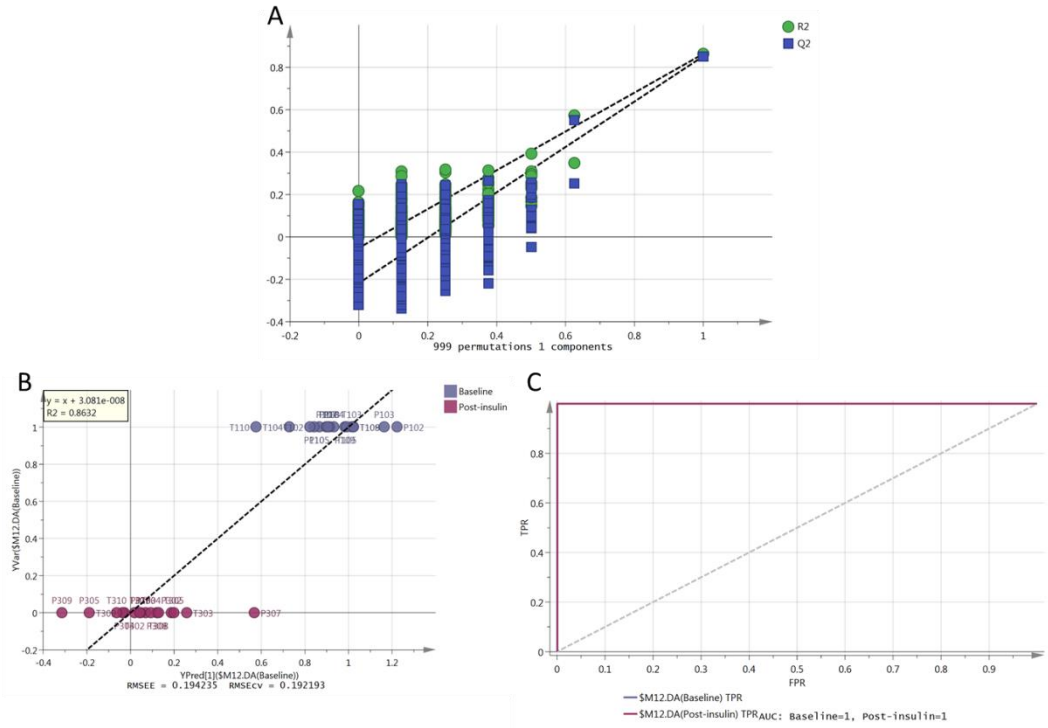

Figure S3.3 (A) Permutations test. The plot shows, for a selected Y-variables, on the vertical axis the values of R^2 and Q^2 for the original model (far to the right) and of the Y-permuted models further to the left. The horizontal axis shows the correlation between the permuted Y-vectors and the original Y-vector for the selected Y. The original Y has the correlation 1.0. (B) The plot displays the observed (y-axis) versus predicted (x-axis) values of the selected Y-variable of the model. The R^2 of the regression line indicates the goodness of Fit = 0.86. (C) Receiver Operating Characteristics (ROC) curve shows sensitivity (true positive rate (TPR)) on the y-axis versus (false positive rate (FPR = 1 - Specificity)) on the x-axis. The area under ROC curve (AUROCC) =1 for each group.

Appendices for Chapter 4

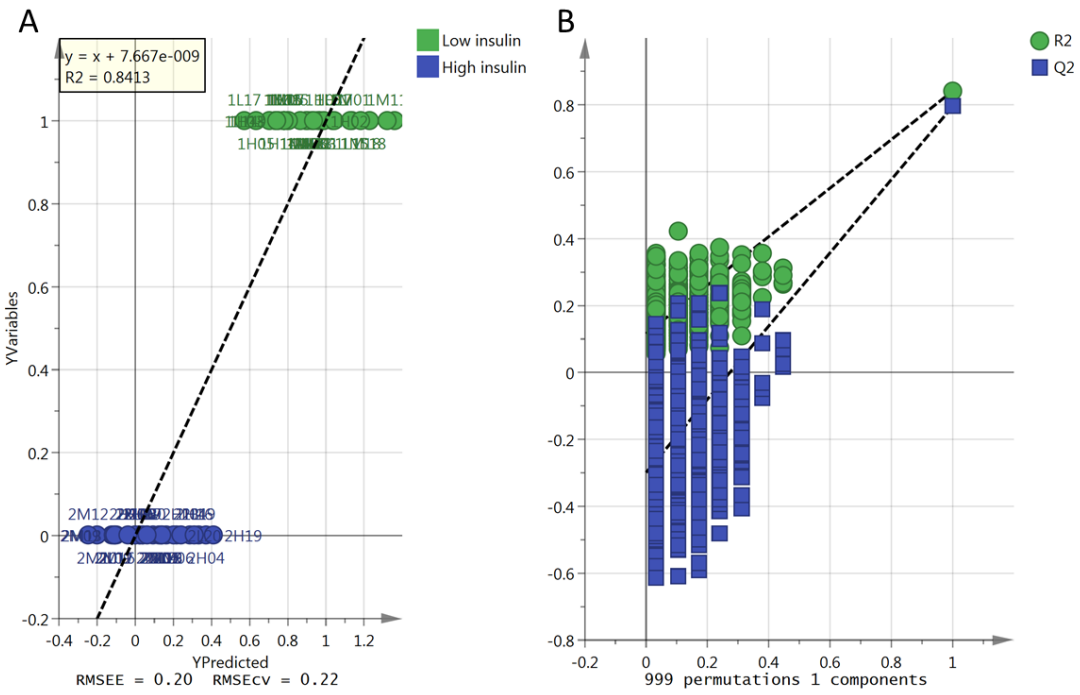

Figure S4.1 (A) The plot displays the observed (y-axis) versus predicted (x-axis) values of the selected Y-variable of the model. The R^2 of the regression line indicates the goodness of Fit = 0.84, with a good model all the observations will fall close to this 45 degree of the line, and with less good models the observations are scattered around the regression line. (B) Permutations test. The plot shows, for a selected Y-variables, on the vertical axis the values of R^2 and Q^2 for the original model (far to the right) and of the Y-permuted models further to the left. The horizontal axis shows the correlation between the permuted Y-vectors and the original Y-vector for the selected Y. The original Y has the correlation 1.0.

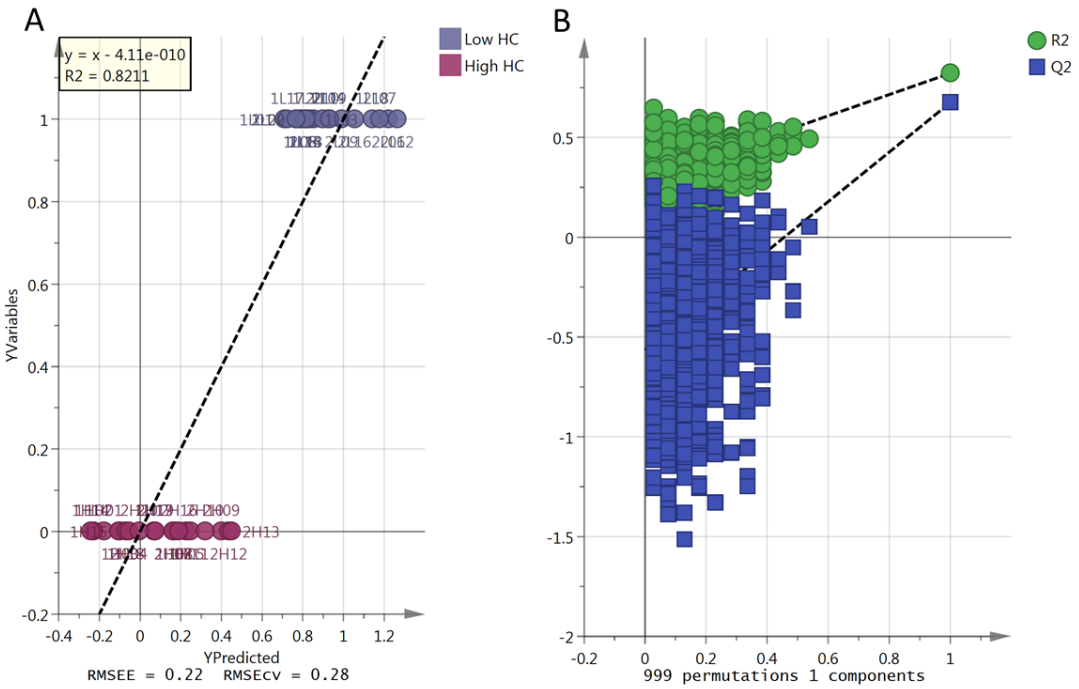

Figure S4.2 (A) The plot displays the observed (y-axis) versus predicted (x-axis) values of the selected Y-variable of the model. The R^2 of the regression line indicates the goodness of Fit = 0.82, with a good model all the observations will fall close to this 45 degree of the line, and with less good models the observations are scattered around the regression line. (B) Permutations test. The plot shows, for a selected Y-variables, on the vertical axis the values of R^2 and Q^2 for the original model (far to the right) and of the Y-permuted models further to the left. The horizontal axis shows the correlation between the permuted Y-vectors and the original Y-vector for the selected Y. The original Y has the correlation 1.0.

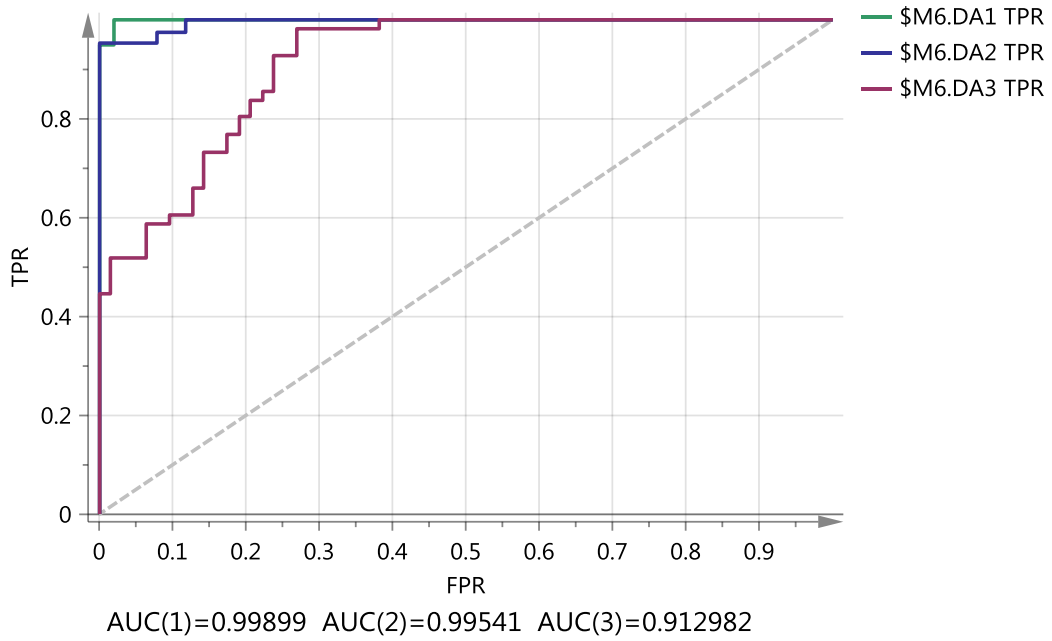

Figure S5.1 Receiver Operating Characteristics (ROC) curve shows sensitivity (true positive rate (TPR)) on the y-axis versus (false positive rate (FPR = 1 - Specificity)) on the x-axis. The area under curve (AUC) of the ROC for the groups; G1=0.99, G2=0.99 and G3=0.91.

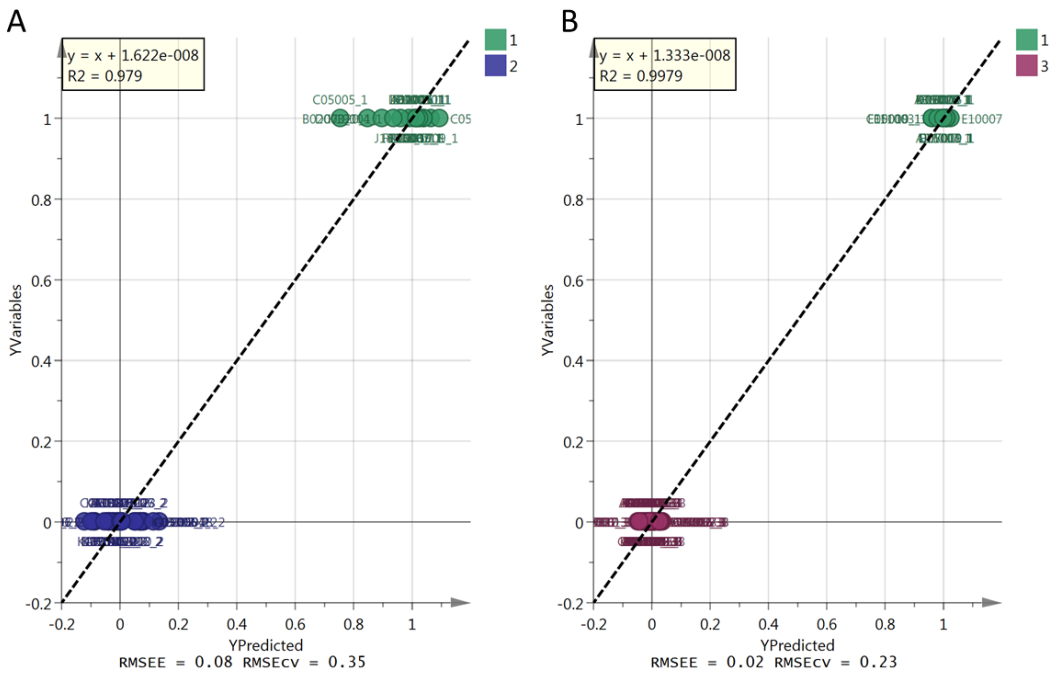

Figure S5.2 (A) The plot displays the observed (y-axis) versus predicted (x-axis) values of the selected Y-variable of the model 1 vs 2. **(B)**The plot displays the observed (y-axis) versus predicted (x-axis) values of the selected Y-variable of the model 1 vs 3. The R2 of the regression line indicates the goodness of Fit, with a good model all the observations will fall close to this 45 degree of the line, and with less good models the observations are scattered around the regression line.

Appendices for Chapter 6

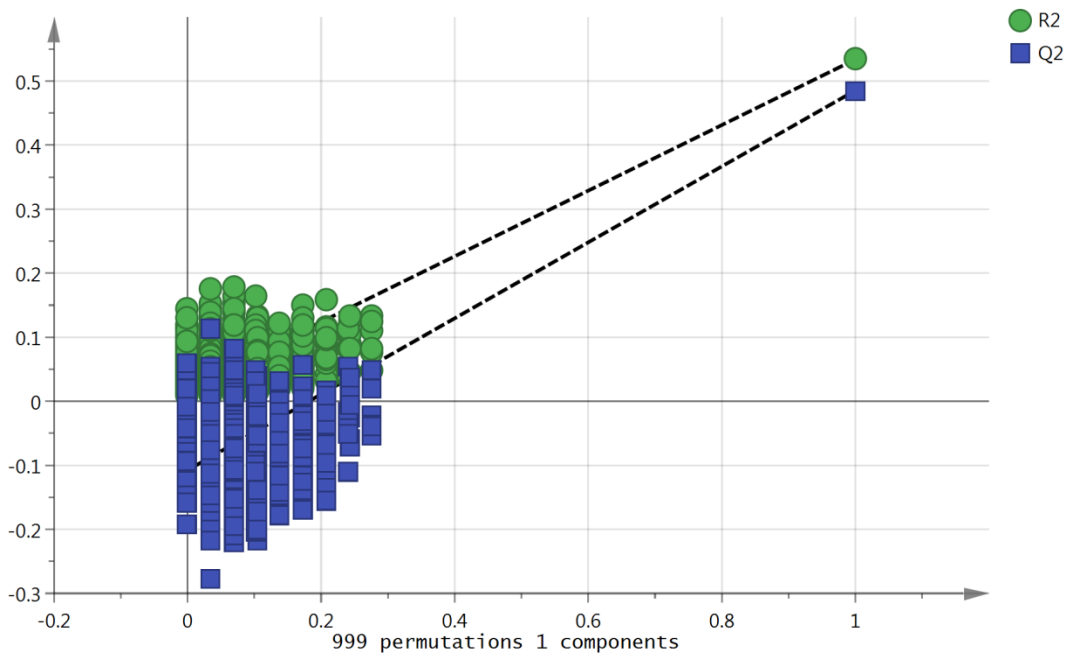

Figure S6.1 Permutations test. The plot shows, for a selected Y-variables, on the vertical axis the values of R^2 and Q^2 for the original model (far to the right) and of the Y-permuted models further to the left. The horizontal axis shows the correlation between the permuted Y-vectors and the original Y-vector for the selected Y. The original Y has the correlation 1.0 with itself, defining the high point on the horizontal axis.